1-1-2013

Abnormal Smooth Muscle Contraction Alters Gut Motility and Propagates Epithelial invasion in the Larval Zebrafish Intestine

Joshua Abrams
University of Pennsylvania, abramsjo@mail.med.upenn.edu

Abnormal Smooth Muscle Contraction Alters Gut Motility and Propagates Epithelial invasion in the Larval Zebrafish Intestine

Abstract
Coordinated smooth muscle contraction is critical for force production and proper functioning of numerous organ systems. Activation at the myosin motor domain via phosphorylated myosin light chain (phospho-MLC) remains the primary signal to initiate contraction, but it is now appreciated that there are additional force modulators also present in smooth muscle. One particularly well studied modulatory protein is Caldesmon (CaD), which has been implicated in controlling contractile force in vascular smooth muscle, however little is known of CaD's physiological role in vivo. Studies in vitro have shown that CaD inhibits actomyosin interactions and that this effect is reversed after phosphorylation, allowing for greater force propagation. Since a number of gastrointestinal (GI) tract and vascular disorders are known to be a result of aberrant force production, closely monitoring CaD's functional properties may provide insight into common contractile defects. We took advantage of the transparent nature of the intestine in larval zebrafish to study CaD's effect on smooth muscle contraction in a vertebrate model. We initiated these studies by examining propulsive peristalsis in the larval intestine after knockdown of endogenous smooth muscle CaD protein. We next measured the role of CaD in the absence of phospho-MLC to better understand its function in disease states where myosin activation is perturbed. Using extensive live imaging analysis, we show that disrupting CaD function within intestinal smooth muscle can significantly increase GI motility, with and without phospho-MLC, highlighting CaD's ability to independently modulate contractile force. In addition, previous work on a mutant, meltdown (mlt), in our lab has uncovered a smooth muscle myosin (myh11) mutation leading to increased contractile force and premature CaD phosphorylation. Interestingly, in the mlt mutant intestinal epithelial invasion was observed pointing to the unique role for force propagation in initiating cell invasion. We show that CaD is necessary for mlt epithelial invasion to occur, as knockdown of CaD causes the invasive phenotype in heterozygous mlt, which otherwise appear wild type. To gain a better understanding of the crosstalk between muscle contraction and epithelial invasion, we performed a genetic screen for modifier mutants of the mlt phenotype. From the screen, we discovered two enhancer mutants of mlt that contained missense mutations in unique protein domains of MYH11 that alter the contractile function of smooth muscle. These mutations (S237Y and L1287M) occur in both the motor domain and helical tail domain of the protein, suggesting that alterations in distinct regions of myosin can result in abnormal contraction and potentially lead to invasion in underlying cells. Since a number of myosin mutations have been implicated in vascular disease and colon cancer, these studies provide insight into the diversity and mechanistic consequences of mutated myosin in altering smooth muscle contraction and epithelial cell invasion.

Degree Type
Dissertation

Degree Name
Doctor of Philosophy (PhD)

Graduate Group
Cell & Molecular Biology

ABNORMAL SMOOTH MUSCLE CONTRACTION ALTERS GUT MOTILITY AND PROPAGATES EPITHELIAL INVASION IN THE LARVAL ZEBRAFISH INTESTINE

Joshua M. Abrams

A DISSERTATION

in

Cell and Molecular Biology

Presented to the Faculties of the University of Pennsylvania

in

Partial Fulfillment of the Requirements for the

Degree of Doctor of Philosophy

2013

Supervisor of Dissertation:

Michael A. Pack, MD _____

Professor of Medicine

Graduate Group Chairperson:

Daniel S. Kessler, PhD _____

Associate Professor of Cell and Developmental Biology

Dissertation Committee:

Shannon Fisher, MD, PhD, Assistant Professor of Cell and Developmental Biology

Brian D. Keith, PhD, Adjunct Professor of Cancer Biology

Catherine Lee May, PhD, Assistant Professor of Pathology and Laboratory Medicine

Paul A. Janmey, PhD, Professor of Physiology

Acknowledgements

I would first like to thank my mentor, Mike Pack for his guidance and intellect as this has kept me enthused as a student and has motivated me to continue my growth as a scientist. Several current and past members of the lab have provided invaluable advice and expertise. Christoph Seiler was the first person to teach me many of the methods used in this project and his proficiency and patience was instrumental throughout my time in lab. Gangarao Davuluri, Weilong Gong, Jie He, and Mani Muthumani, all of whom I'd like to thank for providing technical help throughout my graduate career. I especially thank Ben Wilkins, Kristen Lorent, and Zev Einhorn for providing helpful feedback on a number of scientific presentations and for providing valuable insight on experiments, politics, sports, and life.

I am also greatly indebted to several people who have generously shared their time and expertise. I thank my thesis committee, Shannon Fisher, Brian Keith, Catherine Lee May, and Paul Janmey for their support and honesty on the project and for invaluable advice on a future in science. I also need to thank all of the members, past and present, of the zebrafish group here at Penn in particular members of the Mullins, Granato, and Fisher labs who aside from being great resources scientifically allowed the labs to feel like a community which made coming to work truly enjoyable. I'd also like to give a big thanks to the members of the fish facility Dave and Erin Cobb and Mona Finch-Stephen for their help and for making the zebrafish experience a fun one.

I'd also like to thank the collaborators that we have been fortunate enough to work with on this project. Paul Janmey for providing thoughtful insight and invaluable resources on the biophysical questions within the project, and Jeff Byfield from the Janmey Lab for all of his time and patience optimizing tissue stiffness measurements in the very small and sometimes frustrating zebrafish tissues. Lee Sweeney for graciously making time for us to review data with him and for sharing his expertise on myosin dynamics that allowed the project to become immensely clearer. Dan Safer from the Sweeney Lab for his guidance and for conducting the myosin *in vitro* assays. Roshan Jain for making time for us on the high-speed camera for vascular recordings and for patiently training us and troubleshooting.

Finally, I would not be where I am today without the love and support from my family and especially my mother, Anne. She prioritized education from the time I was young, and this thesis would not have been possible without her commitment to my success.

ABSTRACT

ABNORMAL SMOOTH MUSCLE CONTRACTION ALTERS GUT MOTILITY AND PROPAGATES EPITHELIAL INVASION IN THE LARVAL ZEBRAFISH INTESTINE

Joshua M. Abrams

Michael A. Pack

Coordinated smooth muscle contraction is critical for force production and proper functioning of numerous organ systems. Activation at the myosin motor domain via phosphorylated myosin light chain (phospho-MLC) remains the primary signal to initiate contraction, but it is now appreciated that there are additional force modulators also present in smooth muscle. One particularly well studied modulatory protein is Caldesmon (CaD), which has been implicated in controlling contractile force in vascular smooth muscle, however little is known of CaD's physiological role *in vivo*. Studies *in vitro* have shown that CaD inhibits actomyosin interactions and that this effect is reversed after phosphorylation, allowing for greater force propagation. Since a number of gastrointestinal (GI) tract and vascular disorders are known to be a result of aberrant force production, closely monitoring CaD's functional properties may provide insight into common contractile defects. We took advantage of the transparent nature of the intestine in larval zebrafish to study CaD's effect on smooth muscle contraction in a vertebrate model. We initiated these studies by examining propulsive peristalsis in the larval intestine after knockdown of endogenous smooth muscle CaD protein. We next measured the role of CaD in the absence of phospho-MLC to better understand its function in disease states where myosin activation is perturbed. Using extensive live imaging analysis, we show that disrupting CaD function within intestinal smooth muscle can significantly increase GI motility, with and without phospho-MLC, highlighting CaD's ability to independently modulate contractile force. In addition, previous work on a mutant, *meltdown (mlt)*, in our lab has uncovered a smooth muscle myosin (*myh11*) mutation leading to increased contractile force and premature CaD phosphorylation. Interestingly, in the *mlt* mutant intestinal epithelial invasion was observed pointing to the unique role for force

propagation in initiating cell invasion. We show that CaD is necessary for *mlt* epithelial invasion to occur, as knockdown of CaD causes the invasive phenotype in heterozygous *mlt,* which otherwise appear wild type. To gain a better understanding of the crosstalk between muscle contraction and epithelial invasion, we performed a genetic screen for modifier mutants of the *mlt* phenotype. From the screen, we discovered two enhancer mutants of *mlt* that contained missense mutations in unique protein domains of MYH11 that alter the contractile function of smooth muscle. These mutations (S237Y and L1287M) occur in both the motor domain and helical tail domain of the protein, suggesting that alterations in distinct regions of myosin can result in abnormal contraction and potentially lead to invasion in underlying cells. Since a number of myosin mutations have been implicated in vascular disease and colon cancer, these studies provide insight into the diversity and mechanistic consequences of mutated myosin in altering smooth muscle contraction and epithelial cell invasion.

Table of Contents

List of Figures

Chapter 1: Introduction

1.1: Summary

Coordinated smooth muscle contraction serves a critical role in both visceral tissues and in the vasculature where it contracts rhythmically and functions to maintain muscle tone. Signaling at the myosin filament initiates ATP hydrolysis leading to actin filament sliding and ultimately force production from the smooth muscle. The modulation of force output from contraction has been studied in vascular tissues, where actin bound regulatory elements have been identified as key mediators of muscle tone (Wang 2001, Smolock et al. 2009, Katsuyama et al. 1992). In particular, the actin binding protein Caldesmon (CaD) has shown a unique ability to fine-tune contractile force in smooth muscle tissue. CaD's role in force modulation has been well documented at the level of actomyosin interactions, but its functional relevance in coordinating contraction and tissue maintenance *in vivo* remains unknown. Our lab has previously shown that when endogenous myosin activation is perturbed, through inhibition of light chain (MLC) phosphorylation, intrinsic actomyosin interactions persist raising the question of whether CaD is able to modulate contraction independently of MLC phosphorylation. We therefore hypothesize that CaD is capable of controlling contractile tone irrespective of myosin activation and to test this we have devised an *in vivo* assay to monitor smooth muscle tone within the larval zebrafish intestine.

In addition to the many key regulatory elements that initiate or fine-tune smooth muscle contraction, specific domains within the myosin protein also have profound

effects on contractile output. At the myosin head, the motor domain tightly coordinates actin binding, ATP hydrolysis and the release of ADP/P_i. Each ATP-dependent movement by a myosin dimer along actin requires orchestrated changes in critical structural domains and mutations in certain protein regions can affect contraction in unique ways. Both activating and loss-of-function mutations of myosin have been implicated in human vascular disease and cardiomyopathies, but the mechanism of smooth muscle dysfunction remains unclear. We have previously characterized a unique gain-of-function mutation of smooth muscle myosin (*myh11)* in a zebrafish mutant, *meltdown (mlt)*. The *myh11* mutation resulted in constitutive ATPase activity of the protein and a striking cellular invasion phenotype was observed in the intestinal epithelia of mutant larvae, leading to the question: How can altered contraction dramatically change the cell behavior in an underlying tissue?

Additional evidence from *mlt*, including abnormal CaD function, has led us to hypothesize that the myosin mutation leads to increased contractile force and alters the stiffness of the underlying stromal layer. According to this model, the altered tissue stiffness in *mlt* provides a mechanical cue to epithelial cells, which then respond by initiating cellular invasion. To address this we have examined the crosstalk between the smooth muscle and epithelial layer in *mlt* mutants and have performed biomechanical assays to better understand the link between the contractile defect and epithelial invasion. In addition to biomechanical signaling, *mlt* also raises the question of how specific myosin mutations elicit altered contractile force and if abnormal contraction is a common defect in human disorders caused by myosin variants. We further hypothesize that

multiple myosin protein domains are capable of regulating contractile force output through altered ATPase activity, and that these changes can lead to physiological effects similar to what we have observed in *mlt*. To test these hypotheses, we performed a genetic modifier screen in the *mlt* background where we set out to shed light on the signals that link the contractile defect with epithelial invasion. Ultimately, we discovered additional regions of MYH11 that are also able to propagate the invasive phenotype and this enabled us to further our understanding of myosin domains in both contractile force modulation and their potential link to disease states.

1.2 Smooth Muscle Contraction

The proper functioning of diverse tissue types ranging from the vasculature and respiratory system to the digestive tract and reproductive organs all rely on coordinated smooth muscle contraction. Depending on the tissue type the nature of this contraction can be quite different. In the vasculature for example, smooth muscle contracts tonically permitting slow, sustained contraction during the modulation of vascular tone. Tonic contraction specifically allows smooth muscle to maintain constant force for a prolonged period of time with little energy utilization. In contrast, intestinal contraction occurs phasically with rapid contraction and relaxation to enable food to be propulsed through the gut at a steady rate allowing for nutrient absorption and expulsion of waste. In each of these types of contraction, subtle differences occur in the myosin heavy chain and light chain resulting in distinct contractile patterns and kinetics. The changes that occur on myosin and its regulatory components have long been appreciated and additional modulatory factors have been identified that act at the myosin or actin filament to further

regulate smooth muscle contraction. However, given the diverse functional properties of each smooth muscle tissue the precise coordination between myosin, actin, and their regulatory elements remains poorly understood *in vivo.*

1.2.1 Initiating Contraction at Myosin

In smooth muscle, force is generated by coordinated interactions between actin and myosin, where cross-bridge formation and cycling is a tightly regulated process. This is largely due to the N-terminal ends of myosin heavy chains as they form globular heads that hydrolyze ATP and enable binding to smooth muscle actin. As a result of myosin's enzymatic ability to hydrolyze ATP it serves as the primary force generating protein in smooth muscle. Smooth muscle myosin is made up of two heavy chains and two corresponding light chains that are physically associated to the head domain. The primary, regulatory MLC is considered the central activator of smooth muscle myosin, and if MLC phosphorylation is blocked through inhibition of its kinase (MLCK) normal contraction cannot proceed. A second light chain protein, the essential light chain, is also directly bound to the myosin heavy chain, but its role in regulating protein function is less clear and therefore the regulatory light chain is generally considered the primary regulatory protein of smooth muscle contraction.

In smooth muscle, contraction initiates in response to Ca^{2+}-dependent MLCK activity, with additional Ca^{2+}-independent kinases contributing as well. As the primary initiator of contraction, MLCK becomes active in response to its interaction with the calcium-binding protein Calmodulin following an influx of cytoplasmic Ca^{2+}. These

signaling events lead to MLC phosphorylation, which initiates cross-bridge cycling between myosin and actin leading to contractile force production. In order to maintain contractile tone in smooth muscle, the phosphatase of MLC counteracts MLCK activity, providing a balance of MLC phosphorylation and dephosphorylation between individual myosin heads. This balance of phospho-MLC is especially critical for tissues such as the vasculature where small changes in contractile tone can ultimately lead to severe consequences, such as hypertension due to altered smooth muscle contraction.

There are four isoforms of mammalian smooth muscle myosin (*Myh11*); two C-terminal splice isoforms (SM1 and SM2) and two head domain splice isoforms (SM-A, SM-B) and different combinations have distinct expression in smooth muscle tissues. A mouse mutant of SM-B has normal physiology and survival but displays a significant decrease in maximal force generation and velocity of smooth muscle shortening (Babu et al. 2001). Relative to SM-A, SM-B contains an extra seven-residue insert that resides in a domain adjacent to the ATP-binding pocket of the myosin head and its expression is specific to the intestine, small arteries, and bladder smooth muscles. In vitro motility experiments have shown that the seven-residue insert can alter the kinetics of the cross-bridge cycle and generate higher ATPase activity. Interestingly, knock out mice in which all *myh11* isoforms are deleted display low levels of contraction during early gut development due to a compensatory effect of non-muscle myosins, an effect dependent upon developmental timing as the myosin knockout is eventually lethal (Morano et al. 2000). Although smooth muscle myosin is well understood for its importance during

contractile force production, the specific contributions of each protein domain as well as interacting, modulatory factors in diverse smooth muscle tissues remains elusive.

1.2.2 Modulating Contraction at Caldesmon

As the primary regulation of contraction, MLC is physically associated with the neck domain of individual myosin heads (Kamm and Stull 1985, Murphy 1989) and MLCK phosphorylation induces a conformational change in myosin that activates its ATPase. ATP hydrolysis induces cross-bridge cycling within the actomyosin complex and ultimately the generation of contractile force. Interestingly, in *ex vivo* tissues and culture cells where phospho-MLC levels are greatly reduced, endogenous actomyosin interactions are able to generate and sustain low-level smooth muscle contractile force (Siegman et al. 1984, Haeberle et al. 1985, Gerthoffer 1987, Moreland and Moreland 1987). To account for this, it has been proposed that contraction is also regulated by actin binding proteins that alter actomyosin interactions independently of phospho-MLC (Gusev 2001).

One actin binding protein that has been extensively studied for its regulatory role in smooth muscle is Caldesmon (CaD) (Sobue et al. 1981). CaD exists as two predominant isoforms that are generated by alternative splicing of a single mRNA transcript (Kordowska et al. 2006). The low molecular weight isoform (l-CaD) is expressed in most cell types, including at low levels in smooth muscle, where it mediates actin and non-muscle myosin interaction in the cortical cytoskeleton (Helfman et al. 1999). The high molecular weight isoform (h-CaD) is expressed specifically in smooth

muscle and is distinguished from l-CaD by the presence of a peptide spacer domain that is functionally not well understood, but is thought to facilitate structural rearrangements of h-CaD (Wang et al. 1991). Interestingly, in an h-CaD knockout mouse it was observed that l-CaD expression levels increased in intestinal and bladder smooth muscle pointing to a compensatory mechanism by the light isoform in certain smooth muscle tissues (Morano et al. 2000).

Binding of h-CaD to the phosphorylated actomyosin complex reduces contractile force by inhibiting myosin ATPase activity (Szpacenko et al. 1985, Horiuchi et al. 1986, Earley et al. 1998), possibly by restricting myosin binding to actin or by stabilizing a less active configuration of the actin filament (Ansari et al. 2008) (Figure 2.1A, based on prior model (Wang 2001)). h-CaD's inhibition of the smooth muscle actomyosin complex can be reversed by Erk-mediated phosphorylation or through its interaction with Calmodulin in the presence of calcium (Smith and Marston 1985, Ikebe and Reardon 1990, Childs et al. 1992). This results in increased contractile force by enhancing myosin binding to actin (Katsuyama et al. 1992) (Figure 2.1B) which in turn may stabilize an active configuration of the actin filament (Ansari et al. 2008). In smooth muscle with low levels of phospho-MLC, phospho-h-CaD is thought to promote the interaction between non-phosphorylated myosin heads and actin (Horiuchi and Chacko 1989) (Figure 2.1C, D). Taken together, h-CaD provides an additional mode of contractile tone regulation in smooth muscle in the presence or absence of the primary signaling event at MLC.

1.2.3 Contractile Regulation of Gut Motility

Myosin activation relies on neural signaling that results in MLC phosphorylation, and in the gastrointestinal tract (GI tract) the enteric nervous system (ENS) provides this initial stimulus. The way in which ENS stimulation initiates smooth muscle contraction is through a Ca^{2+}-mediated signaling cascade that activates Calmodulin, which then triggers MLCK, culminating in increased phospho-MLC. In the GI tract ENS-dependent, coordinated contraction is critical in order to process food, absorb water and nutrients, and expel waste. The smooth muscle tissue layers of the gut are innervated allowing for coordinated contraction that causes intestinal contents to be mixed and eventually moved through the intestine. GI smooth muscles are autonomous in that they possess an ability to generate low-level spontaneous rhythmicity and contraction that can be driven by intrinsic pacemakers called interstitial cells of Cajal (ICC). Therefore, smooth muscle cells (SMCs) in the GI tract have the ability to independently contract, though without electrical and mechanical coupling between cells coordinated contraction and peristalsis cannot occur (Sanders et al. 2012). Additional inputs from enteric motor neurons are required in the GI tract to generate coordinated and rhythmic contractions. There are also two types of muscle cells in the GI tract, circular and longitudinal, each providing contractile force in different directions and thus requiring fine coordination to produce rhythmic movements. Coordinated motility in the GI tract is required for efficient digestion and absorption of food and relies on the interplay between each of the factors listed above as well as the intrinsic activity of individual muscle cells.

One example of the autonomous activity of SMCs is highlighted in the small intestine. In this region of the GI tract, pacemaker activity organizes the spontaneous contraction of individual cells into phasic contraction, a process that does not depend on neural inputs. Although this basal activity within SMCs is able to generate low amplitude spontaneous contraction, neural inputs are required to heighten the strength and rhythmicity of contractions. In smooth muscle cells, the primary regulators of such spontaneous contraction are the ICC. In cardiac smooth muscle, pacemaker cells are only detected in distinct sites, however in the GI tract they form networks of cells throughout the entire tissue suggesting a more prominent role. The importance of the ICC was underscored in experiments on cultured gastrointestinal SMCs that alone do not generate electrical rhythmicity, but upon adding ICC exogenously spontaneous rhythmicity occurs that resembles intact smooth muscle. Additional studies determined that slow wave, basal electrical rhythm originates in ICC and that they are coupled to SMCs, allowing the signal to be transmitted (Dickens and Morris 1998, Cousins et al. 2003, Kito and Suzuki 2003). These observations are consistent with ICC expression throughout the GI tract where they are able to coordinate contraction and are key in regulating gut motility patterns. Physiological studies have shown that mice with defective c-Kit signaling, which is critical for ICC rhythmicity, have a reduced contractile response after neural stimulation and GI motility defects (Ward et al. 1994, Burns et al. 1997, Beckett et al. 2007). The ENS and ICC represent two well-studied examples of the tight coordination required across multiple cell types to produce rhythmic GI motility. In addition to understanding the interplay between neural and pacemaker cells within smooth muscle, it is essential to comprehend how these inputs translate at the level of actomyosin

interactions and contractile force. By improving our understanding of myosin motor function and smooth muscle modulators *in vivo*, we can begin to comprehend the complex nature of physiological events such as GI motility in greater detail.

1.3 Motor Mechanism of Myosin

In all forms of myosin, the primary site of activation is the myosin head domain. Each head can be divided into two regions: the motor domain (i.e. actin activated ATPase), and the lever arm, an extended helix containing calmodulin-binding sites. Adjacent to the head domain is a large coiled-coil region that is important for dimerization and folding of myosin. More than 35 classes of myosins have been discovered, each with subtle variations of each domain that dictate subtle differences in protein function. Additionally, myosin proteins may have either one or two heads, depending on the specific interactions that occur with the binding partners of each type of myosin.

In the absence of actin, myosin heads retain the ability to rapidly hydrolyze ATP, but product release requires actin interaction. After inorganic phosphate (P_i) and ADP are released, ATP rapidly rebinds to the actin-bound myosin, causing dissociation from actin. All types of myosins maintain this same basic kinetic cycle, but the rate of transition between each state is highly variable allowing for kinetic tuning of myosin. Kinetic tuning occurs by altering the rate at which myosin proceeds through the ATPase cycle and also the relative amount of the cycle that myosin spends in force-generating states (strong actin binding) (De La Cruz and Ostap 2004). The ratio of myosin's

occupancy of the strong states to that of the weak+dissociated+strong states is known as the 'duty ratio' and is often used as a metric of force production from myosin. Since the rates of P_i and ADP release dictate myosin ATPase cycling, they ultimately determine the duty ratio also. In the example of skeletal muscle myosin, which functions in large clusters, a low duty ratio is maintained to maximize the shortening velocity and power output. The low duty ratio allows this particular myosin to spend most of the cycle weakly attached or completely detached from actin to prevent drag when strongly bound heads slide the actin filament. In other types of muscle and in different tissues the myosin duty ratio can be vastly different depending on the force requirements in each setting.

Additional features of the myosin protein were revealed after the high-resolution structure of the myosin head was elucidated in chicken fast skeletal myosin (Rayment et al. 1993, Rayment et al. 1993). An initial observation of the structure revealed the presence of a large cleft in the middle of the myosin head which was thought to close when myosin discards P_i and ADP upon strong binding to actin (Yengo et al. 1998, Coureux et al. 2003, Volkmann et al. 2003). Another feature of the initial myosin structure was the location of the myosin light chains, which were bound to the C-terminal portion of the motor domain. This region is also thought to form a lever arm that can amplify small movements within the rest of the myosin head. This idea is referred to as the 'swinging lever arm' hypothesis and has been shown to be important in myosin's function (Furch et al. 1999, Tyska and Warshaw 2002, Huxley 2007). This hypothesis adds a level of complexity to how myosin head movements produce contractile force and

highlights how alterations in each myosin protein domain indeed has the potential to change the force output.

1.3.1 Phosphate (P_i) Release

As mentioned above, the initial interaction between myosin and actin triggers the release of P_i and in the absence of actin this release is quite slow. For actin-activated P_i release to proceed, a 'back door' mechanism was first proposed whereby a P_i escape route could be created through a conformational change of myosin. Though the specific conformation of this back door is disputed, it is clear that in order for the P_i to dissociate there must be re-arrangement of either the Switch I or Switch II domain which, along with ADP, block dissociation of P_i. It is still unclear exactly how each Switch element can be induced to move after actin binding of myosin, but a mechanism in which Switch I shifts aside to create the back door is currently favored. Multiple studies have observed movements of the upper portion of the myosin motor domain, and this has been interpreted as evidence for Switch I movement being responsible for these movements (Rosenfeld and Sweeney 2004, Kintses et al. 2007). The concept of Switch I movement creating the back door is also derived from previous work confirming that Switch II movement is coupled to movement of the lever arm and thus is an unlikely candidate for controlling P_i release. Evidence has also implicated Switch I in controlling the position of the lever arm, suggesting it is able to rearrange and create the P_i release pocket without altering myosin conformation.

1.3.2 Myosin Dimers

As an additional layer of complexity with myosin activity, heads of the same dimer are able to communicate with one another in a process known as 'gating.' When the heads communicate they can coordinate events such as the number of steps a dimer takes along an actin filament before dissociating. The communication is a response to strain that occurs when the leading head binds to actin and begins its powerstroke, but is then prevented from completing the powerstroke due to its connection with the lagging head. Once the rear head releases ADP, it binds ATP and dissociates from actin to become the new leading head. While the new leading head searches for a binding site on actin, the new rear head transitions from strong ADP-binding to weak binding, the slowest step in the ATPase cycle. This allows time for the leading head to bind, release P_i, and establish strong binding to actin in order to continue the movement along the filament.

It is clear that both myosin heads do not bind simultaneously during force generation, though the second head can increase the displacement or powerstroke of the engaged head (Tyska and Warshaw 2002). It has been shown in the case of myosin II that additional myosin heads rapidly attach in response to stretch activation and it is thought that these heads are indeed the lagging, unattached heads. The stretch presumably creates a type of physical distortion of attached myosin II molecules that positions the second head for rapid attachment to actin. This could provide an explanation of how stretched muscle can rapidly increase its force to resist the stretch (Brunello et al. 2006). In addition, the force-velocity relationship of muscle can be better

understood because as the velocity of shortening increases, fewer myosin heads are attached to actin in a force generating state (Piazzesi et al. 2007). Interestingly, it has been demonstrated that the force per attached myosin head remains constant irrespective of velocity. Therefore, one explanation for a decrease in force with increasing velocity would be a corresponding decrease in myosin heads attached to actin. It has also been appreciated that phosphorylation at MLC is only required for activation when the myosin dimer is in tact as a single head of myosin can contract independently of MLC phosphorylation. In considering myosin function, it is necessary to take into account the complexity of the individual movements as well as their interaction with neighboring heads.

1.3.3 Myosin Mutations In Disease

Mutations in smooth muscle myosin have been linked to a number of vascular diseases, and thus far the most studied of these is the aneurysm and dissection of the thoracic aorta. Thoracic aortic aneurysms tend to be asymptomatic and often are not diagnosed before an aortic dissection occurs. However, thoracic aortic aneurysms leading to acute ascending aortic dissections (TAAD) can be very serious and often cause premature deaths. A subset of patients with TAAD present with the disease and do not have an identified genetic syndrome but have relatives similarly affected, and this is known as familial TAAD. In both sporadic and familial forms of TAAD, mutations in smooth muscle components have been identified and are implicated in the progression of the disease. Although both smooth muscle actin and myosin mutations have been

identified in patients with TAAD, the implications of these mutations on contraction remains an outstanding question.

By contracting in response to blood flow, smooth muscle cells (SMCs) regulate both flow and pressure in the vasculature. Heterozygous mutations of smooth muscle actin (ACTA2) and myosin (MYH11) are together responsible for TAAD disease in 10-14% of families (Guo et al. 2007, Pannu et al. 2007, Zhu et al. 2007). A large French family with TAAD associated with patient ductus arteriousus (PDA) was used to identify the defective gene as *MYH11* (Khau Van Kien et al. 2005), and subsequent analysis from three unrelated families with TAAD associated with PDA identified *MYH11* mutations in two of the three families (Pannu et al. 2007). The *MYH11* mutations identified for the familial TAAD/PDA phenotype are limited to four mutations: a small deletion, a splice site mutation, and two missense mutations. Individuals with ACTA2 or MYH11 mutations can also present with occlusive vascular disease of the aorta due to increased numbers of SMCs (Pannu et al. 2007).

1.4 *Meltdown* Mutant and Mechanotransduction

1.4.1 Meltdown Mutant and Smooth Muscle Myosin

Previous work in our lab characterized *mlt* as a gain-of-function mutation of MYH11 that results in constitutive ATPase activity at the myosin motor domain. The *mlt* missense mutation, W512R, occurs at the rigid relay loop domain that has previously been implicated in motor activity due to its proximity to critical myosin domains (Wallace et al. 2005). Physiologically, the constitutive ATPase activity in *mlt* leads to

abnormal, tonic contraction as time-lapse imaging revealed intestinal contraction beginning, but not rhythmically resting and constricting as is seen in wild type larvae (Seiler et al. 2012). Tonic contraction of this nature could indeed be responsible for increased force production by the smooth muscle layer upon the surrounding stroma, and our previous work showed the blocking contraction, by actin knockdown, was sufficient to rescue the epithelial invasion in *mlt*. Epithelial invasion can also be induced in heterozygous *mlt*, which are otherwise wild type and survive to adulthood, by treatment with a contractile agonist suggesting that contractile force is the primary driver of the phenotype. Finally, premature phosphorylation of h-CaD was detected by Western blot in *mlt* mutants just prior to the onset of the phenotype (Seiler et al. 2012). h-CaD has been studied in detail for its ability to alter contractile tone, and at an early time when the larval zebrafish intestine has very little contractility, h-CaD could certainly cause substantial changes in force output. Taken together, myosin-induced contractile abnormalities have the potential of triggering mechanical signals between the muscle and stromal layer and a better understanding of how this occurs remains and outstanding question.

1.4.2 Mechanotransduction

The structural framework in SMCs is composed of the contractile unit along with cytoskeleton (made up of nonmuscle actin and intermediate filaments), which links to the cell surface through a protein called filamin A (Small and Gimona 1998). Interestingly, filamin A mutations lead to a syndrome of joint laxity and aortic dissections, suggesting that it may provide a link between SMC contraction and disease. Filamin A enables the

actin filaments of the contractile unit to interface with the cytoskeleton at the cell surface, which contain integrin receptors. Integrins provide the primary signaling to the ECM and serve as a transmembrane link between the matrix, the actin cytoskeleton, and contractile units (Moiseeva 2001). This cellular complex, termed the 'mechanotransduction complex,' provides the interface between the contractile machinery on the interior of the SMC and the ECM on the exterior, to which force is transmitted.

In the vasculature, electron microscopy of the mouse aorta has revealed that SMC contractile filaments link to microfibrils in the ECM early in development and these contacts are maintained up through adulthood (Davis 1993). Fibrillin-1 (FBN1) is the major protein component of these microfibrils, raising the possibility that the integrin receptors of the ECM may interact with fibrillin-1. Hence, FBN1 mutations may also disrupt SMC contraction by interfering with the SMC mechanotransduction complex. Interestingly, in FBN1 mouse mutants the first ultrastructural abnormality noted is an unusually smooth surface of the elastic laminae, likely due to the loss of cell attachments that are normally mediated by FBN1 (Bunton et al. 2001).

Taken together, these components link SMC contraction to ECM components that can alter the stiffness of tissue. Tissue stiffness has been appreciated during tumor progression where it can predict the presence of a tumor or the development of pathology with a heightened risk of malignant transformation, yet the relevance of tissue rigidity to tumor pathogenesis has been largely ignored (Khaled et al. 2004). Though breast cancer patients with fibrotic "stiff" lesions have a poor prognosis (Colpaert et al. 2001), the relationship between tissue rigidity and tumor behavior at the molecular level is unclear.

Tumor rigidity likely reflects an elevation in interstitial tissue pressure due to matrix stiffening linked to fibrosis (Paszek and Weaver 2004). However, it is not understood if and how tissue stiffness can actively promote malignant transformation as many current models rely upon three-dimensional culture assays and physiological forces are likely quite different from these substrates.

1.5: Research Summary

Our previous work on the *mlt* mutant has revealed clear roles for increased contractile force, from myosin and h-CaD, in signaling to the epithelium to initiate invasion. However, there is a limited understanding of how contractile force production and epithelial invasion occur *in vivo*. h-CaD has been studied in great detail *in vitro* and in dissected vascular tissue, but a greater understanding of its role *in vivo* remains to be seen. Studies on vascular smooth muscle disorders have revealed that diverse myosin domains can lead to disease progression, and in some instances this is due to altered motor function. Though mouse models of these vascular disorders have been studied, the specific contribution of these myosin mutations on altered contraction and the propagation of the vascular phenotype remains an open question. Cell invasion has also been linked to altered tissue stiffness, but such studies have relied on advanced three-dimensional culturing methods and there is a paucity of *in vivo* studies on invasion.

In order to model the role of myosin and h-CaD during a normal physiological process, we utilized the larval zebrafish intestine to observe smooth muscle contraction in real-time. This allowed us to assay the specific contributions of each contractile protein

in a live vertebrate. Since h-CaD has been strongly associated with force production from smooth muscle, we hypothesized that altering h-CaD's normal function would result in changes in propulsive peristalsis within the intestine. In Chapter 2, I describe the consequences of h-CaD knockdown in both wild type larvae and a mutant that lacks endogenous smooth muscle signaling at MLC. As MLC phosphorylation is the primary activating signal in smooth muscle, this study was important in understanding h-CaD's potential independent role in the process. In Chapter 3, I describe our efforts to characterize the role, in both smooth muscle contraction and epithelial invasion, of two myosin mutations that we identified from a genetic modifier screen of *mlt*.

Chapter 2: Smooth Muscle Caldesmon Modulates Peristalsis *In Vivo* and is Required to Induce Epithelial Invasion in *meltdown*[*]

2.1: Introduction

Previous work from our lab identified a potential role for smooth muscle Caldesmon in the progression of the epithelial invasion we observed in *meltdown (mlt)* mutants. To better understand the contractility of smooth muscle in *mlt,* Western blot analysis was conducted on regulatory proteins involved in contraction (Seiler et al. 2012). Initially, phosphorylated myosin light chain (p-MLC) expression was assayed and found to similar between wild type and *mlt* suggesting that this mode of signaling was intact in mutants. This is consistent with the previous observation that there is unregulated, constitutive ATPase activity in the mutant Myh11 protein, in that it does not respond to MLC phosphorylation (Wallace et al. 2005). However, when regulation of the h-CaD protein was assayed, Western blots indicated that premature phosphorylation of h-CaD was occurring in *mlt*. The phosphorylated h-CaD was detected at 72 hpf in mutants, which is a stage prior to the onset of peristaltic contractions and also when epithelial invasion initiates in *mlt*. These observations are consistent with the hypothesis that resting smooth muscle tone is increased in the intestine of mutant larvae. Outside of its role in propagating the phenotype in *mlt*, we also wanted to gain insight into h-CaD's

[*] The text of this chapter has been published (Abrams et al. Smooth muscle caldesmon modulates peristalsis in the wild type and non-innervated zebrafish intestine. Neurogastroenterol Motil (2012) vol. 24(3) pp.288-99. Protein data presented in Figure 2.3, 2.7, and 2.9 was provided by co-author Gangarao Davuluri and transgenic larvae in Figure 2.6 were generated by co-author Christoph Seiler. Model in Figure 2.1 was generated by Kristen Lorent.

physiological role in vivo as prior studies of this protein have focused on isolated smooth muscle tissue and individual cells.

By measuring contractile force changes in cultured aortic smooth muscle cells, multiple studies have shown that the inhibitory activity of h-CaD can indeed modulate resting tone of individual cells (Lee et al. 2000). These observations were extended to whole tissue studies of contractile force in dissected aortic tissue after h-CaD siRNA knockdown (Smolock et al. 2009). These groups reported the reversal of h-CaD inhibition after knockdown resulting in a net increase in contractile force. These findings point to h-CaD as a critical mediator of contractile force independent of primary myosin activation (via MLC phosphorylation), but analysis of h-CaD during physiological processes *in vivo* have yet to be elucidated. Our lab has previously shown similarities between the zebrafish and mammalian intestinal smooth muscle and enteric nerve patterning (Wallace et al. 2005, Seiler et al. 2010). These conserved aspects of the zebrafish intestine along with its optical clarity during gut development allowed us to directly test the role of h-CaD in vivo during a physiological process: intestinal peristalsis.

The high molecular weight isoform of the Caldesmon (h-CaD) regulates smooth muscle contractile function by binding actin and modulating cross-bridge cycling of myosin heads. Though the primary regulatory mechanism in smooth muscle occurs through myosin light chain (MLC), h-CaD may have the ability to enhance contractile tone independently of MLC regulation. Upon phosphorylation, h-CaD undergoes a conformational shift allowing myosin binding to occur in a 'higher energy' or 'poised' state (Figure 2.1). In homozygous *meltdown (mlt)* mutants, premature phosphorylation of

h-CaD occurs during a time in intestinal development where phospho-MLC levels remain low. We hypothesized that phosphorylated h-CaD was responsible for an increase in smooth muscle contractile tone in *mlt* and was required for inducing epithelial invasion. To test this hypothesis we further investigated the role of h-CaD in *mlt* mutants and in addition examined its more general role *in vivo* during intestinal peristalsis. We performed morpholino knockdown in viable heterozygous *mlt* larvae and determined that perturbing h-CaD could induce epithelial invasion in these larvae. To determine whether h-CaD knockdown could alter intestinal peristalsis we examined live larvae using a fluorescent gut motility assay. Analysis of these larvae determined that h-CaD protein was indeed modulating contractile tone in smooth muscle, as had been suggested from previous work *in vitro*.

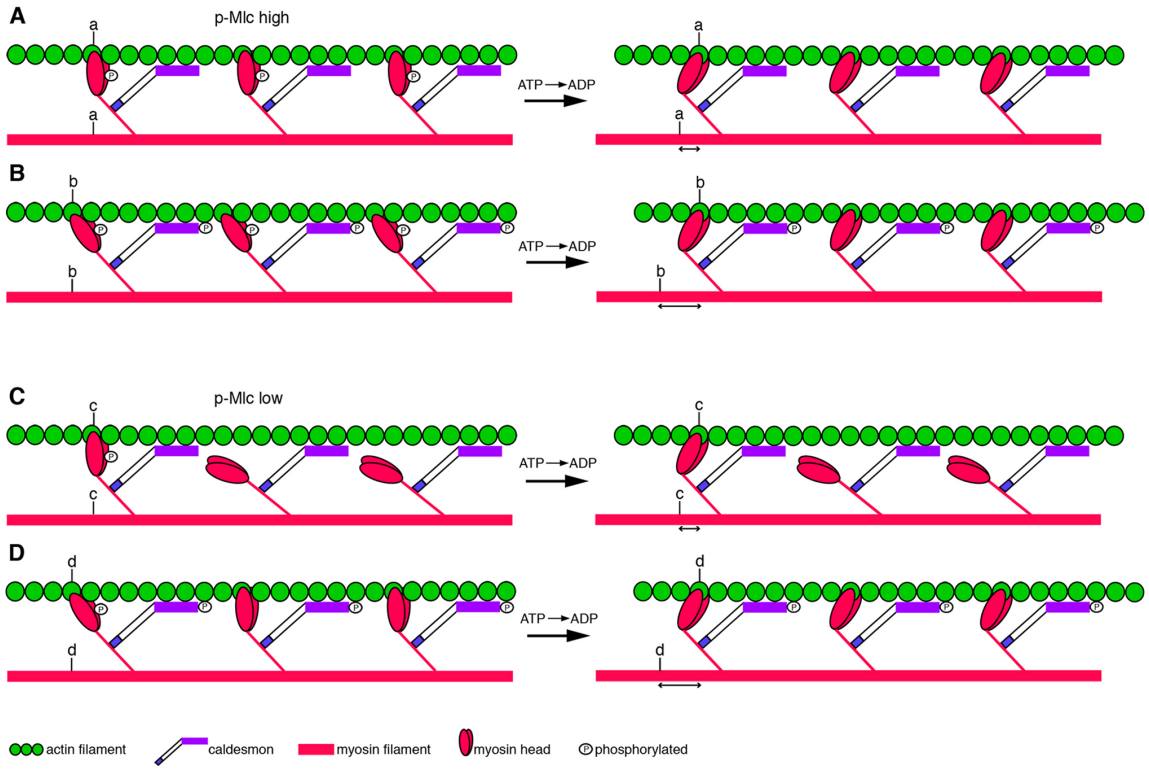

Figure 2.1: Simplified Model of h-CaD Function. Smooth muscle contraction depicted by sliding of actin (green) on myosin (red) filaments following ATP hydrolysis, derived from previous model (Wang 2001). (A) In smooth muscle with high levels of phospho-Mlc (p-Mlc), non-phosphorylated h-CaD restricts binding of myosin heads to the actin filament such that force generation is inhibited. (B) When h-CaD is phosphorylated the myosin heads are able to bind the actin filament in a manner that enhances actomyosin interaction (b). This leads to increased force generation (distance b > distance a). (C) In smooth muscle with low p-Mlc, non-phosphorylated h-CaD prevents binding of non-phosphorylated myosin heads to actin. (D) phospho-h-CaD promotes binding of the non-phosphorylated myosin heads to actin, thereby enhancing contraction; (distance d > distance c). Distances a, b and c, d are not drawn to scale.

2.2: Results

2.2.1: Altered h-CaD Function Induces Epithelial Invasion in mlt

At the onset of epithelial invasion in homozygous *meltdown (mlt)* mutants, smooth muscle signaling via p-Mlc is just beginning in the developing intestine at 3 dpf (Seiler et al. 2012). Interestingly, we have detected high expression of total CaD protein at this early timepoint with markedly low levels of p-CaD expression. This observation suggests a role for endogenous CaD as a contractile 'brake' within the nascent intestinal smooth muscle (Figure 2.1C, D). Phosphorylation of CaD reverses its inhibition and enables propagation of contractile force, and interestingly we found that this phosphorylation occurred prematurely in *mlt* (Seiler et al. 2012). It is important to note that low levels of p-MLC expression were also detected at this stage of development, which implies that coordinated contractions have not yet initiated in the intestine. Since contraction is just beginning in 3 dpf *mlt* larvae, the effects of altered CaD function could become more evident in the absence of mature, coordinated contraction. We postulated that since phosphorylation of CaD reverses its inhibitory function then morpholino knockdown of total CaD protein would mimic this block of inhibition by removing the protein completely.

To investigate the role of h-CaD on the *mlt* phenotype, we utilized a splice blocking morpholino (Cald1a-i4e5 MO, refer to Figure 2.7) that enabled us to reverse h-CaD inhibition in smooth muscle. Using heterozygous *mlt* larvae, we injected Cald1a-i4e5 MO into one-cell embryos and assayed for intestinal abnormalities that resembled

the *mlt* phenotype beginning at 3 dpf. We observed a phenotype in the mid-intestine of Cald1a-i4e5 MO injected heterozygous *mlt* larvae that resembled abnormal ruffling of the intestinal folds (typical of homozygous *mlt*) compared to normal morphology in Cald1a-i4e5 MO injected wild type larvae (Figure 2.2A,C). Age matched Cald1a-i4e5 MO injected wild type larvae displayed normal intestinal morphology, though they had decreased gut motility as described later in this chapter. To determine if the phenotype in *mlt* heterozygotes induced epithelial cell remodeling and basement membrane degradation, we performed histological analysis using antibody labeling of basement membrane (anti-laminin) and epithelial cell junctions (anti-cytokeratin). After antibody labeling of whole mount larvae at 6 dpf, we embedded and prepared serial sections of heterozygous *mlt* with an observable phenotype. Histological analysis revealed abnormalities that resembled homozygous *mlt* whereby intestinal epithelial cells were observed invading into the surrounding stromal layer after basement membrane degradation (Figure 2.2D). Morpholino injected wild type larvae never displayed abnormal epithelial morphology and this was also true of heterozygous *mlt* injected with a control morpholino (Figure 2.2B).

As h-CaD has previously been described *in vitro* to modulate contractile force, these results implicate a role for increased force from the muscle layer to which epithelia are sensitive. We have shown previously that the mutated Myh11 protein in *mlt* has constitutive ATPase activity that is thought to contribute to an increase in contractile force (Wallace et al. 2005). Our current results show that heterozygous *mlt* are also sensitive to increased contractile force, suggesting that there may be a biological

threshold of force that intestinal epithelial cells are sensitive to. In other words, by removing h-CaD inhibition in *mlt* heterozygotes the overall output of contractile force becomes large enough to induce epithelial invasion (for model, see Figure 3.1).

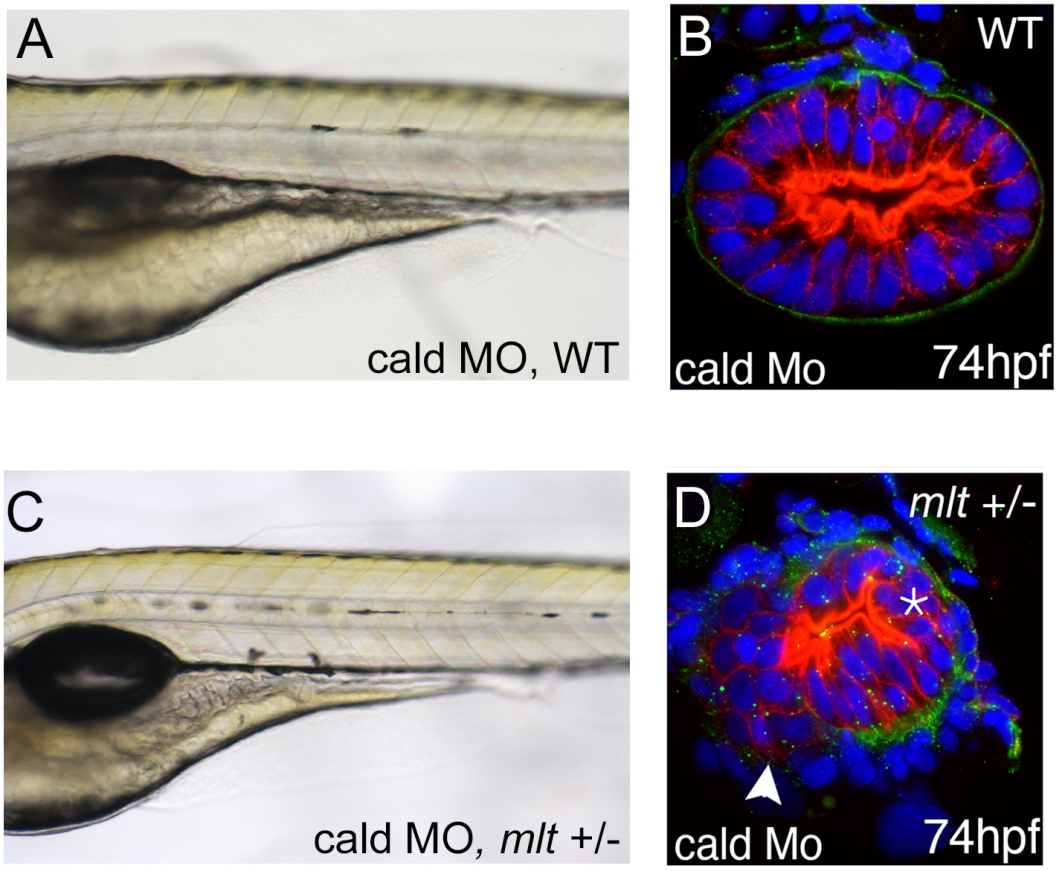

Figure 2.2: **h-CaD Disruption in Heterozygous *mlt* Induces Epithelial Invasion.** (A) Live image of 74 hpf wild type (WT) larvae after injection with a morpholino targeting the large isoform of Caldesmon (Cald1a-i4e5 MO). Cald1a-i4e5 MO has no affect on WT intestinal morphology other than mild developmental delay (B) Histological cross-sections through the intestine of larvae immunostained for laminin (green) and cytokeratin (red) show normal epithelial architecture in WT. (C) Heterozygous *mlt* larvae display abnormal intestinal morphology in the mid-intestinal region after Caldesmon knockdown. (D) Epithelial invasion (arrowhead) and stratification (asterisk) are observed in the mid-intestinal region of the *mlt* heterozygote by histological analysis.

2.2.2: *The Zebrafish Contains Two Caldesmon Gene Paralogs with High Sequence Homology to Human CALD1*

To identify a zebrafish h-CaD ortholog we first performed BLAST analyses of the zebrafish genome assembly using human *CALD1* coding sequence. Two loci encoding genes with relatively high sequence homology to *CALD1* were identified on chromosome 4 and chromosome 25 (*cald1a* and *cald1b*, respectively). The predicted protein encoded by the *cald1a* locus had the greatest degree of homology to human CALD1, particularly in the actin and myosin binding domains (Figure 2.3A).

We also compared syntenic relationships surrounding the *cald1a* and *cald1b* loci with human *CALD1*. We first identified the map positions of the zebrafish orthologs of 65 genes immediately surrounding human *CALD1* (Figures 2.3B and 2.4). Of 34 genes located 5' of *CALD1*, 26 were located in a comparable position with respect to the *cald1a* locus, whereas only 6 mapped to a comparable position with respect to *cald1b*. For 31 genes 3' of *CALD1*, 14 were located surrounding *cald1a* whereas none were located adjacent to *cald1b*. Next, we performed the reciprocal experiment and mapped the position of the human orthologs of genes surrounding the two zebrafish *cald1* loci. 12 of 40 genes 5' of *cald1a* but only 7 of 38 genes 5' of *cald1b* mapped to comparable regions of *CALD1*. Similarly, 9 of 43 genes 3' of *cald1a* but only 3 of 38 genes 3' of *cald1b* mapped nearby *CALD1*. Paralogs for 17 zebrafish genes were identified in the region surrounding the two *cald1* loci (Figure 2.4).

All together, these findings argue that *cald1a* and *cald1b* are gene paralogs that arose from a whole genome duplication that occurred in an ancestral species of ray-

finned fish (Amores et al. 1998). We predicted that the Cald1a protein was likely a functional ortholog of human CALD1 protein based on amino acid sequence homology, and due to more highly conserved gene synteny surrounding the *cald1a* locus.

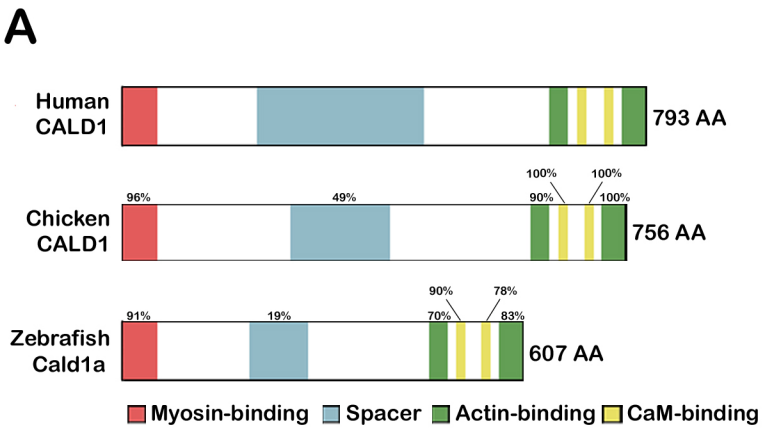

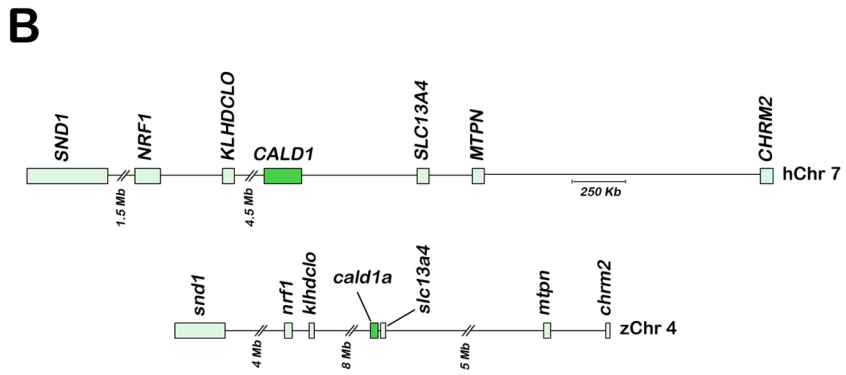

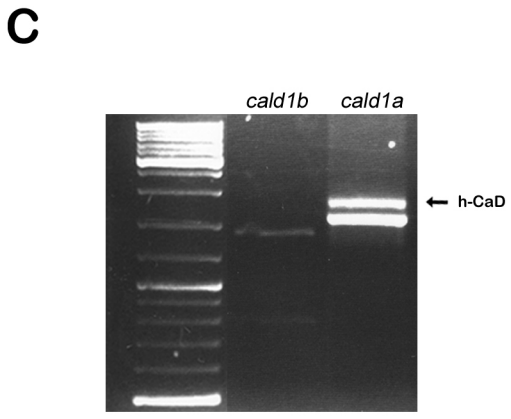

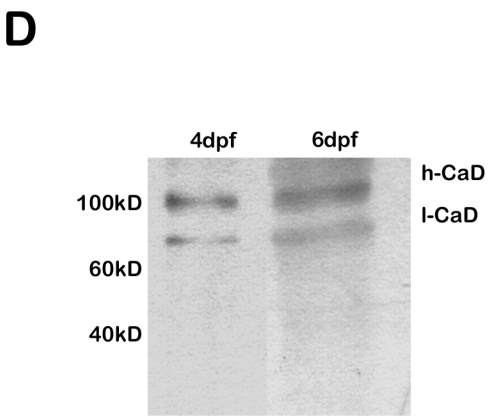

Figure 2.3: Zebrafish Smooth Muscle Caldesmon (h-CaD). (A) Schematic representation of the human, chicken and zebrafish h-CaD orthologs. Conserved protein domains and percent amino acid homology are indicated. (B) Conserved syntenic relationships surrounding the human *CALD1* locus on chromosome 7 and the zebrafish *cald1a* locus on chromosome 4. (C) RT-PCR showing amplification of the full-length cDNA corresponding to the high and low molecular weight zebrafish *cald1a* isoforms from intestinal cDNA. A correctly sized transcript for the predicted low molecular weight *cald1b* isoform is also detected. (D) Western blot showing intestinal levels of CaD isoforms. Molecular weight standards indicated. Mb - megabase; Kb – kilobase; dpf – days post-fertilization.

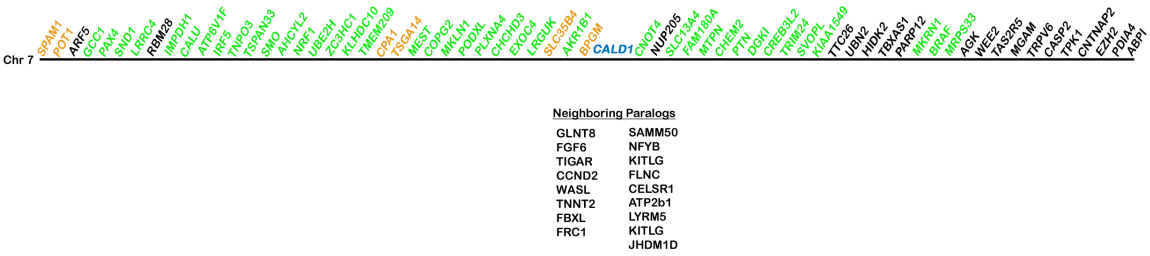

Neighboring Paralogs	
GLNT8	SAMM50
FGF6	NFYB
TIGAR	KITLG
CCND2	FLNC
WASL	CELSR1
TNNT2	ATP2b1
FBXL	LYRM5
FRC1	KITLG
	JHDM1D

Figure 2.4: Conserved Gene Synteny Surrounding the Human *CALD1* and Zebrafish *cald1a* and *cald1b* Loci. Schematic depicts the genes surrounding the *CALD1* locus on human chromosome 7. Genes with zebrafish orthologs in a comparable location surrounding the *cald1a* or *cald1b* loci are depicted in green and orange, respectively. Gene paralogs surrounding both the *cald1a* and *cald1b* loci are listed below.

2.2.3: Cald1a Encodes High and Low Molecular Weight Isoforms Generated By Alternative Splicing

The *cald1b* locus encodes an l-CaD-like ortholog that was previously reported to play a role in cardiovascular development (Zheng et al. 2009). Genomic sequence analysis of this locus did not identify a potential h-CaD transcript nor did BLAST analysis of the zebrafish EST database. To determine whether an alternatively spliced h-CaD mRNA transcript was encoded by *cald1a*, we amplified its full-length cDNA from whole 5 day post-fertilization (dpf) larvae that have functional intestinal smooth muscle. Our primers amplified only a fragment corresponding to the predicted low molecular weight *cald1a* isoform (data not shown). When the same primers were used to amplify RNA recovered from dissected intestines (that were enriched for smooth muscle) a higher molecular weight band was recovered in addition to the low molecular weight band (Figure 2.3C). By contrast, amplification of intestinal cDNA using comparable primers from the *cald1b* ortholog only amplified low levels of a corresponding low molecular weight band (Figure 2.3C). DNA sequence analysis showed that the larger band amplified from *cald1a* encoded a predicted h-CaD ortholog that included an 86 amino acid spacer domain. Genomic DNA analyses indicated that the spacer was encoded by two short exons, 36 and 225 base pairs (bp), respectively. We observed only limited amino acid homology with spacer domains from other vertebrate h-CaD proteins (Figure 2.3A and 2.5). This was expected, as the spacer sequence of h-CaD is not highly conserved across species. Outside of the spacer domain, the h-CaD cDNA sequence was identical to the full-length *cald1a* cDNA, although a splice variant involving the terminal

exon was infrequently detected (Figure 2.6). These findings show that the *cald1a* locus encodes two alternatively spliced transcripts that are orthologs of the mammalian l-CaD and h-CaD isoforms.

To determine whether the h-CaD transcript encoded a functional protein we performed Western blot analysis of 5 dpf intestinal extracts using an antibody directed against mouse CaD protein. This antibody detected both high and low molecular weight bands (Figure 2.3D). The high molecular weight band was first detected around the onset of peristaltic contractions (~ 78 hours post-fertilization; data not shown) when only circular smooth muscle is present (Wallace et al. 2005) and CaD protein levels increased between 4 dpf and 6 dpf. At these later stages longitudinal smooth muscle develops and peristaltic contractions are more pronounced. The estimated molecular mass of the high molecular weight band (125kD) was notably greater than the predicted h-CaD molecular mass (70kD). However, a comparable discrepancy between predicted and observed molecular mass of mammalian h-CaD proteins has been reported and attributed to its large number of acidic amino acids (Bryan 1989). The molecular weight of the presumptive l-CaD protein was similarly affected.

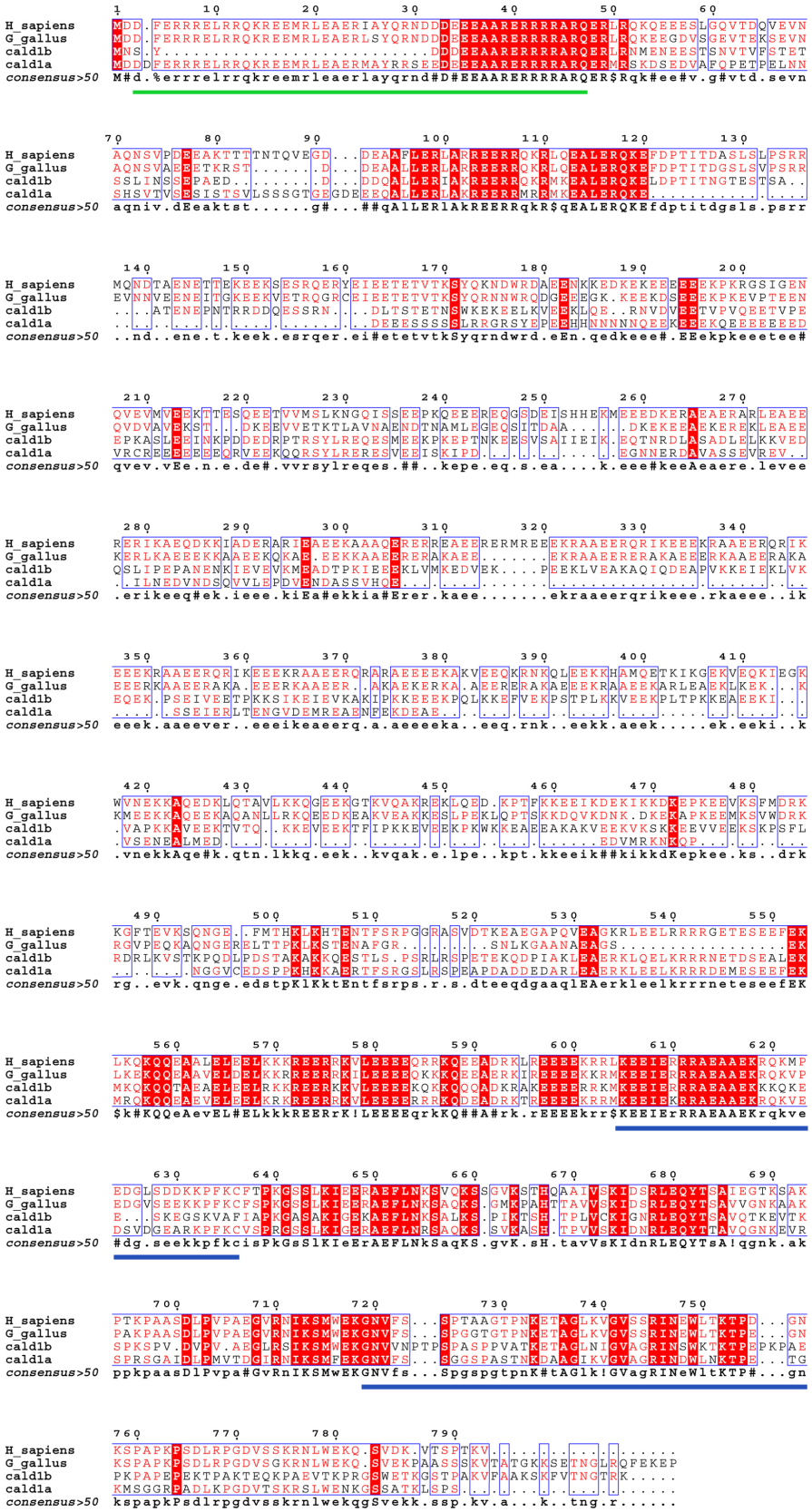
H_sapiens
G_gallus
cald1b
cald1a
consensus>50

Figure 2.5: High Homology at Function Domains in Vertebrate h-CaD Proteins. Note high degree of conservation in the actin and myosin binding domains (blue lines and green lines, respectively). H_sapiens – Human; G_gallus – Chicken; cald1b – zebrafish paralog (chromosome 25); cald1a – zebrafish paralog (chromosome 4).

2.2.4: h-CaD Expression in the Zebrafish Intestine is Restricted to Smooth Muscle

h-CaD expression has been shown in other vertebrates to be restricted to smooth muscle, whereas l-CaD is ubiquitously expressed. RNA in situ hybridization using an isoform specific zebrafish h-CaD probe showed only low level background staining in 5 dpf larvae (data not shown). Therefore, to assay h-CaD expression in intestinal smooth muscle, we recovered epithelial cell and smooth muscle cell RNAs from bigenic larvae that express cell type specific fluorescent reporters (Figure 2.7A). These larvae express GFP from the smooth muscle *sm22a* promoter beginning at 72 hours post-fertilization (Seiler et al. 2010) and mCherry from a *miR194* promoter fragment that is activated in the epithelium at nearly the same time. RT-PCR amplification of established epithelial (*fabp2*, *vil11, and fabp6*) and smooth muscle (*acta2*, *myh11*) markers confirmed purity of the sorted cell populations (Figure 2.7B). The RT-PCR experiments also confirmed that zebrafish h-CaD expression was restricted to smooth muscle while l-CaD was expressed in both smooth muscle and epithelial cells (Figure 2.7C).

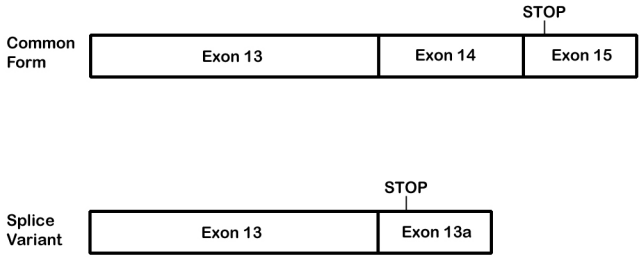

Figure 2.6: Schematic of a Carboxy-Terminal Splice Variant of *cald1a*. Based on sequencing analysis, the most common *cald1a* isoform was comprised of 15 exons (top) while a minority splice variant isoform contained an additional exon containing a premature stop codon (bottom).

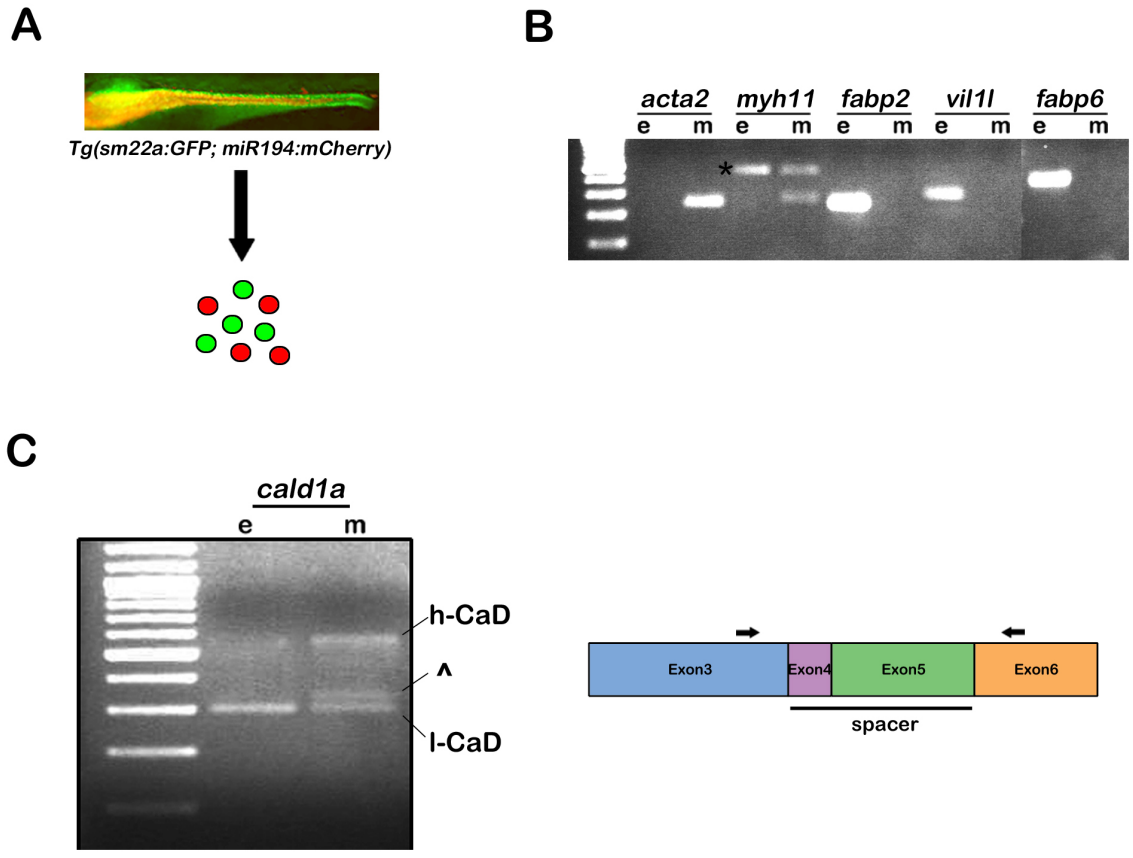

Figure 2.7: Expression of the Zebrafish h-CaD Ortholog in Intestinal Smooth Muscle. (A) Scheme to isolate intestinal smooth muscle (green) and epithelial (red) cells

from *Tg(sm22a:GFP; miR194:mCherry)* larvae. Fluorescent image of a 5 dpf bigenic larval intestine is shown. (B) RT-PCR amplification showing expression of intestinal smooth muscle and epithelial markers in sorted cells. The *myh11* primers amplify a band (*) from contaminating genomic DNA (confirmed by sequencing). (C) Expression of the high molecular weight *cald1a* transcript is restricted to smooth muscle. Infrequently an additional band was amplified from smooth muscle that migrated near the low molecular weight *cald1* transcript (^), however this was detected in only a minority of experiments. Schematic indicates the location of PCR primers (arrows) in exon 3 and exon 6 that were used to amplify the *cald1a* isoforms. e - epithelial; m - smooth muscle.

2.2.5: h-CaD Modulates Propulsive Intestinal Peristalsis in the Larval Zebrafish

To investigate zebrafish h-CaD function in vivo, we generated a *cald1a* splice blocking morpholino (Cald1a-i4e5 MO) that enabled us to specifically disrupt h-CaD translation without affecting translation of the l-CaD isoform. The specificity of Cald1a-i4e5 MO also prevented any disruption of the normal function of *cald1b.* It was crucial not to disrupt l-CaD function as this isoform is predicted to be essential for a wide range of non-muscle phenotypes. For this study, we designed a morpholino complementary to the exon 5 splice acceptor of the h-CaD pre-mRNA (Figure 2.8A). This was predicted to generate a novel Caldesmon transcript that encoded only 12 of 87 h-CaD spacer region amino acids.

Zebrafish embryos and larvae injected with Cald1a-i4e5 MO had normal morphology other than mild developmental delay that was also seen in control larvae (Figure 2.8B). In RT-PCR experiments using intestinal RNA and primers surrounding exons 4 and 5, a fragment of the truncated h-CaD transcript that lacked exon 5 but retained exon 4, and the fragment corresponding to l-CaD were both amplified (Figure 2.8C). The truncated h-CaD transcript, which was 36 bp larger than endogenous l-CaD transcript, encoded 12 amino acids in-frame with exon 6. Successful inhibition of translation of the h-CaD transcript was confirmed by Western blot (Figure 2.8D). This showed reduced intensity of the band corresponding to h-CaD with increased intensity of a band corresponding to l-CaD. The apparent increase in l-CaD protein detected by this blot is likely due to the presence of the truncated h-CaD protein generated by the Cald1a-i5e5 MO (as it is only 12 amino acids longer than endogenous l-CaD).

To determine if h-CaD knockdown affected smooth muscle contraction we assayed propulsive peristalsis in the intestine of larvae injected with Cald1a-i5e5 MO that were then fed fluorescent microspheres (Figure 2.8E). Following their ingestion, the microspheres form an aggregate in the intestinal bulb as a result of mixing peristalsis. This aggregate is then transported into the mid and posterior intestine via propulsive peristalsis, and eventually expelled. We measured peristalsis beginning at 4 dpf in Cald1a-i5e5 MO injected larvae by monitoring fluorosphere movement 2 hours after ingestion. As shown in Figure 2.8E, Cald1a-i5e5 MO larvae had an increase in intestinal transit as more larvae in this group had moved fluorospheres into the mid-posterior intestine and/or expelled them. To confirm that contractile rate was unchanged in these

larvae, video recordings of morpholino injected larvae showed that the rate of peristaltic contractions was unaffected by h-CaD knockdown (Figure 2.9, top). The affect on peristalsis was less pronounced at 5 dpf than at 4 dpf, most likely due to the transient nature of the morpholino knockdown. In addition, because levels of phospho-h-CaD have increased by 5 dpf (Davuluri et al. 2010), the overall level of inhibition imparted by endogenous h-CaD is likely to be reduced. Together these data indicate that the normal function of h-CaD is to negatively regulate the force of phasic intestinal smooth muscle contraction, as gut transit is accelerated in the larvae injected with Cald1a-i5e5 MO without a concomitant effect on contractile rate.

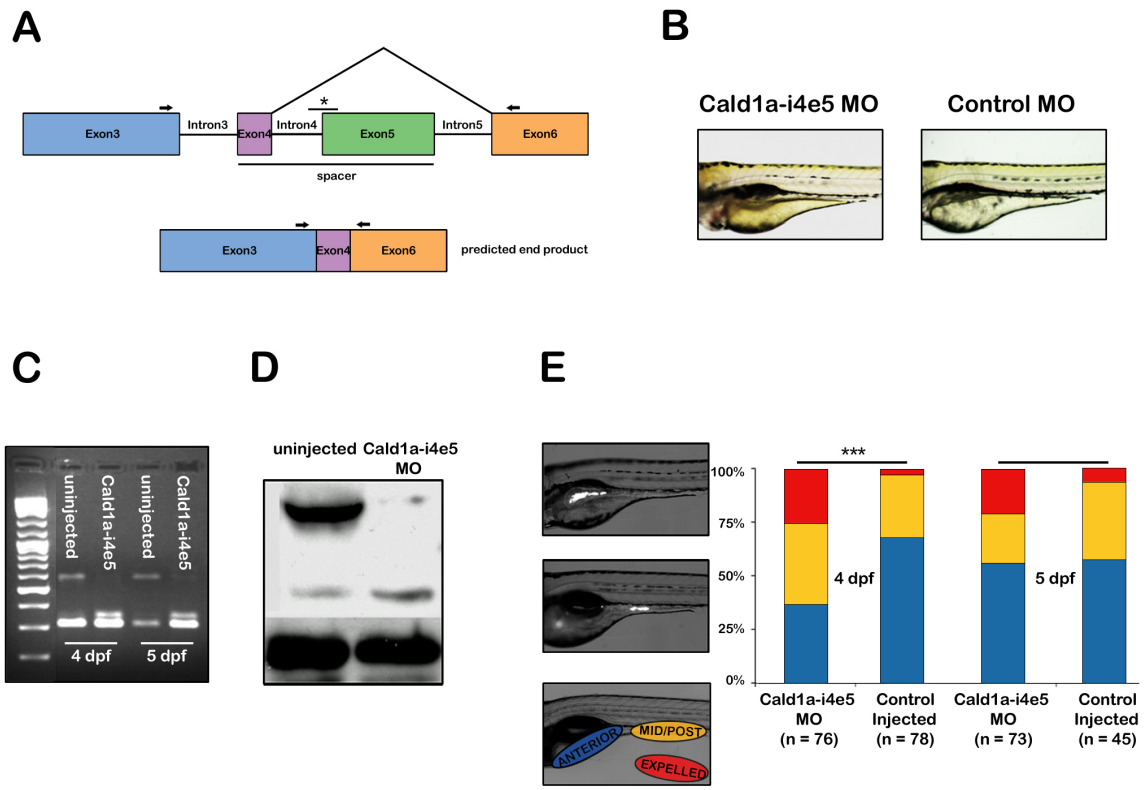

Figure 2.8: h-CaD Deficiency Enhances Intestinal Peristalsis in Zebrafish Larvae. (A) Schematic depicting isoform specific targeting of the high molecular weight *cald1a* transcript by a splice blocking morpholino (Cald1a-i4e5 MO). The exon 5 splice acceptor is targeted (*). (B) Normal morphology of 4 dpf larvae injected with Cald1a-i4e5 MO and a control morpholino. (C) RT-PCR of intestinal cDNA from Cald1a-i4e5 MO larvae using exon 3 and 6 primers (arrows in panel 3A) shows reduced expression of the high molecular weight *cald1a* transcript. (D) Western blot using intestinal protein from Cald1a-i4e5 MO larvae shows reduced levels of h-CaD with slightly increased l-CaD levels. Increased l-CaD expression likely reflects an additional protein translated from a modified transcript only 12 amino acids larger than l-CaD. (E) Images of live 5 dpf larvae that ingested fluorescent microspheres located in anterior and mid – posterior intestine, respectively. Color scheme in bar graph depicts bead location indicated in lateral image of larva (lower panel). Cald1a-i4e5 MO larvae show increased propulsive peristalsis at 4dpf (chi-square test, *** - p<.001). 5dpf p-value = .08, likely due to transient effect of morpholino knockdown.

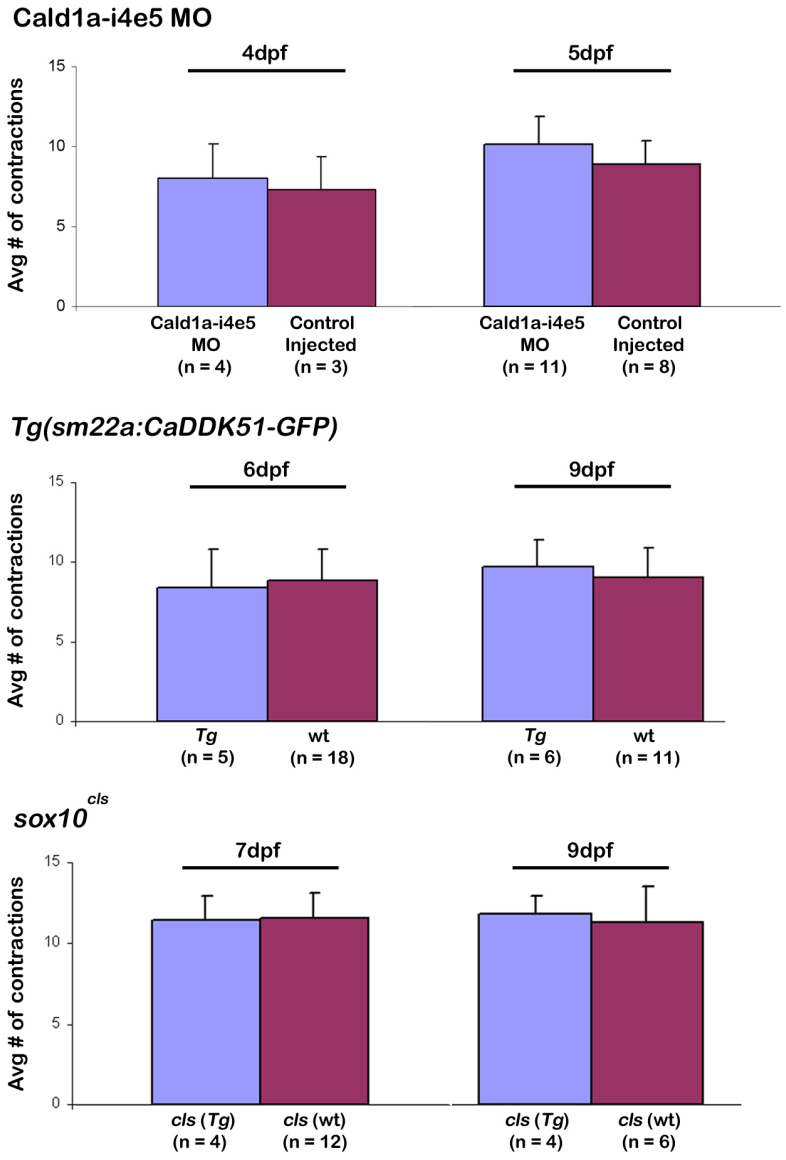

Figure 2.9: **Contractile Rate Remains Unchanged in Larvae After h-CaD Disruption.** Cald1a-i4e5 MO and *Tg(sm22a:CaDDK51-GFP)* larvae in wild type and *colourless* backgrounds. Contractions were counted using live video imaging, t = 2.5 min. Number of larvae assayed and age (dpf) is indicated for each group. Error bars indicate standard deviation. *Tg* - *Tg(sm22a:CaDDK51-GFP)*; wt – wild type.

2.2.6: Interference with h-CaD Binding to Smooth Muscle Myosin and Actin Enhances Intestinal Peristalsis

h-CaD tethers myosin and actin filaments through interactions with its N- and C-terminal domains, respectively (Ikebe and Reardon 1990, Wang et al. 1997). The h-CaD - smooth muscle myosin interaction can be disrupted *in vitro* by expression of a peptide fragment from the myosin-binding domain common to l-CaD and h-CaD (Lee et al. 2000). By inhibiting endogenous h-CaD binding to myosin, actin-myosin interactions are enhanced, thereby increasing basal contractile tone (refer to Figure 2.1). A comparable effect has been reported with a peptide derived from the CaD actin binding domain (Zhan et al. 1991, Katsuyama et al. 1992).

We generated a transgenic line, *Tg(sm22a:CADDK51-GFP)*, with stable smooth muscle expression of a zebrafish ortholog of the mammalian myosin binding peptide (CADDK51). By generating a transgenic line, it enabled us to assay h-CaD function in older zebrafish larvae that have a developed enteric neuromuscular system with robust signaling via p-Mlc. This was not possible in larvae injected with Cald1a-i5e5 MO as its inhibitory effect on translation is transient. In addition to the cDNA encoding the peptide, the expression vector used to generate the transgenic line encoded GFP downstream of a viral 2A recognition motif (Provost et al. 2007). This allowed us to identify fluorescent smooth muscle cells expressing the CADDK51 peptide following its cleavage from GFP. F_0 larvae that had mosaic smooth muscle expression of CADDK51 under control of the zebrafish *sm22a* promoter and F_1 germline transgenic progeny with ubiquitous intestinal smooth muscle GFP expression were both viable (Figure 2.10A). Variable transgene

expression was detected in F_1 larvae, most likely resulting from position effects due to the independent insertion sites of the transgene into the F_0 germline. F_1 transgenic larvae were used to further investigate the in vivo function of h-CaD in intestinal smooth muscle during later developmental stages.

The effect of CADDK51 on h-CaD - myosin filament interaction was examined by measuring levels of h-CaD bound to smooth muscle myosin protein (Myh11) in the transgenic larvae (Figure 2.10B). Because h-CaD remains bound to Acta2 in the actomyosin complex, transgenic larvae were injected with a morpholino targeting smooth muscle actin protein (Acta2) for this immunoprecipitation experiment. This allowed us to determine the effect of CADDK51 on h-CaD - myosin interaction independent of Acta2 interaction. Indeed, Western blot analysis revealed that significantly less h-CaD bound to Myh11 in Acta2 deficient larvae compared with control transgenic larvae. This observation supports binding of CADDK51 to Myh11 and subsequent displacement of endogenous h-CaD.

To determine the effect of CADDK51 peptide on smooth muscle contraction *in vivo* we assayed intestinal peristalsis in the transgenic larvae. Using the intestinal fluorosphere assay (4 hour feeding; assay 4 hours later), we found a significant increase in the propulsive peristalsis of 6 dpf transgenic larvae compared to non-transgenic siblings. This increased peristalsis was determined by transport of fluorospheres to the mid-posterior intestine and their expulsion (Figure 2.10C). When larvae were sorted prior to bead feeding based upon the intensity of GFP expression, we were able to show that increased propulsion was dose dependent as GFP expression levels, which are a

surrogate for the level of CADDK51, correlated with changes in intestinal propulsion (Figure 2.10D). Importantly, increased intestinal propulsion in transgenic larvae was not related to altered contractile rate (Figure 2.9, middle). To confirm this affect we also disrupted actin binding and generated a second transgenic line, *Tg(sm22a:CaDMG101-GFP*), with smooth muscle expression of an inhibitory peptide derived from the h-CaD actin binding domain (Zhan et al. 1991). The CaDMG101-GFP peptide also had a pronounced enhancing effect on intestinal motility similar to the CADDK51 peptide (Figure 2.10C).

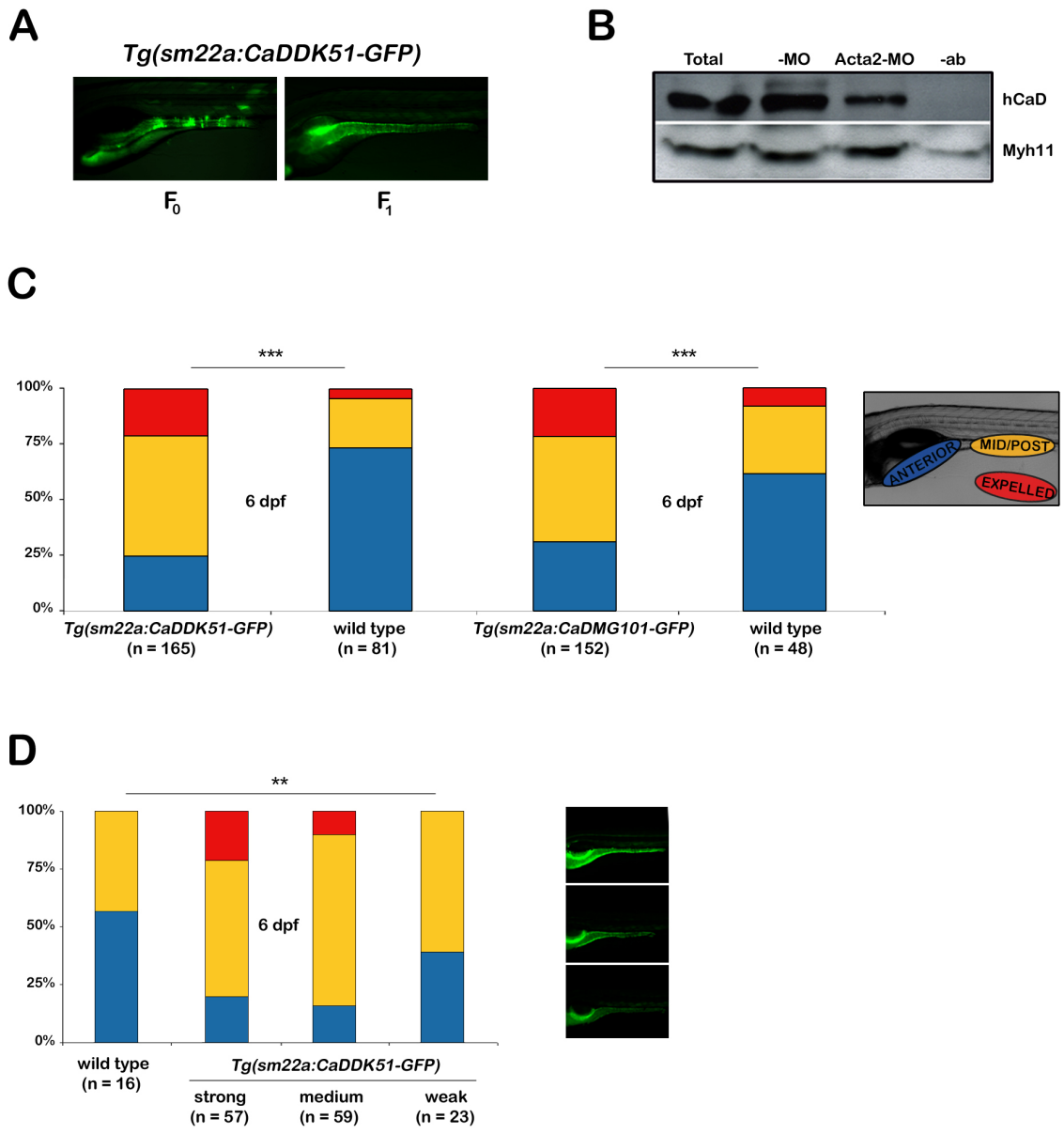

Figure 2.10: Expression of a Peptide Blocking h-CaD - Myh11 Interaction Increases Intestinal Propulsive Peristalsis. (A) Lateral images of live 5 dpf F_0 and F_1 *Tg(sm22a: CaDDK51-GFP)* larvae showing mosaic and widespread smooth muscle GFP expression, respectively. (B) IP-Western blot confirms that CaDDK51 myosin binding domain peptide blocks interaction of h-CaD with Myh11. Total intestinal protein was IP'ed with Myh11 antibody and blotted as indicated. (C) Bar graph shows increased propulsive peristalsis in unsorted *Tg(sm22a: CaDDK51 -GFP)* larvae and *Tg(sm22a: CaDMG101 -*

GFP) larvae, in which peptides block h-CaD interaction with myosin and actin, respectively (chi-square test, *** - p<.001). (D) Enhanced peristalsis in *Tg(sm22a: CaDDK51 -GFP)* larvae correlates with the level of transgene expression (determined by GFP fluorescence). Images show larvae with strong, medium and weak GFP expression (Fisher's exact test, ** - p<.05). -MO – control larvae; Acta2-MO – larvae injected with smooth muscle actin morpholino; -ab - control IP without antibody; Myh11 - smooth muscle myosin.

2.2.7: h-CaD Modulates Endogenous Smooth Muscle Contraction Independent of phospho-Mlc

To address the role of thin filament regulation of intestinal peristalsis independent of phospho-Mlc, we utilized a zebrafish mutant, *sox10* ^{colourless} (*cls*), that lacks enteric nerves (Kelsh and Eisen 2000, Dutton et al. 2001). In previous work, we showed that *cls* mutants have nearly undetectable levels of intestinal phospho-Mlc and phospho-h-CaD, but normal total h-CaD levels. Surprisingly, though *cls* larvae had little if any intestinal phospho-Mlc, they had a significant amount of residual peristaltic activity (Davuluri et al. 2010). This suggested that peristalsis was driven by smooth muscle contraction arising from intrinsic actomyosin interactions. Also, low phospho-h-CaD levels in *cls* suggested that baseline peristalsis was inhibited and may be enhanced by h-CaD disruption. To determine if the lack of phospho-h-CaD inhibited peristalsis in the absence of neuronal input, we repeated the Cald1a-i4e5 MO experiments in *cls* mutant larvae (Figure 2.11A). As in the Cald1a-i4e5 MO wild type larvae, intestinal motility in *cls* was assayed at 5 dpf

because of the transient effects of the morpholino knockdown. Because of reduced feeding by the mutants, they were exposed to the fluorospheres for approximately 14 hours and assayed 6 hours later. Indeed, we observed enhanced propulsive peristalsis in h-CaD deficient *cls* larvae (Figure 2.11A). While fewer of the Cald1a-i4e5 MO *cls* larvae expelled the beads (2%, compared to 21% of wild type larvae), many more had transported the beads to the mid-posterior intestine compared with control *cls* larvae (68% vs. 15%, respectively).

Next, we assayed peristalsis in older (7 and 9 dpf) *cls* larvae that express the myosin binding peptide in intestinal smooth muscle. Because these larvae were older than the morpholino injected larvae, an 8 hour feeding was sufficient. Peristalsis was assayed 20 hours after feeding because the larvae had ingested a larger amount of beads. Fluorosphere analysis of these larvae showed that both transport of the fluorescent beads to the mid-posterior intestine and their expulsion was significantly greater in the transgenic *cls* larvae (Figure 2.11B). The increased propulsion in transgenic *cls* larvae was not related to altered contractile rate (Figure 2.9, bottom). The peristaltic defect in *cls* was not fully rescued by h-CaD disruption, as wild type control larvae at both stages completely cleared all ingested beads (data not shown). This was expected given that the enteric nervous system is the primary stimulus for smooth muscle contraction. However, these findings do show that h-CaD mediated inhibition of intrinsic actomyosin interactions contributes to reduced intestinal motility in the non-innervated intestine of zebrafish larvae.

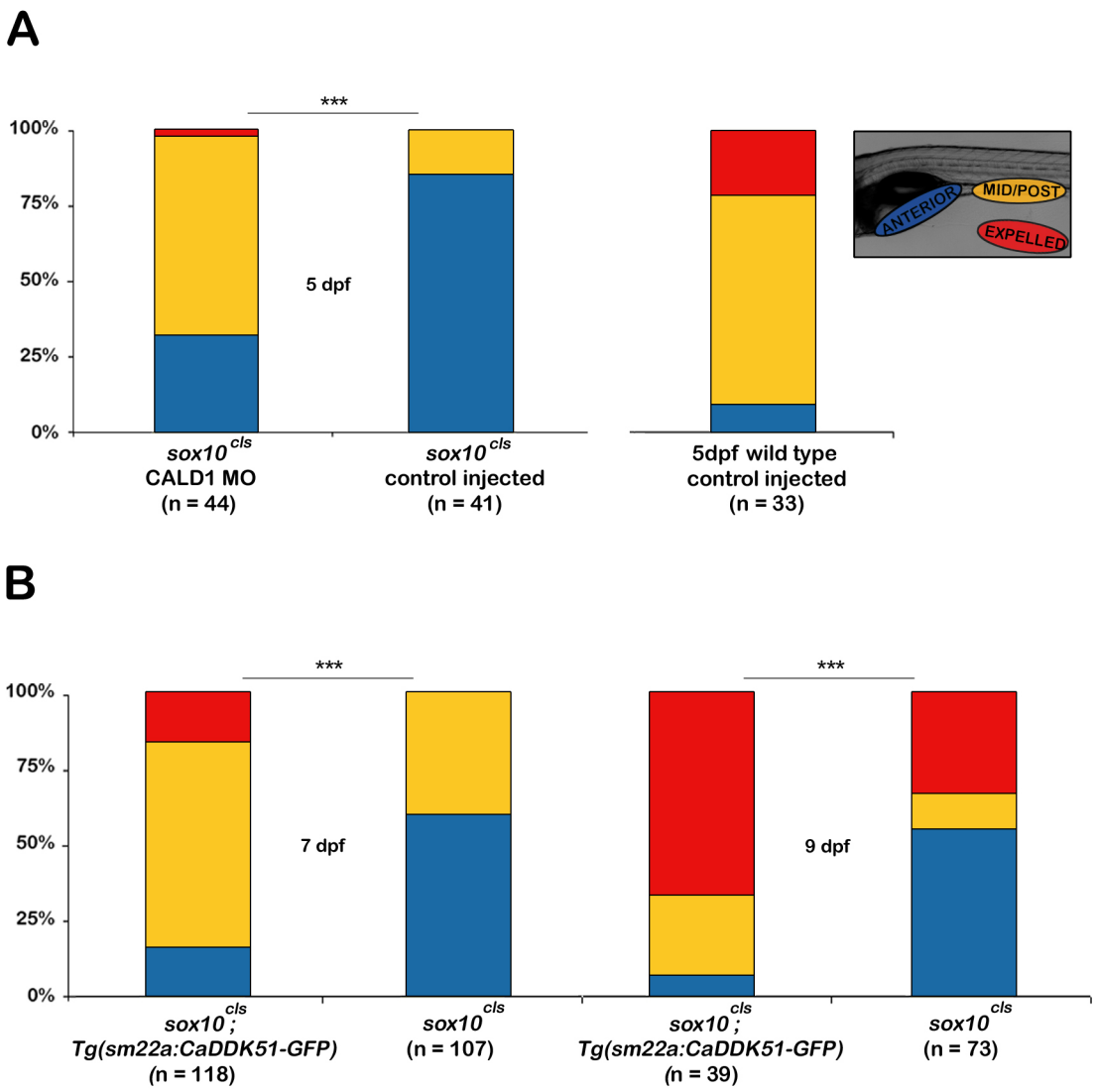

Figure 2.11: Intestinal Peristalsis is Increased in h-CaD Deficient *colourless (cls)* Larvae. (A) Bar graph shows partial rescue of intestinal peristalsis in h-CaD deficient 5 dpf *cls* larvae. (B) *Tg(sm22a: CaDDK51 -GFP) cls* larvae show partial rescue of propulsive peristalsis at 7 dpf and 9 dpf (chi-square test, ***p<.001).

2.3: Discussion

Although regulation of smooth muscle contraction principally occurs at the myosin (thick) filament through phosphorylation of regulatory Mlc, a potentially important role for regulation of contraction at the actin (thin) filament has long been recognized. However, the physiological importance of this mode of regulation has never been directly assayed *in vivo*. Here we show that the smooth muscle actin binding protein h-CaD regulates intestinal peristalsis in the wild type and non-innervated intestine of zebrafish larvae. We also provide evidence for h-Cad's critical role in the epithelial phenotype in *meltdown*; where we have observed h-CaD modulates contractile tone in heterozygous *mlt* leading to epithelial invasion.

2.3.1: Zebrafish h-CaD Paralogs

The h-CaD isoform we identified arises from alternative splicing of a pre-mRNA transcribed from *cald1a*, one of two *cald1* paralogs we show are present in the zebrafish genome. The *cald1a* locus also encodes an l-CaD isoform expressed in intestinal smooth muscle. Predicted translation of the h-CaD protein showed high sequence homology of the actin and myosin binding domains compared with other vertebrate h-CaD proteins. By contrast, there is less sequence homology between the various spacer domains, possibly because of its proposed structural role as a charged single α-helix (Mabuchi and Wang 1991, Suveges et al. 2009). The *cald1b* locus encodes an l-CaD isoform expressed at low levels in intestinal smooth muscle that was previously reported to play a role in vascular development (Zheng et al. 2009). Expression of a *cald1b* h-CaD ortholog was

not detected. Together with functional analyses described below, these findings showed that *cald1a* encodes the zebrafish ortholog of the h-CaD isoform expressed in mammalian intestinal smooth muscle. These findings also argue that *cald1a* and *cald1b* have non-overlapping functions in smooth muscle, similar to other zebrafish gene paralogs that arose from genome duplication events.

2.3.2: Caldesmon's Role in Intestinal Peristalsis and Vascular Tone

We examined the role of h-CaD in intestinal peristalsis and smooth muscle contraction using a previously described simple in vivo assay. Propulsive peristalsis was increased in h-CaD deficient wild type larvae generated via isoform specific antisense targeting. Similarly, peristalsis was increased in larvae that express peptide transgenes designed to interfere with h-CaD binding to either the myosin or actin filament. Because the rate of smooth muscle contraction was not increased in transgenic larvae, our findings argue that h-CaD normally functions to inhibit the force of smooth muscle contraction, as previously reported (Smolock et al. 2009). Whether h-CaD affects contraction velocity or the distance of contraction in the intestine could not be determined using our methods. Although these results are consistent with the predicted role of h-CaD in modulating smooth muscle contractile force from phosphorylated cross-bridges, to our knowledge they are the first evidence for this phenomenon *in vivo*. h-CaD deficient mice have been generated through gene targeting, however the effect of h-CaD disruption on intestinal motility has not been reported (Guo and Wang 2005). Given the similarities of intestinal anatomy and physiology in zebrafish and other vertebrates, we would predict a

comparable effect of h-CaD deficiency on mammalian intestinal motility (Rich et al. 2007, Shepherd and Eisen 2011).

h-CaD function has been studied extensively in vascular (tonic) smooth muscle. Besides functioning as a brake on contraction arising from phosphorylated myosin heads, h-CaD is also thought to sustain contractile force generated by non- or de-phosphorylated myosin heads, thus accounting for force generation at low levels of phospho-Mlc. The mechanism of this aspect of h-CaD function is not known but it has been postulated to occur through either physical stabilization of the actomyosin complex, or the cooperative activation of non-phosphorylated and phosphorylated myosin heads (Albrecht et al. 1997). This presumably occurs when h-CaD itself has been inhibited, such as occurs with phosphorylation.

2.3.3: Role of h-CaD Independent of Light Chain Phosphorylation

Whether h-CaD functions comparably in the phasic smooth muscle of the intestine and colon is not known. Analyses of *cls* larvae allowed this question to be addressed in vivo, as *cls* have nearly undetectable levels of intestinal phospho-Mlc (Davuluri et al. 2010). Surprisingly, *cls* larvae retain a significant degree of peristaltic function, presumably from ENS-independent smooth muscle contraction, which has been observed in the embryonic mouse and zebrafish intestine (Holmberg et al. 2007, Roberts et al. 2007, Roberts et al. 2010). In addition to very low phospho-Mlc levels, *cls* larvae also have undetectable levels of phosphorylated h-CaD. A low ratio of phospho-h-CaD to total h-CaD in *cls* suggests that the basal level of smooth muscle contraction is

inhibited. Our observations indicate that this is indeed the case as both Cald1a-i4e5 MO injection and transgenic expression of the CADDK51 inhibitory peptide enhanced propulsive peristalsis in *cls*. Although it is difficult to make mechanistic inferences regarding h-CaD function from this study, our findings are consistent with the idea that h-CaD restricts binding of non-phosphorylated myosin heads to actin (Figure 1C), as h-CaD knockdown enhances peristalsis in *cls* mutants that have low levels of p-Mlc. The knockdown experiments in wild type larvae (high levels of p-Mlc) argue that h-CaD restricts binding of phosphorylated myosin heads to their preferred site on the actin filament (Figure 1A) and that this constraint is relieved in the absence of h-CaD.

2.3.4: h-CaD and Human Intestinal Disorders

h-CaD is widely expressed in human smooth muscle and has also been used extensively as a tumor marker (Miettinen et al. 1999, McCluggage 2004). Its best characterized physiological role is during pregnancy when total h-CaD levels increase (Word et al. 1993), thus inhibiting premature stretch induced uterine contraction (Li et al. 2009). At the time of delivery, phospho-h-CaD levels increase dramatically and this is thought to enhance the force of uterine contractions. A role for premature phosphorylation of h-CaD in a rodent model of pre-term labor has also been reported (Li et al. 2004). In addition, recent findings have also implicated CaD (via Sox4 interaction) in skeletal muscle myoblast differentiation (Jang et al. 2013). In this study, siRNA was used to reduce CaD expression in myoblasts resulting in decreased cell spreading and differentiation. Their findings suggested a unique role for CaD where, through its

interaction with Sox4, it becomes involved in actomyosin organization in myofibrils during skeletal muscle development.

Relatively little is known about the regulation or function of h-CaD in the human intestine. In rabbit colonic smooth muscle, h-CaD serine-789 is phosphorylated upon exposure to the enteric neurotransmitter acetylcholine, which also drives phosphorylation of Mlc (Somara and Bitar 2006). h-CaD phosphorylation by acetylcholine argues that its normal function is to enhance ENS-mediated smooth muscle contraction. This further suggests that in the setting of ENS dysfunction, levels of both phospho-Mlc and phospho-h-CaD are reduced, as occurs in zebrafish *cls* mutants. Surprisingly, *cls* larvae retain peristaltic activity, which is likely a function of smooth muscle physiology and intestinal anatomy at larval stages. ENS disruption in the adult human intestine, as modeled by conditional *Mlck* disruption in mice (He et al. 2008), is predicted to cause irreversible intestinal motility defects. However, with only a modest reduction in ENS function it is conceivable that modulation of h-CaD could be used to enhance motility in humans. Targeting h-CaD could therefore be a therapeutic strategy to treat hypomotility caused by enteric neuropathies and disorders associated with reduced phospho-Mlc. These disorders are likely to occur with aging and also related to Cajal pacemaker cells defects (Somara et al. 2007, Farrugia 2008).

Chapter 3: Altered Myosin Motor Activity and h-CaD Dysfunction Propagate Contractile Force and Cause Epithelial Invasion in *mlt*

3.1: Introduction

An outstanding question remains during the process of cell invasion as to what signals are responsible for initiating invasion and how such a signal is transmitted from the surrounding stroma to the cell to trigger invadapodia formation and cell motility. From our laboratories previous work on the *meltdown (mlt)* mutant we have mounting evidence that increased contractile force in the intestinal smooth muscle could initiate invasion of the underlying epithelial cells (Wallace et al. 2005, Seiler et al. 2012). As the process of cell invasion had yet to be studied *in vivo* using a genetic model, we aimed to utilize *mlt* as a means to better understand how physical signaling can induce invasion. To elucidate the molecular signaling occurring in *mlt* mutants between the smooth muscle and the underlying epithelial layer our laboratory previously performed microarray transcriptional profiling. We found a significant increase in the expression of reactive oxygen species (ROS)-responsive genes and in particular glutathione peroxidase (gpx), a protective enzyme of oxidative damage was upregulated in the intestinal epithelium.

ROS signaling has been studied extensively for its role in cancer cell invasion where it can activate both metalloproteinases and epithelial-to-mesenchymal transition (EMT) genes. To test the importance of oxidative stress in the progression of the *mlt* mutant, heterozygous larvae were treated with menadione, an intracellular ROS generator, and were found to develop an epithelial phenotype comparable to *mlt* mutant larvae

(Seiler et al. 2012). Interestingly, the treated heterozygotes did not develop cysts or epithelial expansion; features which are indicative of the late *mlt* phenotype. In addition, ROS treated heterozygotes had increased expression of phosphorylated h-CaD, comparable to that seen in *mlt* mutants. Taken together, these observations point to a crosstalk between the intestinal epithelium (where ROS is produced) and the smooth muscle, resulting in the propagation of contraction and ultimately epithelial invasion (Figure 3.1). To test this, we investigated the possibility of a physical signal occurring at the level of the intestinal tissue by measuring tissue stiffness directly. To shed light on the interplay between smooth muscle contraction and epithelial invasion, we performed cell dissociation experiments to establish if crosstalk between the muscle layer and epithelium is indeed necessary in the progression of the *mlt* phenotype. The mechanical signal in *mlt* was found to be independent of overall tissue stiffness, an observation that we ascribe to local alterations between the stroma and the basal surface of epithelia. We also found that it is necessary for each cell type to remain adjacent to one another, as in the organized intestine, as dissociation of the tissue is sufficient to diminish the signaling between them.

We have also investigated the importance of myosin motor activity on smooth muscle contraction and the propagation of the *mlt* phenotype. The *mlt* myosin mutation (W512R) occurs at a conserved region of the motor domain called the rigid relay loop, and the missense mutation results in constitutive ATPase activity of myosin (Wallace et al. 2005). A number of unique smooth muscle myosin mutations have been described in vascular disease, suggesting that altering myosin's motor function can have widespread

outcomes *in vivo*. We therefore performed a genetic modifier screen in zebrafish to identify additional myosin mutations that can contribute the invasive phenotype in *mlt.* Two dominant enhancers of *mlt* were identified harboring unique mutations in vastly different myosin domains, the motor region and C-terminal helix. These mutant proteins work in concert with the *mlt* mutation to initiate epithelial invasion, presumably by increasing contractile tone. We therefore provide the first *in vivo* evidence for these three distinct myosin mutations sensitizing the intestinal epithelium for invasion, and provide an initial analysis of additional oncogenic signals and ROS responsiveness in each genetic background.

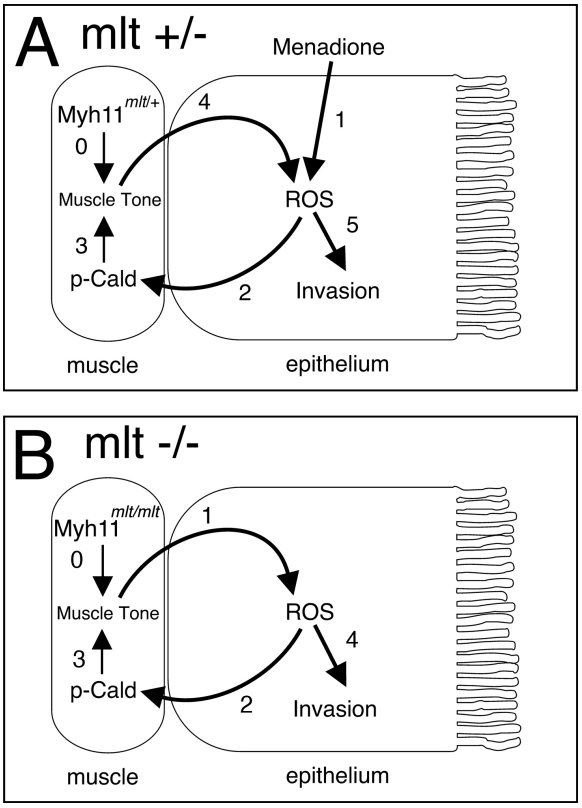

Figure 3.1 Amplification Feedback Signaling Loop Controls Smooth Muscle Contraction and Invasion in *mlt* (A) In *mlt* heterozygotes the expression of mutant Myh11 protein does not generate sufficient smooth muscle tension to induce epithelial invasion or stratification (0). Menadione treatment induces ROS production in the epithelium (1). Epithelial ROS signaling leads to premature phosphorylation of Caldesmon in heterozygous smooth muscle cells (2). The resulting increase in smooth muscle tone (3) leads to an amplified ROS response in the epithelium (4), establishing a feed forward loop causing additional h-CaD phosphorylation and increased smooth muscle tension. Together these stimuli induce invasive remodeling of the epithelium (5). (B) Endogenous smooth muscle tone in *mlt* homozygous larvae (0) induces epithelial ROS (1) and h-CaD phosphorylation via epithelial signaling (2, 3). Ultimately, this culminates in epithelial invasion (4), as in menadione treated *mlt* heterozygotes. Figure provided by Christoph Seiler and published in Seiler et al. 2012.

3.2: Results

3.2.1: Smooth Muscle Tension Activates a Feed Forward Signaling Loop That Amplifies Epithelial Redox Signaling

In homozygous *mlt,* the activation of redox signaling in the intestinal epithelium along with the premature phosphorylation of h-CaD during the onset of the phenotype suggest that there could be crosstalk between the smooth muscle and epithelial tissue. We have previously tested the nature of this crosstalk by assaying for phosphorylated h-CaD in heterozygous *mlt* larvae that were treated with menadione, an ROS generating compound (Seiler et al. 2012). These experiments revealed that redox signaling was indeed altering contractile force through h-CaD, but it was not clear whether it was signaling from the epithelium or if the menadione treatment had a direct effect upon the smooth muscle. Initial *in situ* hybridization experiments suggested that redox signaling was restricted to the epithelial layer as ROS-responsive genes, such as *gpx,* were expressed exclusively in epithelial cells after menadione treatment. These observations led us to hypothesize that h-CaD phosphorylation in menadione-treated heterozygotes was triggered by an epithelial signal rather than by a direct effect on the smooth muscle.

To test this hypothesis, we asked whether menadione could induce h-CaD phosphorylation in dissociated smooth muscle cells from heterozygous *mlt*, as crosstalk with the epithelium would presumably be lost after tissue dissociation. Intestines were dissected from 3 dpf heterozygous *mlt* and wild type larvae then promptly treated with trypsin to dissociate the tissue into a suspension of epithelial and smooth muscle cells. The dissociated cells were then treated with menadione and immediately prepared for

Western blot analysis. A control group consisting of dissected intestines that were treated with menadione was used to ensure that redox signaling affected *ex vivo* tissue in the same manner as we observed in live larvae. Western blots revealed that indeed h-CaD phosphorylation occurred in the non-dissociated heterozygous intestines after menadione treatment, whereas untreated intestines lacked any phosphorylation (Figure 3.2A). In contrast, phosphorylated h-CaD was not detected in dissociated smooth muscle cells from heterozygous *mlt* that were treated with menadione (Figure 3.2B, n = 3 independent experiments). Importantly, phosphorylated h-CaD was present in dissociated homozygous *mlt* smooth muscle cells showing that this form of the protein was not degraded during the incubation period of the assay (Figure 3.2B, lane 3). These observations point to crosstalk from the smooth muscle to the epithelium as being an essential component of the phenotype and thus we next wanted to better understand if physical signals were being transmitted from the smooth muscle.

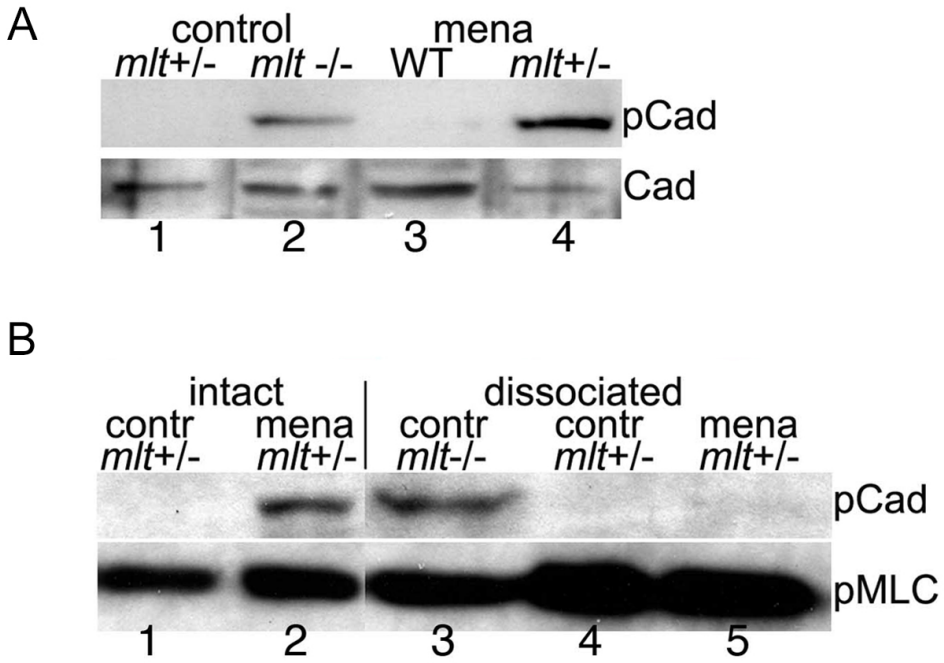

Figure 3.2: Crosstalk Between Smooth Muscle and Epithelium. (A) Western blot showing premature h-CaD phosphorylation (pCad) in dissected intestines from menadione treated heterozygotes but not homozygous WT larvae (lane 4 versus lane 3; ratio phospho-h-CaD WT:*mlt* = 0.02/1, relative to total h-CaD; CaD; in six experiments the ratio averaged 0.016/1; $p<.001$). h-CaD is prematurely phosphorylated in intestines dissected from 74 hpf *mlt* homozygotes versus *mlt* heterozygotes (lane 1 versus lane 2). (B) Western blot showing h-CaD phosphorylation (pCad) in the menadione treated heterozygous intestines prior to dissociation (lane 2) but not after dissociation into free cell populations (lane 5). Phospho-h-CaD persists in dissociated cells from homozygous intestines (lane 3), but is not detected in control intestines dissected from *mlt* heterozygotes, before (lane 1) or after (lane 4) dissociation into free cell populations. No phospho-h-CaD was detected in any dissociated samples in three independent experiments. Loading control, phospho-Myosin light chain (pMlc).

3.2.2: Distinct Mechanosensory Mechanisms Are Activated in Invasive Cells in Response to Smooth Muscle Tension

One conceivable outcome of increased contractile force from the smooth muscle is the stiffening of the extracellular matrix surrounding the intestinal epithelial cells. Matrix stiffening promotes cell invasion in breast cancer models, in part through activation of focal adhesion kinase (FAK) (Paszek et al. 2005, Levental et al. 2009) and we therefore hypothesized that we were observing a similar biomechanical phenomenon in *mlt* mutants. To determine whether a comparable mechanical signaling mechanism was activated in *mlt* we initially dissociated intestinal tissue and cultured the smooth muscle cells. Using atomic force microscopy (AFM) we aimed to measure the stiffness of individual cells, however AFM measurements yielded variable results that were difficult to interpret (data not shown). We therefore proceeded with whole tissue elasticity measurements of mutant larvae using a force displacement assay (Levental et al. 2010). For this assay, we utilized freshly dissected intestines and plated tissues on Cell-Tak™, a biological adhesive, to prevent shifting during the measurements. Before invasive remodeling is detected in *mlt* (70 hpf), tissue compliance was nearly identical in mutant larvae and their wild type siblings throughout the range of tissue indentations tested (Figure 3.3A, $n = 6$ *mlt* and 21 wild type larvae). When remodeling is first detected at 74 hpf, this compliance was slightly increased at the surface of the *mlt* intestine but similar to wild type controls at greater tissue depths, the measured difference is potentially due to the basement membrane degradation that occurs at this stage (Figure 3.3B; $n = 7$ *mlt* and 12 wild type larvae examined). Although small changes were

observed at 74 hpf, force values indicative of significant intestinal stiffening, as would be predicted from models of breast cancer invasion, were not detected in dissected *mlt* intestines.

To assay for changes in extracellular matrix stiffness at the molecular level, previous work in our laboratory examined the phosphorylation of a known mechanotransducer, FAK, in *mlt* using immunohistochemistry (Snow and Henry 2009) and Western blot analyses. However, neither method detected elevated p-FAK in *mlt* (Seiler et al. 2012). Western blots also showed that levels of Collagen-1 and Fibronectin, additional markers of matrix stiffening, were not significantly elevated in the *mlt* intestine. All together, these data argue that mechanical force triggers epithelial invasion in *mlt* independently of changes in matrix composition or increases in tissue rigidity. One possible interpretation is that focal changes in force within the intestinal lumen occur without a corresponding change in total tissue stiffness. Altered blood pressure has been observed in smooth muscle disorders within the vasculature, but without available methods to detect altered force within the intestinal lumen of the larval zebrafish we cannot know definitively.

Together with the h-CaD morpholino data from chapter 2, these findings support a model in which h-CaD phosphorylation in *mlt* smooth muscle cells arises from a ROS-activated epithelial signal (Figure 3.1). Phosphorylation of h-CaD then enhances smooth muscle tone, thereby generating additional oxidative stress within the epithelium. This establishes a feed-forward signaling loop with the adjacent smooth muscle that further enhances contractile tone, amplifies epithelial ROS production, and culminates in

epithelial invasion. In heterozygous *mlt*, activating redox signaling allows the epithelium to increase contractile tone in the smooth muscle through the phosphorylation of h-CaD that leads to further ROS production and culminates in cell invasion. Removing h-CaD inhibition directly by morpholino knockdown also increases contractile tone and drives the epithelial phenotype, further emphasizing the importance of this protein as a modulator of smooth muscle contraction. These observations raised two important question that we aimed to address: 1) Since the epithelia in *mlt* mutants are responding to altered contractile tone, how can this tone be altered to initiate invasion? 2) How is the specific myosin mutation in *mlt* (W512R) contributing to increased contractile tone and can mutations in different domains of the myosin protein produce a similar affect?

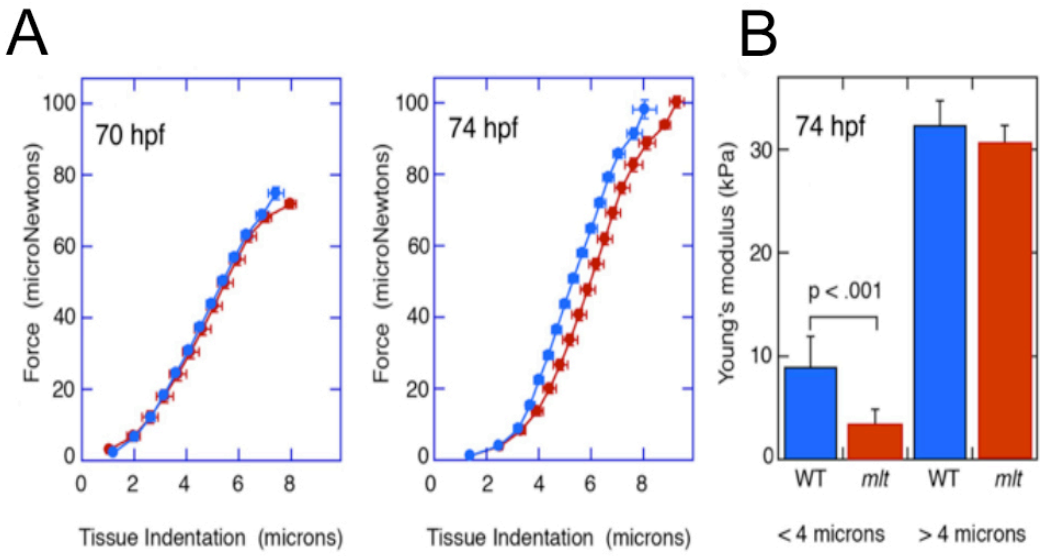

Figure 3.3: Mechanical Signaling in *mlt* and Wild Type Intestines. (A) Force displacement measurements show identical compliance of intestines dissected from *mlt* and WT larvae before the phenotype develops at 70 hpf, and a modest decrease in compliance at the outer surface of the intestine (<4 micron indentation) when invasion is present at 74 hpf. (B) Compliance is indicated by Young's modulus, which is proportional to the slope of the Force versus Tissue indentation curve.

3.2.3: Dominant Modifier Screen Identified Two Enhancer Mutants of meltdown

We next sought to gain additional insight into the potential mechanosensory cues and smooth muscle contractile dynamics that are responsible for the increased force in the *mlt* intestine. From our h-CaD and ROS observations, we hypothesized that epithelial cells in *mlt* initiate redox signaling in response to changes in the overall force output by the smooth muscle tissue. If this hypothesis were true we should in principal be able to find additional mutations within the smooth muscle that alter force output or in epithelial

components that are sensitive to ROS and mechanical signaling, and to test this we performed a forward genetic screen for modifier mutants.

We chose to perform a modifier screen due to a number of advantages that allowed us to better elucidate the critical signaling occurring in *mlt.* Traditional forward genetic screens in zebrafish have identified numerous mutants that affect conserved developmental pathways (Driever et al. 1996) as well as mutants with human disease phenotypes, however many of the underlying mechanisms are not well understood. Modifier screens are a useful way to address this and have been used extensively in other organisms where they have aided in the understanding of major developmental and regulatory pathways (Jorgensen and Mango 2002, St Johnston 2002). In addition, traditional genetic screens, from which *mlt* was initially characterized, relies on incrossing of the second generation (F_2) to produce homozygotes where recessive mutations are scored by phenotype, but in a modifier setup you can screen one generation earlier. As a powerful approach to elucidate the mechanisms of know recessive mutants, modifier screens identify second-site mutations that specifically enhance (worsen) or suppress (ameliorate) the phenotype of a given mutant (Bai et al. 2011). Traditionally, the screen is performed in a sensitized genetic background in which the function of a particular pathway is only partially disrupted and therefore viability of the mutant animal is not affected. Such a genetic background can be achieved by using a heterozygous mutant with a haploinsufficient phenotype or a homozygous mutant of a weak allele. However, due to embryonic lethality and a lack of heterozygous phenotypes most existing zebrafish mutants are not suitable for modifier screens. Fortunately, from our

laboratory's previous work on the *mlt* mutant we have discovered an inducible heterozygous phenotype that allows us to use this background for modifier genetics.

From our previous work we know that although heterozygous *mlt* survive normally through adulthood, they can develop epithelial invasion as larvae under certain conditions where ROS is abundant or when gut contraction is exogenously increased (Seiler et al. 2012). This sensitized heterozygous background in *mlt* makes it an attractive mutant for a modifier genetic screen. We first generated our founder (F_0) population by treating adult males in the long-fin wild type background (TLF) with the chemical mutagen, ENU. Due to the toxicity of ENU, we had two surviving, fertile male founders out of 50 that were mutagenized from which we derived our screen.

Importantly, we crossed our F_0 population with heterozygous *mlt* adults to generate an F_1 generation consisting of 50% trans-heterozygotes (*mlt*/ENU mutations) and 50% heterozygotes for only the ENU induced mutations (Figure 3.4). To screen for mutants that enhance or suppress epithelial invasion in *mlt,* we performed a modifier screen by initially carrying out a genetic cross in the F_1 generation between the mutagenized founder generation and heterozygous *mlt* adults (Figure 3.4, F_1). The resulting F_2 generation contains trans-heterozygote individuals that carry a single *mlt* allele combined with the allele carrying the new mutation induced by ENU mutagenesis. By randomly crossing together F_2 trans-heterozygotes, screening can be performed on two unique mutations in each cross. This crossing scheme also allows for screening of both enhancers of heterozygotes and suppressors of homozygous *mlt (*Figure 3.4, F_2*)*. Using this method, screening was performed on more than 1000 unique F_1 genomes and

from this two enhancer mutants were identified that induced a phenotype in the heterozygous *mlt* larvae.

3.2.4: Characterization and Sequencing of Dominant Enhancer Mutants

Both modifier mutants caused a generally similar phenotype in the *mlt* heterozygote epithelium whereby invasive epithelial cells were observed in the mid-intestine at 6 dpf. In one mutant we identified, S237Y, the *mlt* trans-heterozygote phenotype was observed in a higher percentage of larvae compared to the second mutant, L1287M. In addition, a subset of S237Y mutants displayed a more severe phenotype in the mid-intestine (Figure 3.5B). Histological evaluation of trans-heterozygote larvae from both enhancer mutant backgrounds revealed the hallmarks of epithelial invasion occurring at 6 dpf, whereby basement membrane degradation coincided with abnormal epithelial cell motility (Figure 3.5C).

To determine the chromosomal location of each mutation, map crosses were carried out by mating each F_1 mutant adult with a polymorphic wild type background (WIK). This crossing scheme typically enables large numbers of mapping markers to be identified due to the presence of a high number of SNPs between the two wild type strains. However, while performing F_2 crosses between adult modifier heterozygotes and *mlt* heterozygotes we observed a very strong linkage, where no instances of recombination were seen in over 400 individuals screened. In other words, we never observed the *mlt* mutation and the modifier mutation in the same individual suggesting tight linkage and a very low recombination frequency.

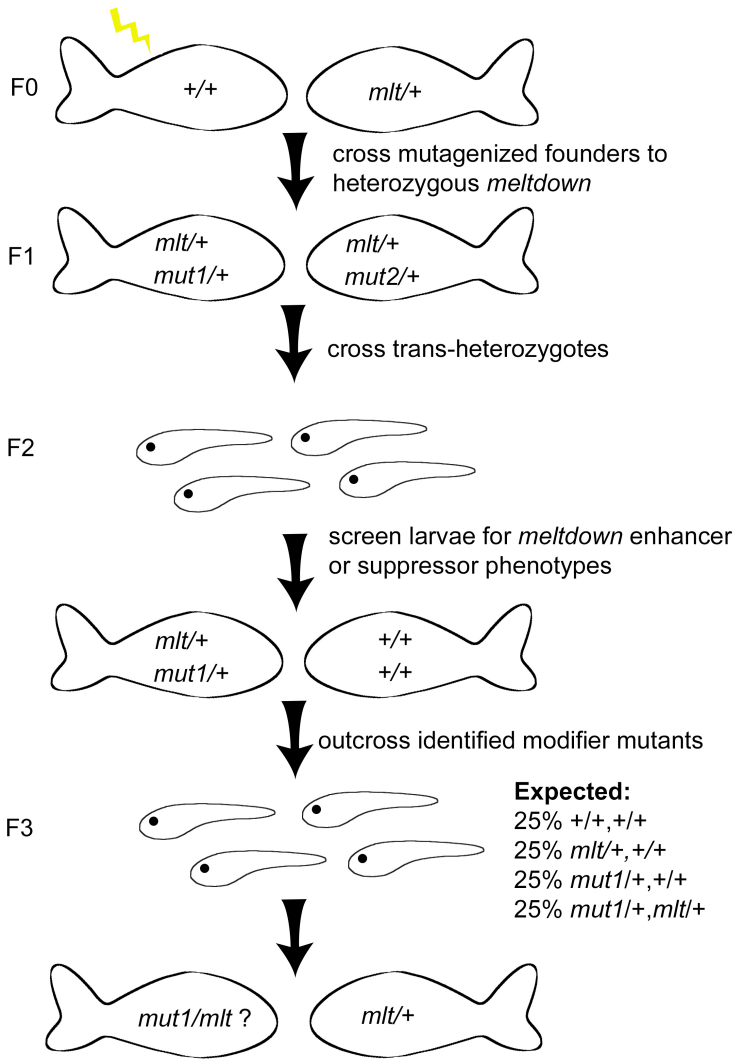

Figure 3.4: Dominant Modifier Screen to Identify Enhancers and Suppressors of *mlt*. The male parent is mutagenized, such that a subset of its sperm contains a mutant allele. The mutagenized male is then mated with a heterozygous *mlt* female. The F_1 progeny of this mating were genotyped for heterozygous *mlt* and mated randomly with additional mutant progeny. Each F_1 contains a unique mutation (i.e. 'mut1', 'mut2', etc.) and incrossing these adults allows for multiple mutations to be screened in a single clutch of F_2 larvae. The low number of modifier mutants identified reflects the specificity of the intestinal phenotype that was screened for. In addition, F_1 larvae with a modifier phenotype may not have survived to adulthood due to the intestinal defects observed.

From this observation it was reasoned that the *mlt* mutation and new mutation (S237Y or L1287M) were either a very small difference apart in their chromosomal location or were indeed new alleles of *myh11*. In combination with both modifier phenotypes being similar in appearance to *mlt* epithelial invasion, we reasoned that there was a high likelihood that these mutations were indeed two additional mutant alleles of *myh11*. To validate the new mutations and because of their tight linkage with *mlt*, the 5922 basepair coding region of zebrafish *myh11a* was sequenced from intestinal cDNA in each modified trans-heterozygote. Sequence data was analyzed manually and instances of double peaks were recorded (one peak corresponding to *mlt*, the other to the new mutation). Each short nucleotide polymorphism (SNP) identified was compared to the translated sequence to determine if it resulted in an amino acid substitution or in-frame STOP codon. From this analysis, we confirmed that both mutants were new *myh11* alleles and that both were missense mutations (Figure 3.5E-H). Interestingly, each mutation occurred in vastly different domains of the Myh11 protein; one at the N-terminal motor domain (S237Y), and the other at the C-terminal coiled-coil tail domain (L1287M)(Figure 3.5G-H). Given that the *mlt* mutation, W512R, occurs in a unique protein domain of MYH11 compared to these two modifier mutants, the new alleles presented us the opportunity to tease apart myosin function *in vivo*.

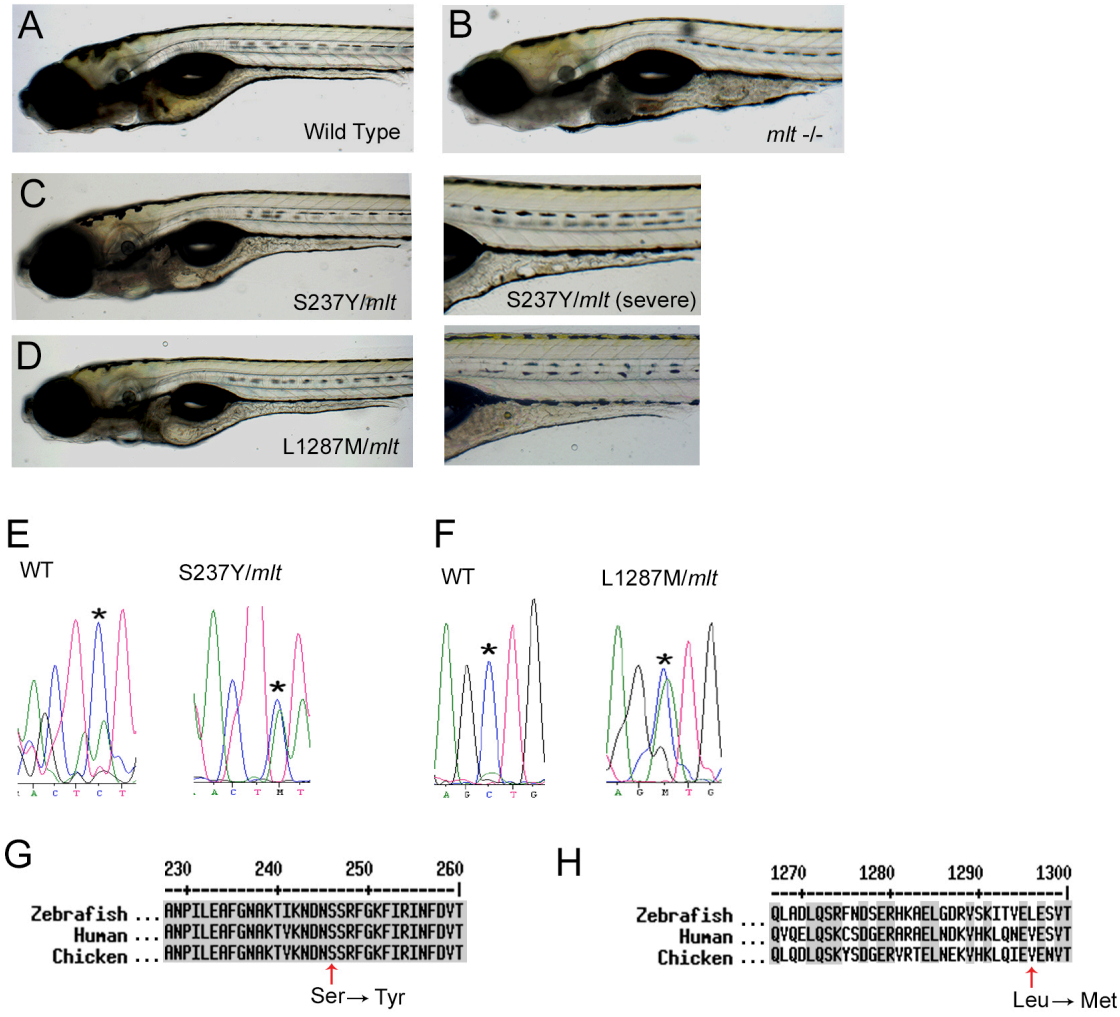

Figure 3.5: Two Dominant Enhancer Mutants Contain Unique Missense Mutations on MYH11. (A) Wild type larvae at 6dpf, arrow depicts mid-intestine connecting anterior and posterior regions (B) *mlt* mutant larvae at 6dpf, arrow depicts cyst-like expansion of mid and posterior intestine (C) S237Y/*mlt* trans-heterozygous larvae at 6dpf, arrow depicts partial phenotype in mid-intestine. Note normal appearance of anterior and posterior intestine at this stage. Severe phenotype was observed in a fraction of S237Y/*mlt* trans-heterozygotes. Arrows indicated sites of cyst-like expansion that was only observed in larvae with severe phenotype. (D) L1287M/*mlt* trans-heterozygotes, arrows indicate partial phenotype in mid-intestine that was similar to S237Y/*mlt*. (E+F)

Sequencing of the *myh11* exome in S237Y/*mlt* larvae identifies distinct mutations. Asterisk indicates the location of each mutation where double peak represents the mutant and *mlt* alleles at a given locus. (G+H) Both mutations result in missense amino acid substitutions in Myh11. Arrow indicates affected amino acid on Myh11 for each mutant.

Since we initially observed the trans-heterozygote phenotypes of the modifier mutants at 6 dpf, where invasion was present in the mid-intestine, we wanted to determine if epithelial cells initiated a response earlier in development. Smooth muscle contraction begins to organize at 3 dpf, and this is when the phenotype in homozygous *mlt* is first observed, therefore we wanted to assay for invasion at this timepoint in the trans-heterozygotes. As no morphological changes were observed in the intestine at this stage, we utilized a transgenic line, *Tg(miR194:Lifeact-GFP)*, in which a GFP-labeled peptide that binds F-actin (Lifeact-GFP) is expressed in the intestine (Seiler et al. 2012). By crossing *Tg(miR194:Lifeact-GFP)* into the modifier mutant background we could visually score for invadopodia in these larvae by cross-section analysis. To do this we immunostained wild type and trans-heterozygous larvae with antibodies against laminin and GFP and found that protrusions localized to sites of extracellular matrix degradation, and that epithelial cells invade the surrounding stroma through sites of degraded basement membrane (Figure 3.6C,D). Whereas in wild type *Tg(miR194:Lifeact-GFP)* the basement membrane remains in tact and no actin-rich protrusion were observed (Figure 3.6A,B).

3.2.5: S237Y, A Myosin Switch I Mutant Affecting Motor Function

Recent work on myosin V has determined that a protein domain termed 'switch II' plays a critical role in stabilizing the conformation of the nucleotide-binding pocket in the presence of actin (Trivedi et al. 2012). The same group also demonstrated, by mutation analysis of the switch II domain, that the region is essential for communication between the active site on myosin and the actin-binding region, which is required for ATP-induced dissociation from actin. A proximal domain, 'switch I', has been shown to cooperate with switch II to maintain the proper structural alignment that enables release of P_i through the 'back door' of the myosin active site (Lawson et al. 2004). Mutagenesis of amino acids within the switch I region generally had little affect on ATPase activity, though certain side chains were able to alter the ATPase binding pocket (Shimada et al. 1997). A neighboring serine was also mutated in myosin II (S237C) in *Dictyostelium discoideum* that was shown to cause defective ATP hydrolysis upon binding to actin (Cochran et al. 2013). The homologous serine in myosin V was mutated (S217A) and shown to slow both actin-activated ATP hydrolysis and reduce the duty ratio, a measure of how long myosin spends in strong actin-bound states (Forgacs et al. 2009). Switch II was also shown to be critical in mediating a key conformational change in the nucleotide-binding pocket that leads to the release of ADP. Additional mutations in the switch I domain of smooth muscle myosin (F344W and F248W) showed increased basal ATPase activity (Robertson et al. 2005, Decarreau et al. 2011). A hearing loss-associated mutation in myo1c was also found to be located at the start of the switch I domain (R156W). This mutation was shown to inhibit actin-activated ATP hydrolysis and had a

lower duty ratio that was attributed to a slowed rate of phosphate release (Lin et al. 2011). Structural changes in switch I are also thought to be tightly coupled to the strength of actin-myosin interaction (Kintses et al. 2007). Interestingly, the homologous tryptophan (W501) in *Dictyostelium discoideum* to that which is mutated in *mlt* (W512) has been implicated in probing the movements in the switch I and switch II domains and the interplay between these domains may very well alter ATP hydrolysis or ADP and P_i release (Zeng et al. 2004, Malnasi-Csizmadia et al. 2005). Taken together, this myosin domain has a strong link to myosin's motor function and has structural implications that would enable it to interact with the helix loop helix domain in *mlt*.

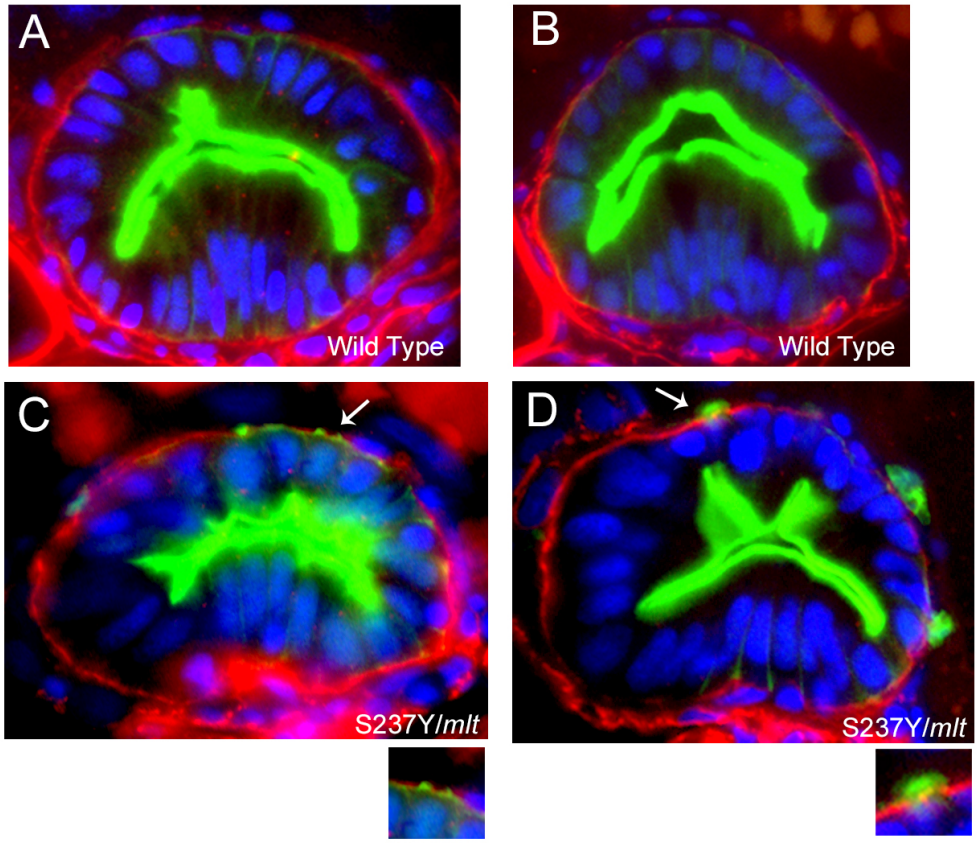

Figure 3.6: Invadopodia Formation in the Invasive Epithelial Cells of the S237Y/*mlt* Trans-Heterozygotes. (A,B) Histological cross-sections through the intestine of 74 hpf immunostained wild type larvae. Basement membrane is labeled in red (laminin immunostain) and actin labeled green (GFP immunostain in Lifeact-GFP transgenics). Nuclei labeled by DAPI (blue). In wild type no actin-rich regions are observed adjacent to the basement membrane. (C) Actin rich protrusions, indicating invadopodia formation, in S237Y/*mlt* co-localize with sites of basal lamina degradation (arrow). (D) During progression of the phenotype epithelial cells invade the tissue stroma through degraded regions of the basal lamina (arrow).

The mutation that we identified in the myosin motor domain, a serine to tyrosine substitution occurring at amino acid 237, was located within the switch I domain of Myh11. As noted earlier, this specific region of Myh11 has been shown to play a critical role in the ATPase function of myosin. The domain forms a pocket out of which ADP can be efficiently released during ATP hydrolysis, and changes in the amino acid make up of the switch I or switch II domain can slow the release of ADP during contraction. Delaying the release of ADP slows the uncoupling of myosin and actin during contraction, and thus allows the myosin head to remain bound to actin longer. This has been described previously in *Dictyostelium discoideum*, as mutation of the homologous serine, S236, resulted in slowed ADP release and altered ATPase function (Cochran et al. 2013). To test if the MYH11 S237Y mutation altered ATPase function similarly to S236, in vitro ATPase measurements were performed. For this assay, it was necessary to introduce the S237Y mutation into a truncated form of the human MYH11 protein (HMM), as full-length myosins form large filaments *in vitro* that disrupt ATPase measurements. The S237Y HMM was transfected into insect cells and exposed to an increasing concentration of smooth muscle actin to measure ATPase hydrolysis as described previously (Sweeney et al. 1998). Strikingly, unphosphorylated S237Y HMM protein displayed a significant increase in ATPase activity when compared to wild type HMM that only had low, baseline activity due to the lack of pMLC (Figure 3.7A). This increased ATPase activity was not due generalized activation of the mutant protein, as phosphorylated S237Y HMM returned to normal levels of ATPase activity comparable to wild type (Figure 3.7A, phosphorylated).

In addition to ATPase function, the rate of inorganic phosphate (Pi) release was examined for the S237Y mutant. This step is considered rate-limiting for the ATPase cycle and has been shown to be the entry point into force generating states (Sweeney and Houdusse 2010). Pi release was faster in S237Y and this increase was not affected by MLC phosphorylation (Figure 3.7D,E). Additionally, the release of ADP can be measured as a readout for myosin detachment from actin, as its release limits detachment. The rate of ADP release was decreased nearly 2-fold in S237Y and also was not affected by MLC phosphorylation (Figure 3.7B,C). Using these measurements, the duty ratio can be determined which determines the relative amount of the cycle myosin spends in strong actin-binding (force-generating) states. As shown in Table 1, S237Y maintains a higher duty ratio when compared to wild type in the phosphorylated and unphosphorylated states of myosin. Taken together, these results suggest that MYH11 S237Y protein exits nonforce generating states faster (higher Pi release) while maintaining force-generating states longer (slower ADP release) and that the overall force output will increase in the mutant.

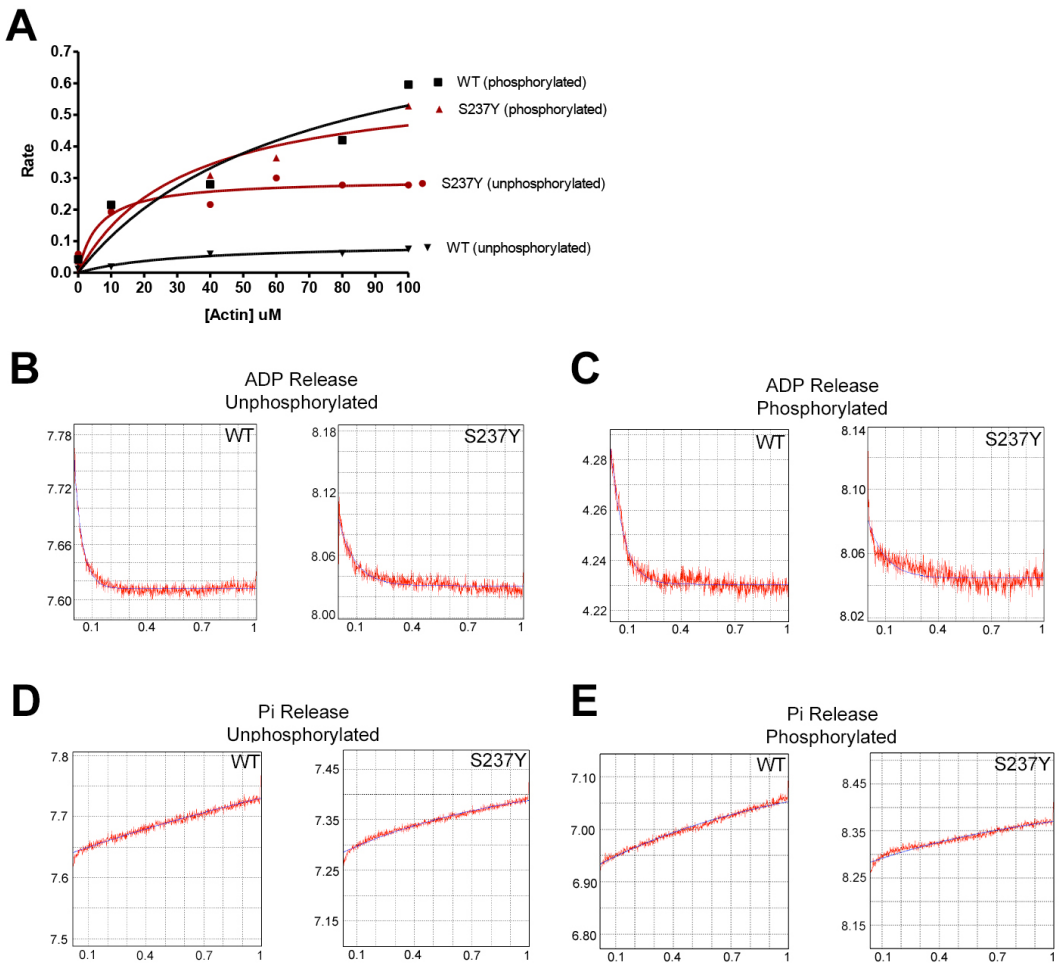

Figure 3.7: S237Y Mutation Causes Aberrant ATP Hydrolysis *In Vitro*. (A) Myosin ATPase assay of heavy meromyosin protein (HMM) harboring the homologous S237Y mutation in human myosin. Unregulated ATPase activity is detected in unphosphorylated S237Y mutant protein compared to wild type protein that only shows baseline activity (compare ● to ▼). Changes in S237Y mutant ATPase activity after MLC phosphorylation were not detected (compare ▲ to ■). (B-C) Myosin ADP release assay of S237Y mutant HMM where time is represented on the horizontal axis and overall fluorescence is depicted on the vertical axis. The release of ADP from actomyosin is measured using a fluorescently labeled nucleotide and quantifying the rate at which fluorescence is lost to determine the rate of dissociation. In both phosphorylated

and unphosphorylated S237Y protein the rate of dissociation was slower (required more time to decrease fluorescence, also see Table 1). (D-E) The release of P_i from myosin was measured using a fluorescent probe for P_i based on a phosphate binding protein (White et al. 1997, De La Cruz et al. 1999) (also see Table 1).

3.2.6: Myh11L1287M, A Myosin Tail Domain Mutant

While the domains within the myosin motor unit have been characterized in some detail for their role in ATP hydrolysis and actin binding, the coiled-coil tail of myosin is far less understood. It is known, however, that the charge along the coiled-coil is important in assembling thick filaments and for structural modification. Myosin tail mutations have been described in cardiac smooth muscle (MYH7) as being implicated in dilated cardiomyopathy, but the functional consequences of these mutations are less clear than those occurring on the motor domain. One possibility is that altered coiled-coil structure could affect myosin incorporation into thick filaments and indirectly affect force output over the longer term (Wolny et al. 2013). Wolny et al. tested 6 different MYH7 tail mutations that had been implicated in cardiac disease, and looked at their ability to form filaments and contract normally using a cell culture assay. They found that mutations that disrupted α -helical content of peptides also had reduced thick filament formation in culture, but no changes in contraction were observed. One particular MYH7 mutation at a highly conserved amino acid, E1356K, was found to be thermodynamically instable, hindering its ability to form filaments (Armel and Leinwand 2010). Two unique mutations at the same tail domain amino acid (R1500P and R1500W) have been shown to cause dilated cardiomyopathy, but both cause decreased thermodynamic stability and

overall filament self-assembly (Armel and Leinwand 2010). These observations suggest that alterations at the myosin tail domain and its corresponding helical structure can have the potential to alter motor function indirectly. Importantly, these structural changes at the myosin rod can lead to tissue-wide defects as it has been demonstrated in cardiac smooth muscle and is likely the case in other smooth muscle tissues as well.

The C-terminal modifier mutant, a leucine to methionine substitution which occurred at amino acid 1287, was located in the tail region of Myh11, a protein domain critical for myosin dimerization and filament formation. The domain forms a coiled-coil, bringing together individual myosin proteins to form functional dimers, a process required for actin shortening and thus the production of contractile force. Though we cannot directly measure myosin dimerization in this context, mutations in this region have been previously described and altered myosin contractility has been reported. Myosin tail domain mutations are also known to alter filament assembly of neighboring myosin dimers, which affects muscle contractility. To determine if the L1287M mutant had a defect in motor function we aimed to perform an in vitro ATPase assay, however for this we needed to utilize the full length Myh11 protein as the mutation occurred in the tail domain. The full length protein has been generated, however these measurements are currently ongoing.

	Actin-Activated ATPase (sec^{-1} $head^{-1}$ ± SD)	Rate of P_i Release (sec^{-1} ± SD)	Rate of MgADP Release (sec^{-1} ± SD)	Duty Ratio
MYH11 WT *unphosphorylated*	0.09±0.02	0.62	20.23	.03
MYH11 WT *phosphorylated*	0.88±0.46	0.81	19.93	.04
MYH11 S237Y *unphosphorylated*	0.30±0.03	1.12	10.02	.11
MYH11 S237Y *phosphorylated*	0.62±0.12	0.98	11.10	.09

Table 1: Increased Myosin Duty Ratio in S237Y Mutant. Values presented are taken from same experiment shown in graphical form in Figure 3.7

3.2.7: Redox Signaling in L1287M but Not S237Y

Meltdown mutants have increased expression of ROS responsive genes and heterozygous *mlt* larvae develop invasive epithelia in response to treatment with ROS compounds. We therefore wanted to examine redox signaling in the two modifier mutants. As neither S237Y nor L1287M develop a visible phenotype as homozygotes, we reasoned that ROS treatment could potentially induce epithelial invasion similarly to our previous observations in heterozygous *mlt.* To examine this question, we treated homozygous S237Y and L1287M mutant larvae with 1.5uM menadione to activate ROS in the epithelium as previously described (Seiler et al. 2012). Interestingly, we observed invasive epithelia in 3 dpf homozygous L1287M mutants, this phenotype was similar to the response seen previously in heterozygous *mlt* larvae (Figure 3.8). This observation suggests that two very disparate mutations occurring in Myh11 (W512R and L1287M) can sensitize the intestinal epithelium to redox signaling, likely through the overall

contractile output produced by the smooth muscle. Surprisingly, S237Y homozygotes failed to respond to menadione treatment (data not shown, 3 independent experiments) pointing to the possibility of subtle differences in force output occurring at each myosin domain. Age matched heterozygous *mlt* larvae were included in all menadione treatments to confirm that redox signaling was active in these experiments and the developmental timing was correct (Figure 3.8C), as the staging for treatment is crucial to initiating invasion in *mlt*. To determine if menadione treatment of homozygous S237Y larvae initiated intestinal protrusions without cell invasion, we repeated the menadione treatment experiment in *Tg(miR194:Lifeact-GFP)*. As we have previously reported instances where invadopodia protrude the surrounding basement membrane without causing epithelial cell invasion, we postulated a similar phenomenon could be occurring in menadione treated homozygous S237Y mutant. However, we observed normal Lifeact GFP expression comparable to that of wild type larvae suggesting that S237Y homozygous mutants were not even mildly responsive to redox signaling (data not shown, 2 independent experiments).

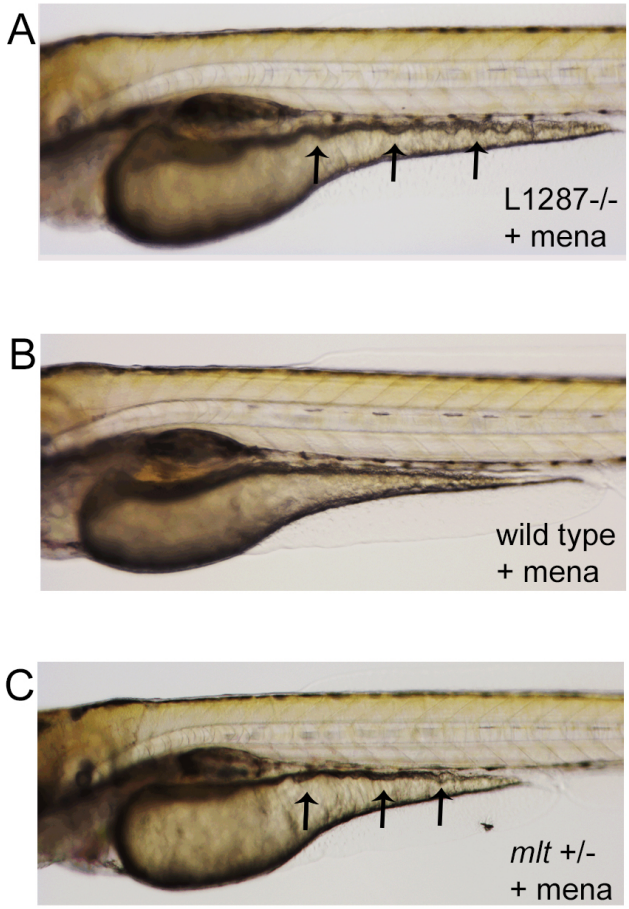

Figure 3.8: Oxidative Stress Induces Epithelial Invasion in Homozygous L1287M Mutant Larvae. (A-C) Lateral images of live homozygous L1287M (A), wild type (B), and *mlt* heterozygous larvae (C). Larvae were treated with Menadione for 3 h beginning at 73 hpf. Menadione treated L1287M homozygous larvae have an intestinal phenotype (arrows) that resembles an untreated *mlt* homozygous larvae (Wallace et al. 2005). No observable phenotype was detected in wild type larvae, and heterozygous *mlt* were used as a positive control.

3.2.8: Normal Intestinal Motility and Survival of Homozygous Modifier Mutants

Homozygous *mlt* mutants begin developing an intestinal epithelial phenotype at 74 hpf and the cells gradually expand into a cyst-like malformation of the entire gut preventing the larvae from processing food and hindering their survival. However, since this lethality is due in large part to the severe epithelial phenotype that disrupts overall gut architecture rescue experiments were conducted to determine if survival could be improved. As the *mlt* mutation is a gain-of-function in Myh11, rescuing the phenotype is achieved by morpholino knockdown of MYH11 protein (Wallace et al. 2005). Morpholino knockdown in zebrafish is transient with normal protein expression typically returning between 5 dpf and 7 dpf. Therefore, contractile function of the mutant Myh11 protein can be monitored in the larval intestine at 7 dpf along with general survival resulting from the smooth muscle defect, independent of epithelial disorganization. In rescued *mlt* mutants, a significant deficit in gut motility was observed when assayed using a fluorescent bead feeding method. Most rescued homozygous *mlt* mutants retained a fluorescent bolus in the anterior gut after being left overnight, whereas nearly 90% of wild type injected larvae had expelled all beads at that time (Fig. 3.9). This result suggests that the mutant Myh11 protein, a constitutively active ATPase, was unable to generate rhythmic contractions necessary for gut motility in the developed intestine. Moreover, time-lapse movies confirmed that only mild contraction was occurring in rescued *mlt*, supporting the idea of an unregulated mutant protein lacking coordinated contraction. When compared to the contractile deficit we see in *cls* mutants (see chapter 2), rescued *mlt* show similarly slowed gut motility but contraction is not visually evident

as it is in *cls,* highlighting the importance of endogenous actomyosin interactions which can occur independent of phospho-MLC in *cls* (Davuluri et al. 2010). The lack of visible contraction in rescued *mlt* suggests that the mutant myosin not only cannot respond to phospho-MLC, but also that endogenous actomyosin interactions cannot contract normally in the mutant. Not surprisingly, rescued *mlt* individuals are not highly successful at surviving into adulthood, as only 2 out of 100 rescued individuals were viable, but showed decreased body size and small swellings along their ventral side.

To assess contractility in the Myh11 modifier mutants, gut motility was assayed in homozygous larvae from S237Y and L1287M. Incrossing heterozygous carriers of each mutant allele never yielded a visible phenotype in the homozygous progeny, so fluorescent bead feeding assays were performed to monitor any subtle changes in gut contraction. These assays were performed on all larvae from an incross to assess motility in both homozygous and heterozygous larvae. In both S237Y and L1287M, we observed normal gut motility at 6dpf when larvae were assayed 4 hours after removing the beads and also after an overnight incubation while feeding on paramecia (Figure 3.9). Time-lapse imaging of S237Y homozygotes revealed no detectable changes in rhythmic contractions occurring at 6dpf (data not shown), thus confirming that the ATPase dysfunction in this mutant was not as physiologically severe as in *mlt* with regard to contraction. Additionally, both homozygous modifier mutants are viable throughout adulthood. It should be noted, however, that a subset of L1287M homozygous adults display signs of infertility and can become lethal as adults. The near normal survival and lack of visible contractile defects in homozygous modifier mutants supports the notion

that *mlt* heterozygotes remain highly sensitive to modest changes in contractile force and redox signaling, as single allele of S237Y or L1287M will suffice to induce epithelial invasion.

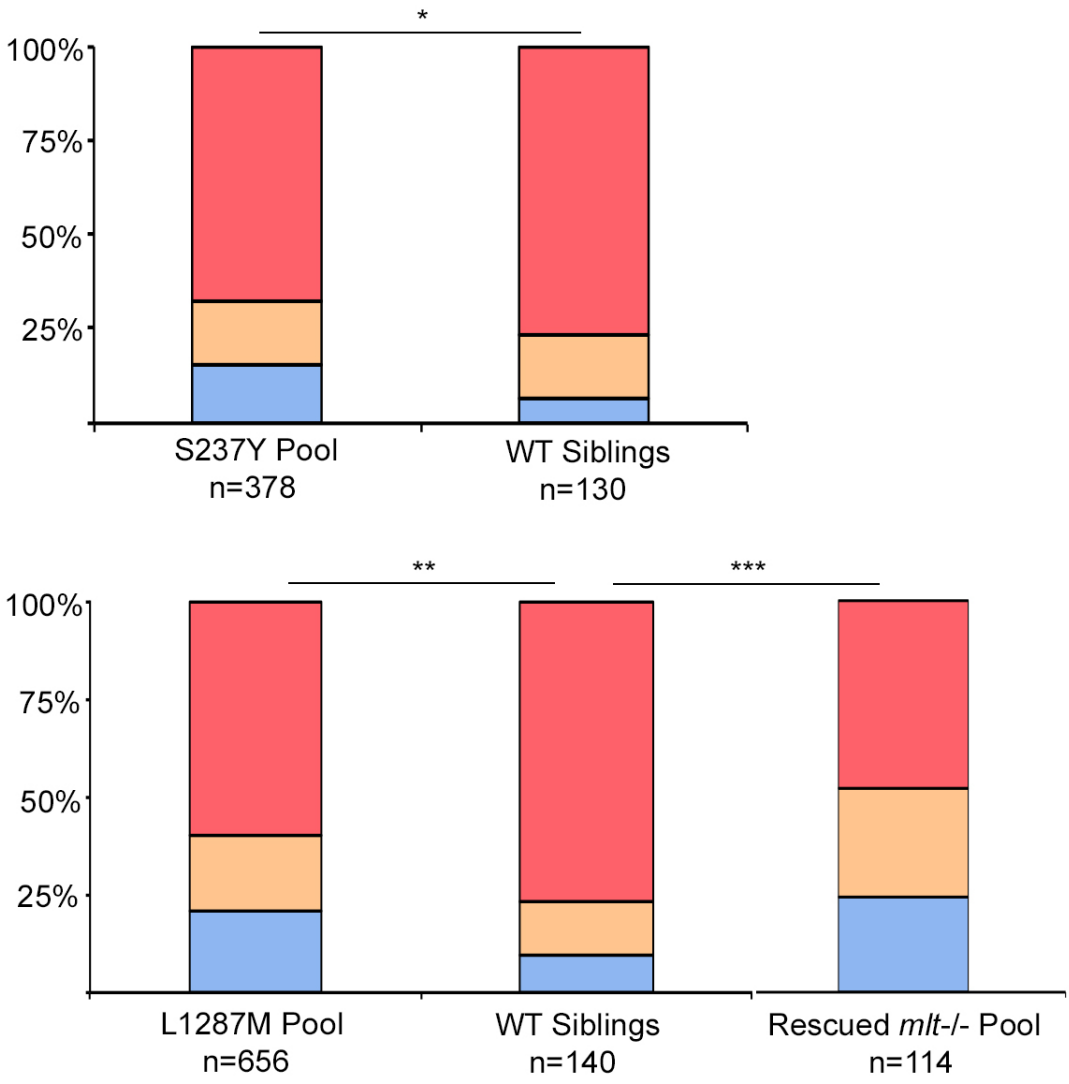

Figure 3.9: Normal Intestinal Motility in S237Y and L1287M MYH11 Mutants. (A) Bar graph represents cumulative results from pooled clutches of S237Y larvae that were

fed fluorospheres at 6 dpf and assayed for intestinal motility the following day. The pooled larvae were derived from a heterozygous incross and contain 25% wild type, 50% heterozygous, and 25% homozygous S237Y mutant larvae. These graphs represent the combined data from 3 independent experiments (chi-squared test, $*P > .05$, not significant) (B) L1287M larvae pool has a small decrease in intestinal motility at 6 dpf (chi-squared test, $**P < .05$). Compare this to WT sibling and rescued *mlt* -/- bar graphs. *mlt* larvae were rescued by injecting *myh11* morpholino as described previously (Wallace et al. 2005). These larvae show nearly 25% having no intestinal motility and serve as a positive control group (chi-squared test, $***P < .001$).

3.2.9: Modifier Mutants are Sensitive to Oncogenic Signaling

Heterozygous *mlt* and homozygous L1287M mutants respond to menadione treatment at 74 hpf, but at later stages of development this response to ROS signaling is lost. At 5 dpf, invasion is not observed after menadione treatment in S237Y and L1287M homozygous mutant larvae (data not shown) and this lack of a response was likely due to a change in the epithelial redox signaling and smooth muscle contractile dynamics compared to 74 hpf. In heterozygous *mlt* larvae, our lab previously reported a response to menadione in older larvae when oncogenic signaling was enhanced (Seiler et al. 2012). Using a transgenic strain that expresses an activated human KRAS allele in the intestinal epithelium (*Tg(miR194:eGFP-KRAS^{G12V}),* intestinal epithelial cell hyperplasia was induced in 5 dpf zebrafish larvae. In addition, these KRAS transgenic larvae were bred into an *axin1* loss-of-function mutant background, which disrupts Wnt signaling and leads to added intestinal hyperplasia, as described previously (Heisenberg et al. 2001). The intestinal epithelial cells in these 'KRAS-axin' larvae are similar to those in

colorectal cancers where activated KRAS and defective Wnt signaling both occur. In the KRAS-axin larvae that were also heterozygous for *mlt*, menadione treatment at 5 dpf generated a dramatic invasive response, whereas siblings that were wild type at the myh11 allele showed no response to menadione (Seiler et al. 2012). To determine if S237Y and L1287M were sensitized to oncogenic signaling in a similar manner to mlt, we crossed each mutant into the KRAS-axin background and performed menadione treatment experiments at 5 dpf. After 5 hours of menadione treatment, both homozygous myh11 mutants displayed epithelial invasion while heterozygous larvae resembled wild type (Figure XX). Importantly, invasion was not detected after menadione treatment of 5 dpf homozygous myh11 mutants that lacked KRAS-axin, suggesting that the observed response was indeed due to oncogenic signaling in these mutants.

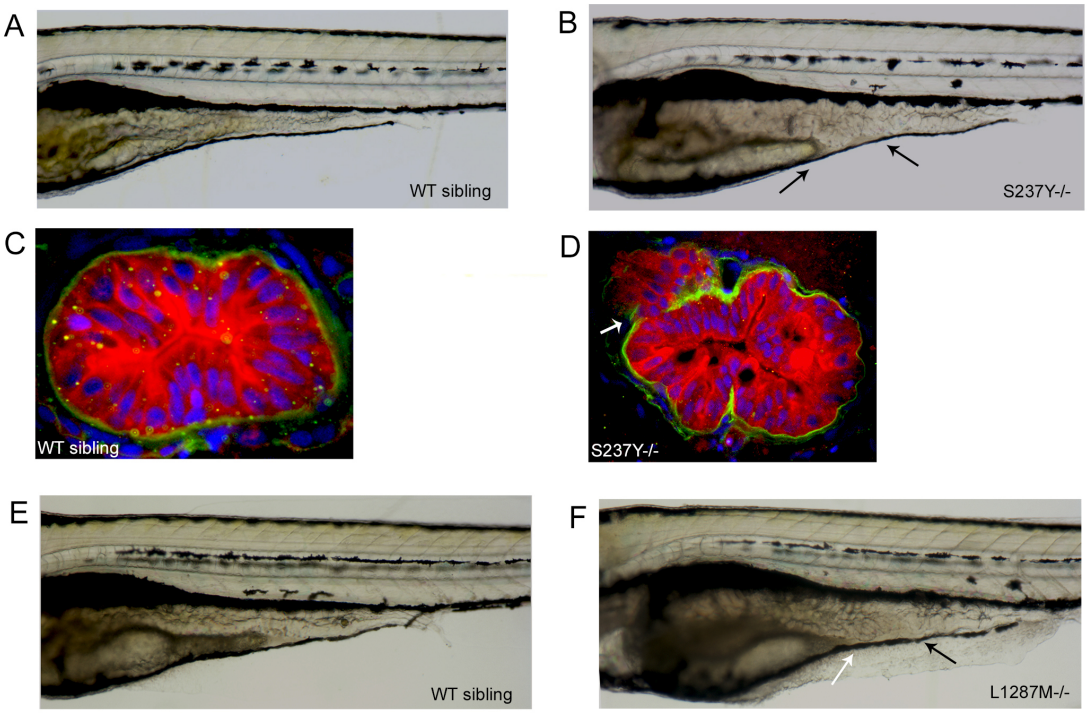

Figure 3.10: Activation of Oncogenic Signaling Enhances Sensitivity of S237Y and L1287M to Oxidative Stress. (A) Lateral views of live, menadione treated 5 dpf *axin* mutant larvae that express mutant *KRAS* in the intestinal epithelium (*Kras-axin*). Hypertrophy of the intestinal epithelium in *Kras-axin* larva is unchanged by treatment with menadione. (B) Menadione treatment causes pronounced cystic expansion of the intestinal epithelium of the *Kras-axin* S237Y homozygote (arrows). (C-D) Histological cross-sections through the intestine of immunostained larvae show invasive cells in menadione treated *Kras-axin* S237Y homozygotes (arrows). Invasion is not detected in menadione-treated *Kras-axin* wild type siblings. (E-F) Similar cystic expansion is observed in *Kras-axin* L1287M homozygotes larvae after treatment with menadione compared to wild type sibling controls.

3.2.10: Altered Vascular Flow Rate After Smooth Muscle Actin Disruption

In many of the human diseases associated with myosin mutations as well phenotypes described in mouse models for thoracic aneurysm and cardiomyopathy, vascular abnormalities remain a common feature. Our findings in the intestinal smooth muscle show that altered contractility can result in striking features such as epithelial invasion, and lastly we sought to determine if smooth muscle abnormalities could lead to vascular phenotypes in zebrafish. We utilized the smooth muscle actin (acta2) morpholino that we described above in chapter 2 and injected into wild type embryos. We raised these larvae to 5 dpf, when vascular smooth muscle expression is first detected in zebrafish and compared the vascular flow rate to age-matched, control injected wild type larvae. We found a significant increase in both arterial and venous flow in acta2 morphant larvae when compared to control injected wild type (Figure 3.11A). Consistent with this, the measured artery and vein width was increased in acta2 MO injected larvae also (Figure 3.11B). Indeed we expect that altered smooth muscle actin function would decrease contraction in the vasculature allowing for the vessels to widen and pass blood faster. This proof-of-principle experiment shows that contractile disruptions can indeed be detected in the vasculature of larval stage zebrafish, presenting this method as a potential way in which to study smooth muscle contraction in addition to the intestine.

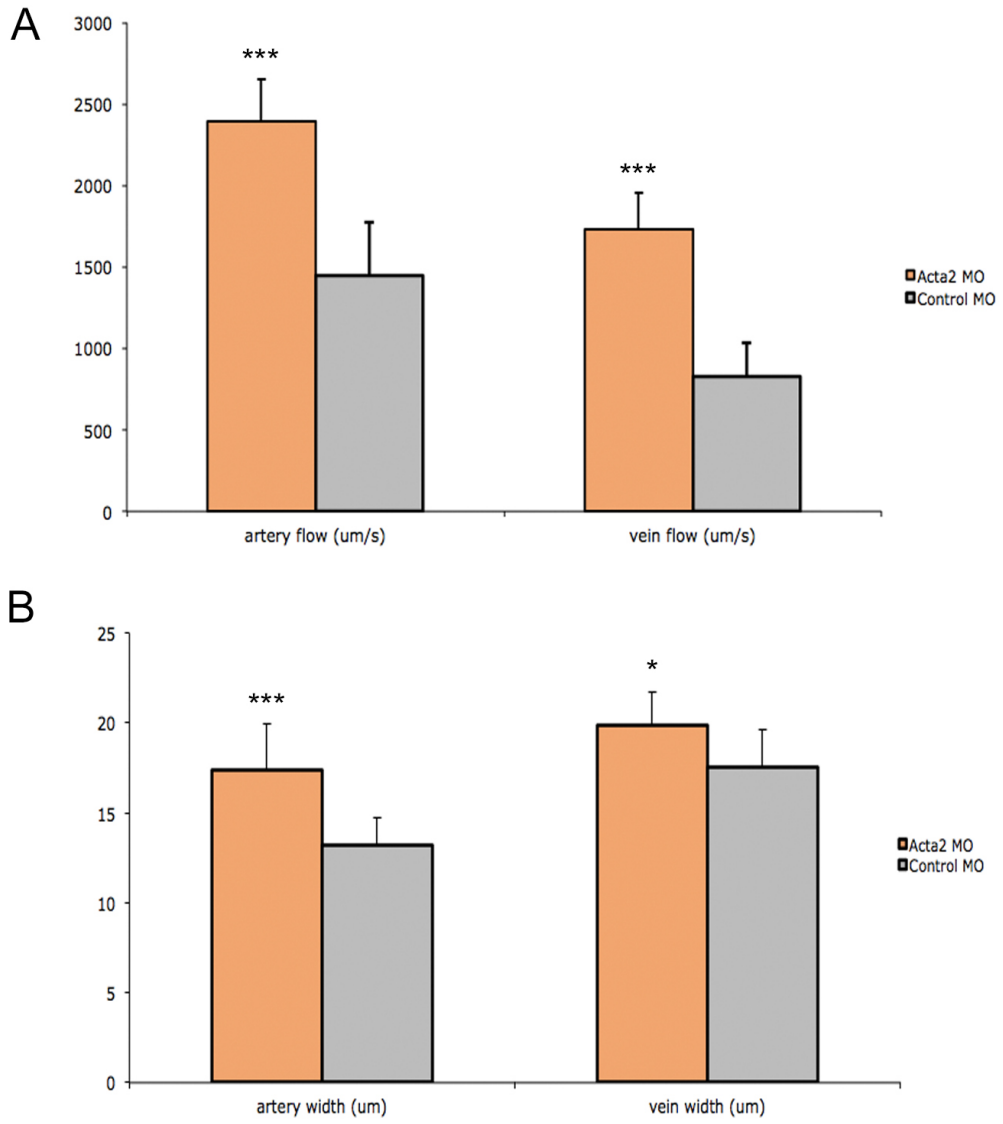

Figure 3.11: Increased Vascular Flow After Smooth Muscle Actin Disruption. (A) Artery and vein flow rate was measured in 5 dpf larvae that were injected with a morpholino targeted to smooth muscle actin (acta2, n=10 larvae) or a mismatched control morpholino (n=8 larvae). (B) Widening of arterial and venous blood vessels using images obtained from the same set of larvae assayed in (A). Values are presented as an average flow rate or average width of all the larvae tested. t-test * $P < .05$, *** $P < .005$

Discussion

Studies of myosin missense mutations in vascular disease and *in vitro* analyses of specific protein domains have provided important links between myosin during contractile modulation and its potential to cause severe disruptions within certain tissues. However, the connection between the specific function of myosin and its tissue-wide effects cannot be realized through these analyses. Our results provide an *in vivo* analysis of the role for S237Y, L1287M, and W512R myosin mutations in both smooth muscle contraction and the propagation of epithelial invasion within the intestine. In our model, each of these mutations alters myosin contractility in a unique way through the dynamic process of ATP hydrolysis and each mutant is different in their response to redox and oncogenic signaling. These results provide a unique avenue with which to study smooth muscle contractility and they lead to a number of additional questions requiring further investigation. For one, it would certainly be interesting to determine the precise nature of the L1287M mutation with regard to its ATPase function and this is something we hope to gain further insight on in the near future. Overall, our data implicate myosin mutations and h-CaD in the tuning of contractile tone and alterations in the function of these proteins can result in striking and biologically interesting disruptions in the GI tract. In the future, applying these observations to vascular abnormalities in the larval zebrafish would provide an interesting connection with known human vascular diseases where Myh11 is mutated.

Chapter 4: Conclusions and Future Directions

In this work, we have addressed how smooth muscle contractile force can be modulated as well as the consequences of abnormal contractility in the intestine. We have revealed an important *in vivo* role for h-CaD during gut motility, which illustrates a modulatory function for this protein during contractile force production. In a previously studied h-CaD knockout mouse, smooth muscle tissues appeared to function normally and this was attributed to a compensatory role of l-CaD in this context. Thus the ability to re-examine h-CaD function using the live imaging capability of zebrafish allowed us to monitor its affect on smooth muscle contraction in the gut. Because of the established role *in vitro* for h-CaD in regulating vascular tone, our findings in the zebrafish intestine may potentially be extended to the vasculature and other smooth muscle tissues as well. We have also characterized a novel mutation in the *myh11* motor domain that leads to altered ATP hydrolysis and initiates epithelial invasion in heterozygous *mlt*, a previously characterized *myh11* mutant. A second mutation in the helical tail domain of myosin was also found to cause invasion in heterozygous *mlt* and was responsive to redox signaling, its role in ATP hydrolysis is currently under investigation. Although the tail domain mutant only responded to redox signaling when homozygous, this observation remains clinically relevant as our assay is conducted with a fairly short exposure to reactive oxygen. In heterozygous human carriers, for example, a longer time period of exposure to reactive oxygen could allow a response to manifest gradually. Taken together, this work suggests that alterations of specific MYH11 domains and smooth muscle regulatory elements, such as h-CaD, can have profound effects on both physiological functions and

biomechanical signaling leading to cellular invasion. In the following section, these conclusions will be investigated in more detail and additional experiments will be proposed to further this work in the future.

4.1: Implications of h-CaD as Force Modulator During Contraction

During smooth muscle contraction, a number of contributing factors work in concert to produce coordinated rhythmicity or maintain muscle tone. The phosphorylation of MLC has been thoroughly described as the regulatory event initiating contraction, but to better understand the diverse roles that smooth muscle plays in each tissue its critical to consider each of the modulatory events which fine tune contraction. It is now appreciated that clear differences exist between longitudinal and circular smooth muscle layers as well as their specific neural inputs and these differences can lead to vast changes in contraction and force output. Prior work from our lab has shown that in a zebrafish mutant lacking enteric nerves and with no phospho-MLC GI motility persists, albeit extremely slowly (Davuluri et al. 2010). These observations point to other contributing factors such as ICC pacemaker activity, hormonal stimulation, intrinsic actomyosin interactions and modulatory proteins, such as h-CaD being critical in tuning the force output and rhythm of smooth muscle contraction. We have used a simplified, readily observable vertebrate system in the larval zebrafish intestine to determine the roles of h-CaD, phospho-MLC, and enteric nerve input *in vivo*. However, our analysis has not determined that these regulatory factors maintain similar importance later in development or in complex mammalian tissues where additional inputs need to be considered. Thus, it will be critical to evaluate whether targeting h-CaD in mature tissues

can generate the same response that we have seen with our observations, as this will shed light on the potential for modulating smooth muscle contraction in human GI and vascular disorders.

Additional evidence of CaD's importance in the regulation of smooth muscle contraction was recently demonstrated using a mouse model of bladder contraction. Mice were generated that carried mutations within the CaD ATPase inhibitory domains and though homozygotes were embryonic lethal, heterozygous mice could produce more contractile force during bladder smooth muscle contractions (Deng et al. 2013). These observations point to CaD's role within diverse smooth muscle tissues as well as the physiological sensitivity to CaD disruption, as contraction was enhanced in heterozygotes. Enteric nerve and smooth muscle tissue grafting are widely utilized procedures in cases where gut motility is disrupted, and both present a number of limitations. CaD and related smooth muscle regulatory proteins present an alternative mode of contractile regulation that has the potential to be fine-tuned using targeted strategies.

Both the inhibitory role of h-CaD and the molecular signaling pathways that regulate its activity have been characterized in smooth muscle cells from the digestive tract and other mammalian tissues (Gerthoffer and Pohl 1994, Earley et al. 1998, Chacko et al. 2004, Lu et al. 2006, Zhang and Zhang 2007, Smolock et al. 2009). Despite these advances in understanding h-CaD function and regulation, its role during complex physiological responses, such as intestinal peristalsis, has not been directly examined *in vivo*. Isoform specific knockout of h-CaD in mice has been reported, however visceral smooth muscle function was not perturbed due to a compensatory increase in l-CaD in

phasic smooth muscle tissues (Guo and Wang 2005). A more recent follow up study found that arterial smooth muscle in h-CaD null mice was abnormally slow at relaxing, supporting the role of h-CaD in controlling vascular tone (Guo et al. 2013). This observation suggested that unphosphorylated crossbridges did not properly detach and importantly, there was no difference in MLC phosphorylation in these mutants indicating that this change in relaxation is only attributed to the loss of h-CaD. One possible explanation of the altered relaxation in the mutants is the slow release of ADP during the myosin ATPase cycle, allowing the dephosphorylated heads to remain attached to actin longer in the absence of h-CaD before they progressively detach.

4.1.1 Smooth Muscle Contraction and Gastrointestinal Disorders

As discussed in Chapter 2, a potential role of h-CaD in mammalian intestinal motility could be to compensate for disruptions in enteric nerve signaling where limited contraction persists, as it would be unlikely to offset a complete loss of MLC phosphorylation. One context where this would be important is in tissue regeneration and transplantation efforts where coordinating contraction remains a major hurdle. Initial tissue engineering approaches of the small intestine that have used transplanted tissue in rat and canine models of severe bowel resection have shown improvement in the basic physiology and enteric nerve regeneration (Chen and Badylak 2001, Grikscheit et al. 2004). However, these tissues did not produce the proper coordination of circular and longitudinal smooth muscle that is crucial to generate appropriate force for gut motility. Similar challenges have been encountered with stomach and colonic smooth muscle, as regenerated tissue demonstrated an absorptive capacity but did not respond to stimulation

by acetylcholine treatment (Hori et al. 2002). Lastly, three-dimensional *in vitro* models have demonstrated that alignment of circular smooth muscle can be achieved around the colonic lumen and rhythmic contraction can occur, but these findings have yet to be validated *in vivo* (Hecker et al. 2005).

One promising study by Pan et al. used neural crest progenitor cells for transplantation into a rat model for colonic dysfunction. In this study, the authors were able to demonstrate a partial rescue of neuronal mediated gut motility in the diseased colon after transplantation (Pan et al. 2011) and previous work has shown that human enteric progenitor cells can repopulate segments of an aganglionic colon (Metzger et al. 2009). In this example, the results are similar to what we have observed with h-CaD's ability to partially rescue motility in *colourless* mutant larvae that lack enteric nerves. It would certainly be compelling to analyze h-CaD function in these transplantation studies. Limited success has also been achieved in studies with engineered sphincteric smooth muscle, as this region of the GI tract is less complex and therefore easier to induce motility. Engineered sphincteric smooth muscle tissues grown in culture and grafted into animals displayed low levels of contractile tone as well as a response to neural input (Raghavan et al. 2010, Raghavan et al. 2012). However, restoring gut motility has not been demonstrated in these studies and regenerating smooth muscle layers with proper orientation and functionality remains a challenge.

As current efforts are focused primarily on enteric nerve replacement or smooth muscle tissue grafting, targeting regulatory elements in these tissues may allow finer manipulations of contraction and possibly better muscle coordination. A number of these

challenges could be addressed *in vivo* using the zebrafish model of intestinal contraction that we have established. For example, by using small molecules one could foreseeably screen for factors that improve or reduce gut motility in the larval intestine. Not only would such an approach carry the potential to uncover targeted compounds to treat motility disorders, but also by understanding the target and mechanism of action such small molecules could provide valuable insight into the regulatory complex guiding smooth muscle contraction. By furthering our understanding of both actomyosin interactions and mediators of force production such as h-CaD, and combining this insight with the current tissue engineering methods, the potential exists to improve coordinated contraction in GI motility disorders and after tissue replacement therapies.

In summary, smooth muscle contraction and gut motility results from coordinated behavior of multiple cell types and modulatory factors at the contractile apparatus. Although much has been elucidated about the function and molecular mechanism of these different cell types, highly specific therapeutics for GI motility disorders remain elusive. In each disorder or region of the GI tract, the regulation of contractile force and the mechanisms that regulate smooth muscle excitability seem to differ considerably. There are also differences between the GI tracts of mice, humans, and zebrafish although understanding the specifics of human smooth muscle regulation will start with modeling the process in other vertebrates. It is also important to consider that motility disorders may not be manifested throughout the entire GI tract. For example, if constipation results from hypomotility in the colon that does not imply that other regions of the GI tract will contract abnormally, and thus treatments devised to increase contraction in one area may

negatively affect motility in a neighboring region. Importantly, there are many similarities between the GI tract and other organs (i.e. the vasculature) with regard to smooth muscle and its regulatory components, and manipulating molecular targets in the gut could alter contraction of other critical organs. Currently, there are very few gut specific smooth muscle targets and a limited number of efficacious compounds to treat motility disorders. Therefore, there is a need to identify additional regulatory elements at the molecular level that can modulate smooth muscle contraction and GI motility, as these discoveries would allow for more targeted therapies.

Additionally, in studies of *c-kit* mutants where ICC are absent contractile responses could be elicited in the stomach and lower esophageal sphincter after repetitive stimulation, suggesting that transmitter overflow can elicit a response without ICC (Sivarao et al. 2001, Huizinga and White 2008). Other inputs from purine interstitial neurotransmission (PDGFRa) generate an electrically coupled complex that allows SMCs to become stimulated after activation of any cells within the complex. Layers of regulation also exist in circulating hormones, paracrine substances and inflammatory mediators. Altering any of these regulatory inputs can change the response of SMCs leading to gut paralysis or hypermotility disorders that affect the movements of food, absorption of nutrients, and waste transit. A greater understanding of the basic contractile apparatus in gut smooth muscle would provide a foundation for improving occurrences where upstream signaling has been disrupted. GI motility disorders commonly arise from developmental defects and disease processes that compromise function, and regenerative medicine has the potential to correct motility problems through

engineering of functional GI smooth muscle and enteric nerves. However, the complex organization and contraction of smooth muscle has presented a challenge in coordinating tissue-wide contraction. Extensive work on vascular smooth muscle, where differentiated SMCs have been used to engineer functional tissue, has shed light on the challenges of providing normal contraction in synthetic tissue. Though fairly successful in vascular tissue, engineering GI smooth muscle has presented several challenges due to the many cell types and neural inputs that regulate carefully orchestrated rhythmic contractions (Bitar and Raghavan 2012). Further studies of both h-CaD and myosin within GI smooth muscle could aid in avoiding some of the setbacks in transplanting tissue when motility is disrupted. With the great strides that have been made in tissue engineering and transplantation, studying contractile modulators could complement this approach when addressing therapeutic validity for motility disorders.

4.2: Muscle Contraction and Increased Force

Mutations of Myh11 have been implicated previously in vascular disease and in our studies we have found a connection between smooth muscle mutations and epithelial invasion in an underlying tissue. In both vasculature disease and in our work in the intestine, Myh11 mutations alter the motor function that ultimately leads to the abnormal physiology observed. This observation suggests that smooth muscle contractility has the capability to dictate the morphology of neighboring cells and underlying tissues. Indeed, muscle contraction has been shown to order tissue morphology in the skeletal system and during embryogenesis. Using both a mouse and zebrafish model, Shwartz et al. showed that chondrocyte morphology during skeletal development was impaired when muscle

contraction was chemically or genetically reduced (Shwartz et al. 2012). They observed rounded, rather than elongated, cells in paralyzed zebrafish and in 'muscle-less' mouse mutants impaired chondrocyte intercalation was noted. Contractile force has also been shown to regulate bone growth earlier during embryogenesis, as mutant mice that lack muscle contraction harbor offspring with abnormally developed bone structures (Sharir et al. 2011). In these 'muscular dysgenesis' mutant mice it was also observed that osteoblasts were improperly distributed due to the altered mechanical load from the muscle layer. While these examples occur in a skeletal muscle system that varies considerably from smooth muscle, they do point to the importance of muscle contractile force output in shaping individual cells or even entire tissues. This raises the question of how altered contractile force can lead to the diversity of phenotypes that have been reported and epithelial invasion that we have described from our observations. In the following section I will discuss the described role of myosin in certain disease states and consider how specific regions of the proteins contributes to certain conditions.

4.2.1: Consequences of Myosin Mutations in Disease

Myosin missense mutations have been well characterized in cardiac smooth muscle where they are known to cause both dilated and hypertrophic cardiomyopathies, the two most common forms of genetic heart disease. More than 300 distinct myosin mutations have been identified in these diseases and are distributed throughout the protein, though most mutations occurred in the head domain (Buvoli et al. 2008, Walsh et al. 2010). More detailed analysis determined that regions of the motor domain adjacent to the ATPase site had a greater frequency of mutations (Moore et al. 2012). Although

the number of mutations linked to cardiomyopathy is large, only a small subset of these mutations have been studied for their effect on myosin mechanics.

Though rare, the MYH11 mutations identified in FTAAD families are deletions and missense mutations primarily located in the coiled-coil domain of the protein (Pannu et al. 2007, Zhu et al. 2007). Identification of many of these mutations has proven to be difficult due to the fact that rare, nonsynonymous variants occur in MYH11 in the general population (0.6% according to the exome rare variant database, Kuang et al. 2012). However, a recurrent MYH11 rare variant, R247C, is located in the motor domain of the myosin heavy chain and disrupts an arginine that is completely conserved across species. Also, a mutation in the corresponding amino residue in cardiac myosin (MYH7), R249Q, causes familial hypertrophic cardiomyopathy. The mutation in both the cardiac and smooth muscle isoforms lies near the ATP binding domain, and in vitro assays of MYH7 R249Q have confirmed decreased ATPase activity and filament velocity (Sata and Ikebe 1996, Roopnarine and Leinwand 1998).

To quantify altered motor function of the R247C MYH11 mutation, Kuang et al. used a fragment containing the myosin motor domain (HMM) and found a decrease in actin-activated ATPase activity after phosphorylation of the MLC. In the absence of MLC phosphorylation, regulation was not altered in the mutant and no ATPase activity was detected, as is seen in wild type myosin (Kuang et al. 2012). They also measured the rate of P_i release after the R247C MYH11 was allowed to bind and hydrolyze ATP and then mixed with actin. As noted earlier, this step is rate-limiting for the overall ATPase cycle in smooth muscle and initiates the force generating states on actin (Sweeney and

Houdusse 2010). P_i release was found to be slower for the mutant myosin and was notably only slightly faster than the overall ATPase cycle rate for both mutant and WT proteins, consistent with it being the rate-limiting step. Lastly, they measured the release of ADP, an event that limits both the rate of myosin detachment from actin and maximal shortening velocity. The rate of ADP release was slower in the R247C mutant, as was the rate of actin filament sliding in an in vitro motility assay.

To reconcile the kinetic findings on R247C it is important to consider the total time that myosin spends bound strongly to actin during the ATPase cycle (i.e. duty ratio) as this will be a major determinant of the total force that myosin produces. In the context of net force, the rate of P_i release controls exit from the weakly bound (i.e. non-force generating) states and ADP release controls exit from the strongly bound (i.e. force generating) states. The calculated duty ratio of the R247C mutant was nearly half that of the WT protein, and thus force production and shortening velocity are both likely decreased *in vivo* due to the mutation. To determine the affect of this mutation *in vivo*, mice carrying the R247C mutation were generated and assayed for aortic force development. These mutant mice were found to have decreased contractile force compared to controls, and importantly had no change in MLC phosphorylation suggesting the changes were indeed due to intrinsic properties of the mutated myosin. This decreased aortic contractility did not cause aortic pathology in these mice, suggesting that contractility alone may not be sufficient to cause TAAD. SMCs explanted from the mutant mice also displayed increased proliferation and dedifferentiation. In contrast to R247C mutants, *Myh11* deficient mice die shortly after

birth due to vascular complications, and from dysfunction of the bladder and intestine (Morano et al. 2000). R247C mutant mice do not display any deficiencies in visceral smooth muscle, which could be due to compensation by the nervous system, hormones, or other type II myosin motors that are sufficient to maintain tissue functionality.

Though the specific role of this mutation in TAAD remains to be seen, R247C can alter duty ratio and contractile force *in vivo* and this suggests that missense motor domain mutations have dramatic affects on smooth muscle contraction. Work has also been described in *MYH7*, the cardiac beta-myosin heavy chain, showing that mutations typically cluster in the functional subdomains of the myosin motor head domain, specifically in the ATP-binding and actin binding clefts, these mutations are correlated with human vascular disease but their specific functional consequences are not known (Buvoli et al. 2008). Aside from R247C, TAAD mutations do not often occur in the head domain, but rather in the coiled-coil rod domain. One additional exception to this is a missense mutation at amino acid 712 near the converter domain, which transduces force from the ATPase motor and allow the flexible movement of the myosin head along actin. However, as more mutations in both the motor and helix domains are studied we will be able to better grasp how these missense mutations can alter the *in vivo* function of smooth muscle tissues and vascular disease.

In the airway smooth muscle of the lung, contraction must be tightly coordinated to maintain a constant force output upon the tissue. The mechanical strain that is placed upon the smooth muscle during lung inflation perturbs the binding of myosin to actin due to the mechanical force acting upon the actomyosin interaction (Seow and Fredberg

2001). This response by the major contractile components allows the tissue to be more amenable to stretch and is required for normal breathing to take place. In situations where more actomyosin bridges are formed the tissue becomes less compliant as the muscle stiffens. When in the so-called 'statically equilibrated' state, the myosin cycling and rate of ATP utilization becomes greatly decreased (Fredberg et al. 1999), and an asthma-associated condition termed airway hyperresponsiveness can occur. This condition occurs in airways that narrow too readily and too much in response to treatment with nonspecific contractile agonists, it is also the feature underlying excessive airway narrowing seen in asthma, but the specific mechanism remains unknown (Woolcock and Peat 1989, King et al. 1999). In the smooth muscle myosin mutants that we have identified, unregulated ATPase activity has been observed in two cases where it is highly likely that additional actomyosin bridges are being formed between unphosphorylated myosin heads and actin. This could have the similar affect seen in the airway and thus generate less compliant intestinal tissue. Although the intestine does not experience the same degree of strain as the lungs do, the tightly coordinated contractile waves are vital for its function. In addition, we have previously demonstrated that increasing gut contraction in heterozygous *mlt* larvae after treatment with L-NAME, a general contractile agonist, can induce epithelial invasion suggesting that a similar 'hyperresponsive' state is achieved in these larvae similar to what has been described in the airway.

4.3: Myosin Domains and Contractile Force Output

4.3.1: The Importance of the Myosin Switch I Domain

Within the myosin motor domain, there are multiple subdomains that are linked through highly conserved 'connector' domains. One domain, the converter, has a high potential for movement due to its connection with two deformable joints, the relay and SH1 helix. It is this conformation that allows small movements at the motor domain to be amplified during contraction. A critical connector, known as the Switch I domain, allows coupling between the actin and nucleotide binding sites. Briefly, during the 'prepowerstroke' state partial closure of the large cleft involves the inner part of the cleft, a domain adjacent to Switch I, trapping the P_i. As has been shown in myosin V, the nucleotide-free rigor-like state causes the outer and inner cleft to close and generates a new actin-binding interface that has a strong affinity to myosin (Fisher et al. 1995, Yount et al. 1995, Coureux et al. 2003). Interestingly, it was reported that the polarity of the amino acid side chain located at S236 in Myh11 impacted the affect each mutation had on ATPase function, suggesting that this serine is critical for myosin motor function (Li et al. 1998, Frye et al. 2010). From what we have found with the S237Y mutant, where ATPase activity persists when myosin in unphosphorylated, it seems clear that this domain of myosin has critical functional implications for ATP hydrolysis. At the level of the intestinal tissue, our *in vivo* assays reveal that this mutation alters the coordination of muscle contraction and production of force. With what is known about Switch I's structural role within the myosin head, it is apparent that small structural changes in myosin can lead to significant changes in contraction as we have observed with S237Y.

4.3.2: Regulatory implications of myosin tail domain

The assembly of myosin dimers and their proper orientation is directed by an alternating 28-residue pseudo repeat of the α-helical coiled-coil domain of the tail domain and this forms the core of the thick filament. The coiled-coil domain of the myosin tail directs both dimerization and the overall conformation of myosin structure. Smooth muscle myosin in particular has been shown to be more prone to bent conformations, but it is still unknown exactly which domains along the helical tail are responsible for the increased bending (Trybus et al. 1982). The physiological relevance of a more bent myosin confirmation is also unknown, though it has been long appreciated that changes in the head domain after phosphorylation of MLC can alter filament assembly at the tail. Additional studies of the importance of the tail domain used various chimeric constructs to determine how each domain of the tail altered actin-activated ATPase function *in vitro* (Trybus et al. 1997). They tested the role of dimerization in the regulation of ATPase activity by the myosin head and determined that a tail domain was required, and needed to be at least the same length as the head domain in order to allow for proper function. Interestingly, the tail domain was shown to be crucially important for myosin to achieve its 'off' state, a state that is absolutely necessary for normal contractile regulation. The role of the tail therefore mediates specific interactions with the myosin head, and if these interactions are obstructed then unphosphorylated crossbridges can slowly continue to cycle.

These observations could be of critical importance when considering L1287M, the tail domain mutant that we have described above. In L1287M/*mlt* trans-

heterozygotes we observe epithelial invasion characteristic of homozygous *mlt*, and we have previously shown that the *mlt* mutation (W512R) results in active cycling of unphosphorylated crossbridges. Therefore, the unphosphorylated heads are likely of critical importance in propagating the epithelial phenotype in *mlt* and in the modifier trans-heterozygotes. We have already shown that activation of unphosphorylated heads occurs in the S237Y mutant and this is likely to be the case in L1287M as well. Further, the L1287M mutant presents us the unique opportunity to better understand how a myosin tail domain mutation can regulate both ATPase activity and smooth muscle contraction *in vivo*.

4.3.3: Trans-heterozygotes: A Potential Interaction Between Mutated Myosin Heads?

At the level of individual myosin heads, each can maximize their duty ratio when actin concentration is high. The higher duty ratio ensures that when one head detaches from actin upon ATP rebinding, the second head in the dimer will be in a strong binding state and remain in this state until the detached head hydrolyzes ATP and rebinds at a distal actin-binding site. In this manner, certain myosins can processively walk along an actin filament in hand-overhand fashion through the cycling of only a single head (Yildiz et al. 2003, Yildiz et al. 2004), a phenomenon that has been seen in vitro and in living cells (Nelson et al. 2009, Pierobon et al. 2009). A well-studied example of this is myosin V, where a high duty ratio is required to support its processive movements and actin-activated P_i release (De La Cruz et al. 1999). Myosin V simultaneously decreases the rate of ADP release such that the strongly attached myosin head becomes the predominant steady-state intermediate of the cycle. The coordinated regulation of ATP

hydrolysis at individual myosin heads can be attributed in part to regulatory mechanisms leading to MLC phosphorylation but the role of the regulatory domains of each myosin protein has been shown to be of critical importance as well.

The double-headed structure of myosin is not necessary for actin binding or ATP hydrolysis, in fact a single-headed molecule can alone move actin filament, albeit less effectively than a two-headed myosin (Margossian and Lowey 1973, Toyoshima et al. 1987, Waller et al. 1995). More recently, it was determined that the step size was twice as large in a two headed myosin when compared to single-headed molecules (Tyska et al. 1999) suggesting that two heads are more effective than one and that they may work together to coordinate contraction. Additionally, the strain produced at the junction between the two heads has been shown to influence actin binding ability, an effect more striking in smooth muscle myosin (Whittaker et al. 1995, Conibear and Geeves 1998, Conibear 1999). Taken together, these observations highlight the complexity of double-headed molecules rather than simply being two kinetically independent heads. In work by Rovner et al., the performance of homo- and heterodimeric double-headed myosins was tested to shed light on the complex nature of their interactions. This study determined that heterodimers with one mutant head only bind actin weakly, but were more efficient than single heads or mutant homodimers. This suggests that the weak binding of the mutant head optimally orients the working head so that it can achieve maximal performance. A second interpretation is that the second head simply maintains the structure of the dimer allowing more efficient movement by the working head, which suggests that actin binding would not be required (Kad et al. 2003, Rovner et al. 2003).

If we extend these findings to our observations in S237Y or L1287M/*mlt* trans-heterozygotes, it suggests that the modifier mutant head binds weakly to actin allowing the *mlt* head to produce maximal force and drive the phenotype. Consistent with this is the observation that heterozygous *mlt* do not develop a phenotype, likely due to the wild type myosin head providing the primary mode of contraction while the *mlt* head serves a structural role. Additionally, this would explain why we do not observe epithelial invasion in S237Y and L1287M homozygotes, as these mutant homodimers can only bind weakly and are not able to reach the contractile force threshold required for epithelial invasion. It is not clear precisely what ratio of homo- and heterodimers exist in each heterozygous state discussed above, but the overall number and specific types of dimers in each context are likely indicators of the contractile force output. Therefore, in addition to the specific myosin mutation with respect its location within the protein, altered dimer function is an important consideration when determining the net effect on muscle contraction.

4.4: Triggering and Responding to Mechanotransduction

In a number of different tissues, the role of force signaling has been shown to cause diverse responses by the neighboring cells. For instance, in kidney epithelial cells respond to levels of fluid shear similar to those produced by urine flow in collecting ducts by increasing calcium influx. Also, changes in gene expression and growth of bladder smooth muscle cells that are triggered by outlet obstruction appear to result from mechanical stretch secondary to overfilling of the bladder (Park et al. 1999). During pregnancy, the onset of labor is triggered by distension of the uterus imposed by the

growing fetus, and pulmonary epithelial cells increase secretion of surfactant when stretched *in vitro*, just as they do in a newborn taking its first breath (Wirtz and Dobbs 1990, Oldenhof et al. 2002). Pulmonary hypertension, urinary frequency, and irritable bowel syndrome have each been associated with muscle cell hypercontractility, though additional factors likely play a role as well. Recent studies suggest that genetic mutations or malfunction of cytoskeletal proteins, ECM molecules or integrins that alter cell and tissue mechanics can lead to impaired vascular smooth muscle and cardiac muscle contractility (Balogh et al. 2002, Loufrani et al. 2002). In contrast, decreased smooth muscle cell contractility results in urinary stress incontinence, as well as defects in male and female sexual function (Italiano et al. 1998, Levin 2002). Abnormal muscle tone also can lead to destabilization of the skeleton and contribute to skeletal and joint diseases. For example, axial muscular dysfunction has been implicated in the development of joint pathology in ankylosing spondylitis (Masi and Walsh 2003). Abnormal fibrillin deposition in patients with Marfan's syndrome alters the vascular endothelial cell response to hemodynamic stresses and results in aortic dissection due to local weakness of the vascular wall (Westaby 1999). Changes in ECM structure that alter tissue mechanics and provide a constitutive stimulus for cell growth may even contribute to cancer initiation and progression (Ingber et al. 1981, Sternlicht et al. 2000, Ingber 2002). For example, overexpression of an ECM-degrading enzyme in transgenic mice results in formation of malignant tumors (Sternlicht et al. 1999). Though each of these examples is quite different, they emphasize the widespread effect that altered mechanical signaling can have and additional examples of this are still being characterized.

Tensional forces are resisted and balanced by external adhesions to ECM and neighboring cells, and by other molecular filaments that locally resist inward-directed tensional forces inside the cytoskeleton. This type of force balance is a hallmark of an architectural system known as 'tensegrity' (Ingber 2003) and the viscoelastic behavior of living cells results from collective mechanical interactions within the tensed molecular cytoskeleton. Cytoskeletal forces are harnessed in muscle to generate tensional forces that are important for cell contractility and movement. The effects of applied stresses on cell shape and mechanics depend on the material properties of the cytoskeletal filaments and the level of isometric tension in the cell. This occurs similarly to the mechanical responsiveness of whole muscle, which is governed by its structural organization and by its contractile tone.

Recognition of the importance of mechanics and cellular mechanotransduction for tissue development also may help to explain the focal incidence of disease. Although high cholesterol and LDL promote atherosclerotic plaque formation, these plaques preferentially form in regions of disturbed blood flow (e.g. near vessel branches) (Davies 1995). Local changes in tissue structure also may explain why genetic diseases, including cancer, often present focally. Mechanical therapies have been used to alter tension using engineered devices that act through alterations in microscale forces (e.g. cell stretching) that activate cellular signal transduction (Langevin et al. 2001, Webb 2002). The therapeutic value of physical therapy, massage, and muscle stimulation is also well known, and even acupuncture therapy appears to result from ECM distortion as associated integrin-dependent changes in mechanotransduction (Langevin et al. 2001). In

our observations of the phenotype in *mlt* we have observed focal regions of invasion occurring, suggesting that forces are also applied locally but currently our assays do not have the resolution to detect these changes.

In smooth muscle cells, mechanical stresses can alter receptor or protein conformation (Shaw and Xu 2003) and also potentially influence the mechanical output of the cells. A number of studies have observed differences in the biomechanical properties of smooth muscle cells in the vasculature (VanDijk et al. 1984), bladder (Yu et al. 2003) and the airway (Smith et al. 2005). Within the GI tract, it has been indicated that smooth muscle strips that lacked enteric nerves could contract in response to stretch, suggesting that mechanosensitivity can occur intrinsically at the level of the smooth muscle cell (Farrugia et al. 1999). In addition to the direct implication of GI smooth muscle contractility, a study by Risse et al. found altered smooth muscle contraction in a mouse model for cystic fibrosis. In this report, it was shown that dissected intestinal muscle strips exhibited higher contractility in mutant mice with cystic fibrosis than in wild type controls (Risse et al. 2012). Mechanical measurements of isolated GI smooth muscle cells were consistent with measurements in other smooth muscle tissues, which overall are notably softer than other cell types (i.e. blood, endothelial cells, and chondrocytes) (Liao et al. 2006). In addition, smooth muscle cells in the GI tract are constantly being deformed due to forces generated by the muscle cells themselves or by the surroundings (Tanaka et al. 2000, Gregersen et al. 2002). Therefore, the intestine represents an environment where local contractile force alterations could certainly reside

and result in focally applied mechanical signals, as we believe is the case in early *mlt* mutants.

4.4.1: Tissue Stiffness and Cancer Invasion

Aside from the genetic and biochemical events that proceed during tumor development, recent findings lend support to the role of biomechanical factors in tissue development and maintenance (Paszek and Weaver 2004). During early tumor expansion, the surrounding tissue becomes compressed and interstitial pressure increases, altering the tissue tension within the stroma. Additional stiffening also happens at the cell contact level, where actomyosin contractions and Rho GTPase activity compromise cell junctions and alter cell polarity, while ECM stiffening drives focal adhesion formation. Force-induced effects can also widely vary based up the direction the force is being applied and its duration. One example of this is TGF- β1 signaling in smooth muscle cells, where transient forces increase its expression but if a constant force is applied both TGF-β1 and collagen I become upregulated (Gutierrez and Perr 1999). This has also been observed in fibroblasts where dynamic forces increase MMP-9 but static force upregulates MMP-2 (Prajapati et al. 2000). An outstanding question remains as to how each applied force can induce different cellular responses that can often occur in the complex environment surrounding a tumor.

Extracellular matrix (ECM) orientation mediates tension-dependent cell migration to orchestrate developmental processes such as gastrulation (Keller et al. 2003), and matrix rigidity influences cell growth, differentiation, and motility (Lo et al. 2000, Engler

et al. 2004, Yeung et al. 2005). Matrix compliance influences Rho activity and ERK-dependent growth (Wang and Bitar 1998, Wozniak et al. 2003), and cytoskeleton tension promotes growth (Roovers and Assoian 2003) and focal adhesion (FA) assembly (Burridge and Wennerberg 2004). It has also been postulated that tissue stiffness could drive transformation by increasing Rho-generated cytoskeletal tension via integrin signaling. Integrins are transmembrane ECM receptors that can function as mechanotransducers (Bershadsky et al. 2003), integrins regulate Rho- and ERK-dependent growth (Lee and Juliano 2004). Integrin expression is higher in epithelia on rigid substrates than complaint surfaces (Delcommenne and Streuli 1995), and matrix rigidity increases integrin expression (Yeung et al. 2005). Thus, tissue stiffness could drive expression of a malignant phenotype through force-dependent regulation of integrin activity. Indeed, integrin levels and signaling are altered in 'stiff' tumors (Guo and Giancotti 2004).

Paszek et al. found that even small increases in matrix rigidity will perturb tissue architecture and enhance growth by inducing Rho-generated cytoskeletal tension to promote FA assembly and increase ERK activation. Their data suggests a mechanoregulatory circuit that functions to integrate physical cues from the ECM (i.e. exogenous force) with FA assembly through ERK- and Rho-dependent cytoskeletal contractility to regulate cell and tissue phenotype (Paszek et al. 2005). Thus, tensional homeostasis may be essential for normal tissue growth and differentiation, and increasing tissue rigidity by stiffening the matrix (fibrosis) or by elevating Rho signaling through, for example, oncogene (*Ras*)-driven ERK activation, could induce cytoskeletal

contractility to enhance integrin-dependent growth and destabilize tissue architecture (Zhong et al. 1997).

4.4.2: ECM Signaling in Response to Stiffness: A Clue From Tissue Development?

Cell growth, differentiation, and motility can all be influenced by physical distortion of cells through their ECM adhesions. Mammary and retinal epithelium can be switched from growth to differentiation by decreasing the stiffness or adhesivity of the ECM, and thereby promoting cell retraction and rounding (Opas 1989). Varying the mechanical compliance (flexibility) of the ECM also influences the rate of cell migration and the direction of motility can be affected by geometric cues from the ECM (Lo et al. 2000, Parker et al. 2002). Changing vascular smooth muscle cell shape through modulation of cell-ECM adhesion or alteration of ECM compliance also regulates its contractile response to vasoagonists (Lee et al. 1998).

Cell shape-dependent changes in the sensitivity of the contractile machinery may ensure 'compliance matching' in muscle cells of the gastrointestinal tract, blood vessels, as well as in epithelial and connective tissues, so that the level of tension exerted by the cell precisely balances the mechanical stress transmitted through the surrounding ECM in response to tissue distortion. During tissue development, local alterations in ECM structure that influence cell shape and mechanics, such as thinning of basement membrane produced by increased ECM turnover (e.g. metalloproteinase activities), also appear to drive regional changes in cell growth and motility. Skin epithelium, bone cells, and embryonic heart muscle cells all increase their growth rates when they experience

mechanical strain (Miller et al. 2000, Hatton et al. 2003). Endothelium sense fluid shear stress and respond by altering expression of proteins involved in handling oxidative stress. Mechanical forces have also been shown to be important in the developing vasculature where pressure and shear stress from pumping blood affects the morphology of the heart and vasculature. Bones are also shaped by forces produced by muscle contraction during development and lungs rely on airway contractions to regulate their physiology.

Mechanotransduction during early development has been proposed from observing the effects of stretching embryos in vitro and altering mechanical forces in vivo (Beloussov et al. 1988, Beloussov 1990). Morphogenetic movements during development can be regulated by physical force as well as the coordinated growth of individual tissues (Orr et al. 2006). In Drosophila, there is evidence suggesting mechanical activation of the transcription factor Twist (Farge 2003). In this system, Twist expression in the anterior foregut and stomodeal primordial appears to be initiated by a force applied onto these tissues by germ band extension. The authors also applied force experimentally and were able to ectopically express Twist. Mechanical tension in Drosophila has also been proposed to regulate transcription in migrating border cells (Somogyi and Rorth 2004). They observed that MAL-D, an SRF cofactor, requires the force from stretch in order to translocate from the cytoplasm to the nucleus and they could block this translocation by preventing cellular elongation.

With the large number of diverse processes being controlled by mechanical signaling or abnormal muscle contraction, there is clearly a number of emerging questions as to how tissues are responding to these stimuli. These questions can be

addressed, in part, by assessing myosins role in force propagation as well as its ability to cooperate with neighboring heads or modulatory proteins such as h-CaD. Understanding smooth muscle contraction *in vivo* as well as its effect on underlying epithelial cells will begin to shed light on biological processes that transmit mechanical signals between neighboring tissues. However, it remains to be determined how widespread mechanical signaling is in disease states and during development. If the underlying mechanistic properties are similar in each context then understanding the modulation of smooth muscle contraction could provide insight into the nature of force propagation in muscle and between cells.

Appendix: Materials and Methods

Morpholino Knockdown

All morpholinos were injected into 1- to 4-cell stage fertilized embryos. Injection of 620 pg of a morpholino directed against the 5' region of the zebrafish smooth muscle myosin heavy chain cDNA that overlapped the predicted translation initiation site rescued *mlt* mutants (5'-ATCATCGCTCAAGCCTTTCTTCGTC-3'). Injection of lower doses generated partially rescued *mlt* mutants that were discarded from further analyses. Fully rescued mutants were identified using Kompetitive Allele Specific PCR (KASP).

For smooth muscle Caldesmon knockdown, fertilized embryos were injected at one cell stage with 20 pg of *cald1* morpholino. Zebrafish embryos were microinjected with a morpholino targeting the splice acceptor site of exon 5 of zebrafish *cald1* (5'-TTATTCCCCTACAAACAGAACTGCA-3'; Gene-Tools, Corvallis, OR, USA). Morpholinos were injected as described. The sequence of the control morpholino is TGCGCGCCAGACAGGGTGATGAC. The h-CaD morpholino was designed against the smooth-muscle-specific exon of Caldesmon (based on acc. # BC158175), which was identified from intestinal smooth muscle cDNA. Injection of ~20 pg caused an in-frame deletion of this exon but had no effect on transcript of the low molecular weight isoform (Abrams et al. 2012).

RT-PCR

Intestines manually dissected from 5 day post-fertilization embryos were homogenized in Trizol (Sigma Aldrich, St. Louis, MO, USA) and total RNA was collected following the manufacturer's protocol. First strand cDNA was synthesized using the SuperScript™ III Reverse Transcriptase (Invitrogen, Carlsbad, CA, USA) according to the manufacturer's procedure. When necessary for sequencing, amplified cDNA fragments were cloned into the pGEM®-T Easy Vector (Promega, Madison, WI USA). Primer sequences are listed in table below.

Gene name	Genbank accession number	Forward primer	Reverse primer
Acta2	NM_212620	AGGAACACCCCACTCTGTTG	GCCAAGTCCAAACGCATAAT
Myh11a	NM_001024448	TGGATTACAATGCCGTAGCA	GCTGTGTGTTGTGCAGTGTG
Fabp2	NM_131431	CAACGTGAAGGAAGTCAGCA	AAATCCTCTTGGCCTCGACT
Vil1l	NM_200238	TGCCAGACCTGACATAGCTG	CTGCACCGGTTCTCCATTAT
Fabp6	NM_001002076.1	CGTCCAGAACGGAGATGACT	TGCGGTTAAACCTTCTTGCT
Cald1a	NM_001114883	TCACAACAACAACAACAACCAA	AGACGCGCATCTTCATCGT
Cald1b	XM_687255	AGGAAACAGTGCCAGAGGAA	ACTGGGGATTTGGGTGATTT

Generation of CALD1 Myosin- and Actin-binding Peptide Transgenic Fish

Primers corresponding to the human *CALD1* myosin binding peptide (Lee et al. 2000) were identified in the zebrafish *cald1*cDNA. Transgenic constructs were generated with the peptide fragment by Tol2kit site-specific recombination-based cloning. A 162 bp fragment was amplified from zebrafish intestinal cDNA and cloned in frame into an expression construct encoding a cDNA for the viral 2A recognition peptide (Provost et al. 2007) upstream of the green fluorescent protein cDNA. The expression construct also included a previously reported promoter fragment from the zebrafish *sm22a* gene (Seiler et al. 2010) and Tol2 inverted repeats at each end. 20ng μL^{-1} of DNA encoding the expression construct was injected into newly fertilized embryos along with 20ng μL^{-1} in

vitro transcribed mRNA for the Tol2 transposase as previously reported. All fragments were cloned using the multisite gateway system (Kwan et al. 2007, Villefranc et al. 2007).

Peristalsis Assay

Wild type, transgenic, morpholino injected, and mutant larvae were fed paramecia in media containing fluorescent latex beads (Fluoresbrite^{TM} YG2.0; Polysciences, Warrington, PA, USA; 5 µL beads per 2 mL of embryo media) for 2 hours - 6 hours. Larvae were then screened for fluorescence in the anterior intestine, placed in media containing only paramecia, and monitored for bead expulsion using a fluorescent dissecting microscope (Olympus, MVX-10). For time-lapse movies of intestinal contraction, larvae were anesthetized with equal amounts of tricaine (64 mg L^{-1}) and mounted in 3% methylcellulose. Images were obtained at 5 second – 15 second intervals for 2 minutes – 6 minutes using an RGB Vision digital camera (Roper Scientific Photometrics, Tucson, AZ, USA) and Image-Pro Plus Version 6.0 software (Media Cybernetics, Bethesda, MD, USA).

Cell Dissociation and FACS

Intestines dissected from 3dpf *Tg(sm22a:GFP; miR194:mCherry)* larvae were collected in DMEM (Gibco) and dissociated in 0.25% trypsin EDTA by pipetting. Cells were collected by centrifugation for 10 minutes at 620 *g* at 4°C and resuspended in 5%FCS/DMEM. Cells were labeled with 0.2µg mL^{-1} DAPI to determine cell survival and sorted using FACSVantage™ SE with FACSDiva™ Software (BD Biosciences, San Jose, CA, USA). Sorted cells were promptly collected by centrifugation and frozen in

liquid N_2. Total RNA was purified using RNAqueous®-Micro Kit (Applied Biosystems/Ambion, Austin, TX, USA) and used as a template for cDNA synthesis.

Western Blot/ Immunoprecipitation

Dissected intestines from 30 larvae at 4 dpf and 6 dpf were homogenized in 1x sample buffer, protein was recovered and used for Western analysis using standard methods (Davuluri et al.). Western blots were probed with anti-human beta-actin (Sigma-Aldrich); anti-mouse Caldesmon (a generous gift of Albert Wang); and anti-rabbit phospho-Caldesmon (serine 789; Upstate Biotechnology) using standard procedures.

For immunoprecipitation, intestines dissected from morpholino injected and uninjected *Tg(sm22a:CaDDK51-GFP)* larvae were fixed in 1% formaldehyde for 15 min at room temperature. Proteins were isolated by adding cell lysis buffer (50mM Tris-Cl, 10mM EDTA, 1%SDS and protease inhibitors), incubated on ice for 10 min and then centrifuged at 14000rpm for 10 min at 4°C. Supernatant was removed and the pellet diluted to 200ml in IP dilution buffer (0.01% SDS, 1.1% Triton X100, 1.2mM EDTA, 16.7mM Tris-Cl, 167mM NaCl). 1ug of rabbit anti-Caldesmon (Albert Wang) or smooth myosin antibody (Sigma Aldrich) was added and the mixture incubated overnight at 4°C. 10ml of Protein A/G Agarose (Santa Cruz Biotechnology) was added to the samples and incubated for 2hr at 4°C. The samples were then washed 3 times with PBST and the pellet was dissolved in 50ml of sample buffer. 25ul of samples were run on a 10% SDS-PAGE gel for western analysis.

Zebrafish Husbandry and Mutagenesis

Maintenance and breeding were performed as previously described (Wallace et al. 2005). *colourless* mutants were purchased from the Zebrafish International Resource Center (Eugene, OR, USA). Larvae were raised at 28°C in E3 medium and were staged by age and morphological criteria (size of yolk extension and pigment pattern around yolk extension). Expression of mCherry, Lifeact-GFP (Riedl et al. 2008), and GFP-$KRAS^{G12V}$ (a generous gift from Steven Leach) in the intestinal epithelium was driven by a 2 kb promoter fragment from the zebrafish *miR194* gene (Seiler et al. 2012). Expression of GFP in smooth muscle was driven by a promoter fragment from the zebrafish *sm22-alpha* gene (Seiler et al. 2010). Zebrafish *axin1* mutants were obtained from the Zebrafish International Resource Center. Mutagenesis was performed on males of Tu and AB strains according to the scheme outlined by Dosch et al. (Dosch et al. 2004).

Immunostaining

3 dpf old larvae were anesthetized with 0.1 mg/ml Tricaine, fixed in 4% PFA/PBS, washed in PBST (PBS+0.1% Tween), dehydrated in methanol, and stored at −20°C. For whole mount staining with anti-laminin and anti-cytokeratin antibodies, larvae were washed in PBST and permeabilized by a 15-min Proteinase K digestion (100 ug/ml in PBST). They were then rinsed in PBST and postfixed in 4% PFA/PBST. The skin above the trunk and intestine was removed using fine forceps. Larvae were stained with antibody in 10% goat serum/PBST. The laminin antibody (Sigma #L-9393) was used at 1:50 or 1:200 dilution; the cytokeratin antibody (Thermo Scientific clone AE1/AE3, MS-

343-PO) was used at 1:100 dilution. Secondary antibodies were labeled with Alexa 568 or 488 (Molecular Probes/Invitrogen). Histological analyses of the mounted specimens were performed as described (Wallace et al. 2005).

Drug Treatments

Larvae were bathed in 1.5 μM Menadione (MP biomedicals) in E3 media for 3 h (3 dpf larvae) or 5 h (5 dpf larvae).

Construction of Human Smooth Muscle Myosin II (MYH11)

The cDNA for human MYH11 (SM1A isoform) was truncated at the codon for threonine 1775 (creates a soluble 'HMM' construct), after which a glycine plus FLAG peptide (DYKDDDDK) was appended to facilitate purification. Site-directed mutagenesis was performed using Quickchange XLII kit (Stratagene) to introduce the S237Y mutation into the same construct. The constructs were subcloned into the baculovirus transfer vector, p2Bac (Invitrogen). Protein expression and purification were as previously described (Sweeney et al. 1998). The HMM construct had been previously subcloned into the baculovirus transfer vector, pVL 1393 (Invitrogen). Baculovirus expression was used to produce HMM fragments of smooth muscle myosin after infection of an insect cell line (Sf9) with recombinant baculovirus (described in detail in Sweeney at al. 1998 (Sweeney et al. 1998)).

Myosin ATPase Assay and Transient Kinetic Assays

As described previously in Kuang et al. 2012 (Kuang et al. 2012), the actin-

activated ATPase activity assay was performed at 25°C in buffer 20/20 (KCl 20 mM, Mg2+ 5 mM, EGTA 1 mM, MOPS 20 mM pH 7.0), ATP 1 mM final concentration and actin concentration ranging from 0 to 150 μM. Actin was purified from rabbit skeletal muscle and stabilized by phalloidin. Phosphorylation of HMM WT and mutant constructs was performed as previously described 10. Both unphosphorylated and phosphorylated forms of WT and mutant human smooth myosin 2 HMM constructs were assayed at 0.2 nM final concentration. Curves were fitted with Kaleidagraph software TM. Triplicate assays were performed with three different preparations of each protein. Transient kinetic measurements (Pi release from myosin and ADP release from actomyosin) were made in buffer 20/20 at 25°C with an Applied Photophysics SX.18MV stopped-flow instrument following previously published protocols (De La Cruz et al. 1999). Assays were performed with three different preparations of each protein.

Tissue Tension Measurements

The elastic moduli (Young's modulus) of intestines isolated from wild type and *mlt* larvae were measured using a microprobe indenter device (Levental et al. 2010). This assay measures the upward force generated by the intestine in response to indentation of the probe applied to the outer (serosal) surface. Tissue compliance (Young's modulus) is the slope of the force versus probe indentation curve. Briefly, a tensiometer probe (Kibron, Inc., Helsinki) with a 100 μm radius flat-bottom needle was mounted on a 3-D micromanipulator with 160 nm step size (Eppendorf, Inc.) attached to an inverted microscope. The tissue was adhered to the bottom of a plastic dish filled with DMEM and imaged by bright field illumination. The bottom of the probe was brought through the air-

water interface until it rested at the surface of the cylindrical tissue with a diameter of approximately 80 microns. The probe was calibrated using the known surface tension of a pure water/air interface, and the stress applied by the tissue to the probe as it was lowered was measured as a function of indentation depth. In principle, this deformation geometry is that of an infinite plane compressing a cylindrical object, and the absolute values of elastic modulus can be calculated from appropriate models that require assumptions about the adherence of the tissue to the probe and the glass slide, whether the sample is modeled as a uniform cylinder or an elastic shell, and other structural factors that confound calculation of the absolute value of elastic modulus from the force-indentation data.

In this study the primary interest is in the relative stiffness of wild type and mutant tissue, and therefore we present only the primary data, which consists of the elastic resistance of the tissues as a function of indentation depth. Indentations (≥13 per intestine) spanned the range from 160 nm, which would measure small strain reflecting linear elasticity to indentations, up to 20 microns, which would reveal differences in large strain deformation or rupture. After the largest indentations, measurements were repeated at small strains to confirm that the deformations were recoverable. For statistical analyses, a one-tailed Student's *t* test for data sets with unequal variance was performed to determine the significance of differences between Young's moduli of wild type and *mlt* intestines samples.

Vascular Recordings

5 dpf larval zebrafish were anesthetized with equal amounts of tricaine (64 mg L^{-1}) and mounted in 3% methyl cellulose. All larval vascular flow was recorded for 5 seconds using a high-speed camera (Motionpro 2000; Redlake, Tuscon, AZ) at 250 fps with a 640 x 480 resolution. Heart rate imaging was recorded for 5 seconds at 125 fps with a 512 x 512 resolution. Quantification of blood flow rate was performed by tracking individual cells (5/larvae) over a fixed distance within both the artery and vein.

Bibliography

Abrams, J., G. Davuluri, C. Seiler and M. Pack (2012). "Smooth muscle caldesmon modulates peristalsis in the wild type and non-innervated zebrafish intestine." Neurogastroenterol Motil **24**(3): 288-299.

Albrecht, K., A. Schneider, C. Liebetrau, J. C. Ruegg and G. Pfitzer (1997). "Exogenous caldesmon promotes relaxation of guinea-pig skinned taenia coli smooth muscles: inhibition of cooperative reattachment of latch bridges?" Pflugers Arch **434**(5): 534-542.

Amores, A., A. Force, Y. L. Yan, L. Joly, C. Amemiya, A. Fritz, R. K. Ho, J. Langeland, V. Prince, Y. L. Wang, M. Westerfield, M. Ekker and J. H. Postlethwait (1998). "Zebrafish hox clusters and vertebrate genome evolution." Science **282**(5394): 1711-1714.

Ansari, S., M. Alahyan, S. B. Marston and M. El-Mezgueldi (2008). "Role of caldesmon in the Ca2+ regulation of smooth muscle thin filaments: evidence for a cooperative switching mechanism." J Biol Chem **283**(1): 47-56.

Armel, T. Z. and L. A. Leinwand (2010). "A mutation in the beta-myosin rod associated with hypertrophic cardiomyopathy has an unexpected molecular phenotype." Biochem Biophys Res Commun **391**(1): 352-356.

Armel, T. Z. and L. A. Leinwand (2010). "Mutations at the same amino acid in myosin that cause either skeletal or cardiac myopathy have distinct molecular phenotypes." J Mol Cell Cardiol **48**(5): 1007-1013.

Babu, G. J., E. Loukianov, T. Loukianova, G. J. Pyne, S. Huke, G. Osol, R. B. Low, R. J. Paul and M. Periasamy (2001). "Loss of SM-B myosin affects muscle shortening velocity and maximal force development." Nat Cell Biol **3**(11): 1025-1029.

Bai, X., Z. Yang, H. Jiang, S. Lin and L. I. Zon (2011). "Genetic suppressor screens in haploids." Methods Cell Biol **104**: 129-136.

Balogh, J., M. Merisckay, Z. Li, D. Paulin and A. Arner (2002). "Hearts from mice lacking desmin have a myopathy with impaired active force generation and unaltered wall compliance." Cardiovasc Res **53**(2): 439-450.

Beckett, E. A., S. Ro, Y. Bayguinov, K. M. Sanders and S. M. Ward (2007). "Kit signaling is essential for development and maintenance of interstitial cells of Cajal and electrical rhythmicity in the embryonic gastrointestinal tract." Dev Dyn **236**(1): 60-72.

Beloussov, L. V. (1990). "Mechanics of animal development." Riv Biol **83**(2-3): 303-322, 227-345.

Beloussov, L. V., A. V. Lakirev and Naumidi, II (1988). "The role of external tensions in differentiation of Xenopus laevis embryonic tissues." Cell Differ Dev **25**(3): 165-176.

Bershadsky, A. D., N. Q. Balaban and B. Geiger (2003). "Adhesion-dependent cell mechanosensitivity." Annu Rev Cell Dev Biol **19**: 677-695.

Bitar, K. N. and S. Raghavan (2012). "Intestinal tissue engineering: current concepts and future vision of regenerative medicine in the gut." Neurogastroenterol Motil **24**(1): 7-19.

Brunello, E., P. Bianco, G. Piazzesi, M. Linari, M. Reconditi, P. Panine, T. Narayanan, W. I. Helsby, M. Irving and V. Lombardi (2006). "Structural changes in the myosin filament and cross-bridges during active force development in single intact frog muscle fibres: stiffness and X-ray diffraction measurements." J Physiol **577**(Pt 3): 971-984.

Bryan, J. (1989). "Caldesmon, acidic amino acids and molecular weight determinations." J Muscle Res Cell Motil **10**(2): 95-96.

Bunton, T. E., N. J. Biery, L. Myers, B. Gayraud, F. Ramirez and H. C. Dietz (2001). "Phenotypic alteration of vascular smooth muscle cells precedes elastolysis in a mouse model of Marfan syndrome." Circ Res **88**(1): 37-43.

Burns, A. J., T. M. Herbert, S. M. Ward and K. M. Sanders (1997). "Interstitial cells of Cajal in the guinea-pig gastrointestinal tract as revealed by c-Kit immunohistochemistry." Cell Tissue Res **290**(1): 11-20.

Burridge, K. and K. Wennerberg (2004). "Rho and Rac take center stage." Cell **116**(2): 167-179.

Buvoli, M., M. Hamady, L. A. Leinwand and R. Knight (2008). "Bioinformatics assessment of beta-myosin mutations reveals myosin's high sensitivity to mutations." Trends Cardiovasc Med **18**(4): 141-149.

Chacko, S., S. Chang, J. Hypolite, M. Disanto and A. Wein (2004). "Alteration of contractile and regulatory proteins following partial bladder outlet obstruction." Scand J Urol Nephrol Suppl **215**(215): 26-36.

Chen, M. K. and S. F. Badylak (2001). "Small bowel tissue engineering using small intestinal submucosa as a scaffold." J Surg Res **99**(2): 352-358.

Childs, T. J., M. H. Watson, J. S. Sanghera, D. L. Campbell, S. L. Pelech and A. S. Mak (1992). "Phosphorylation of smooth muscle caldesmon by mitogen-activated protein (MAP) kinase and expression of MAP kinase in differentiated smooth muscle cells." J Biol Chem **267**(32): 22853-22859.

Chin-Sang, I. D., S. E. George, M. Ding, S. L. Moseley, A. S. Lynch and A. D. Chisholm (1999). "The ephrin VAB-2/EFN-1 functions in neuronal signaling to regulate epidermal morphogenesis in C. elegans." Cell **99**(7): 781-790.

Cochran, J. C., M. E. Thompson and F. J. Kull (2013). "Metal Switch-controlled Myosin II from Dictyostelium discoideum Supports Closure of Nucleotide Pocket during ATP Binding Coupled to Detachment from Actin Filaments." J Biol Chem **288**(39): 28312-28323.

Colpaert, C., P. Vermeulen, E. Van Marck and L. Dirix (2001). "The presence of a fibrotic focus is an independent predictor of early metastasis in lymph node-negative breast cancer patients." Am J Surg Pathol **25**(12): 1557-1558.

Conibear, P. B. (1999). "Kinetic studies on the effects of ADP and ionic strength on the interaction between myosin subfragment-1 and actin: implications for load-sensitivity and regulation of the crossbridge cycle." J Muscle Res Cell Motil **20**(8): 727-742.

Conibear, P. B. and M. A. Geeves (1998). "Cooperativity between the two heads of rabbit skeletal muscle heavy meromyosin in binding to actin." Biophys J **75**(2): 926-937.

Coureux, P. D., A. L. Wells, J. Menetrey, C. M. Yengo, C. A. Morris, H. L. Sweeney and A. Houdusse (2003). "A structural state of the myosin V motor without bound nucleotide." Nature **425**(6956): 419-423.

Cousins, H. M., F. R. Edwards, H. Hickey, C. E. Hill and G. D. Hirst (2003). "Electrical coupling between the myenteric interstitial cells of Cajal and adjacent muscle layers in the guinea-pig gastric antrum." J Physiol **550**(Pt 3): 829-844.

Davies, M. J. (1995). "Acute coronary thrombosis--the role of plaque disruption and its initiation and prevention." Eur Heart J **16 Suppl L**: 3-7.

Davis, E. C. (1993). "Smooth muscle cell to elastic lamina connections in developing mouse aorta. Role in aortic medial organization." Lab Invest **68**(1): 89-99.

Davuluri, G., C. Seiler, J. Abrams, A. J. Soriano and M. Pack "Differential effects of thin and thick filament disruption on zebrafish smooth muscle regulatory proteins." Neurogastroenterol Motil **22**(10): 1100-e1285.

Davuluri, G., C. Seiler, J. Abrams, A. J. Soriano and M. Pack (2010). "Differential effects of thin and thick filament disruption on zebrafish smooth muscle regulatory proteins." Neurogastroenterol Motil **22**(10): 1100-e1285.

De La Cruz, E. M. and E. M. Ostap (2004). "Relating biochemistry and function in the myosin superfamily." Curr Opin Cell Biol **16**(1): 61-67.

De La Cruz, E. M., A. L. Wells, S. S. Rosenfeld, E. M. Ostap and H. L. Sweeney (1999). "The kinetic mechanism of myosin V." Proc Natl Acad Sci U S A **96**(24): 13726-13731.

Decarreau, J. A., N. G. James, L. R. Chrin and C. L. Berger (2011). "Switch I closure simultaneously promotes strong binding to actin and ADP in smooth muscle myosin." J Biol Chem **286**(25): 22300-22307.

Delcommenne, M. and C. H. Streuli (1995). "Control of integrin expression by extracellular matrix." J Biol Chem **270**(45): 26794-26801.

Deng, M., E. Boopathi, J. A. Hypolite, T. Raabe, S. Chang, S. A. Zderic, A. J. Wein and S. Chacko (2013). "Amino acid mutations in the caldesmon C-terminal functional domain increases force generation in bladder smooth muscle." Am J Physiol Renal Physiol.

Dickens, G. R. and P. E. Morris (1998). "Cyclosporine-induced beta-adrenergic receptor down-regulation in bovine pulmonary artery smooth muscle cells: a pilot study." Pharmacotherapy **18**(2): 341-344.

Dosch, R., D. S. Wagner, K. A. Mintzer, G. Runke, A. P. Wiemelt and M. C. Mullins (2004). "Maternal control of vertebrate development before the midblastula transition: mutants from the zebrafish I." Dev Cell **6**(6): 771-780.

Driever, W., L. Solnica-Krezel, A. F. Schier, S. C. Neuhauss, J. Malicki, D. L. Stemple, D. Y. Stainier, F. Zwartkruis, S. Abdelilah, Z. Rangini, J. Belak and C. Boggs (1996). "A genetic screen for mutations affecting embryogenesis in zebrafish." Development **123**: 37-46.

Dutton, K. A., A. Pauliny, S. S. Lopes, S. Elworthy, T. J. Carney, J. Rauch, R. Geisler, P. Haffter and R. N. Kelsh (2001). "Zebrafish colourless encodes sox10 and specifies non-ectomesenchymal neural crest fates." Development **128**(21): 4113-4125.

Earley, J. J., X. Su and R. S. Moreland (1998). "Caldesmon inhibits active crossbridges in unstimulated vascular smooth muscle: an antisense oligodeoxynucleotide approach." Circ Res **83**(6): 661-667.

Engler, A., L. Bacakova, C. Newman, A. Hategan, M. Griffin and D. Discher (2004). "Substrate compliance versus ligand density in cell on gel responses." Biophys J **86**(1 Pt 1): 617-628.

Farge, E. (2003). "Mechanical induction of Twist in the Drosophila foregut/stomodeal primordium." Curr Biol **13**(16): 1365-1377.

Farrugia, G. (2008). "Interstitial cells of Cajal in health and disease." Neurogastroenterol Motil **20 Suppl 1**: 54-63.

Farrugia, G., A. N. Holm, A. Rich, M. G. Sarr, J. H. Szurszewski and J. L. Rae (1999). "A mechanosensitive calcium channel in human intestinal smooth muscle cells." Gastroenterology **117**(4): 900-905.

Fisher, A. J., C. A. Smith, J. Thoden, R. Smith, K. Sutoh, H. M. Holden and I. Rayment (1995). "Structural studies of myosin:nucleotide complexes: a revised model for the molecular basis of muscle contraction." Biophys J **68**(4 Suppl): 19S-26S; discussion 27S-28S.

Forgacs, E., T. Sakamoto, S. Cartwright, B. Belknap, M. Kovacs, J. Toth, M. R. Webb, J. R. Sellers and H. D. White (2009). "Switch 1 mutation S217A converts myosin V into a low duty ratio motor." J Biol Chem **284**(4): 2138-2149.

Fredberg, J. J., D. S. Inouye, S. M. Mijailovich and J. P. Butler (1999). "Perturbed equilibrium of myosin binding in airway smooth muscle and its implications in bronchospasm." Am J Respir Crit Care Med **159**(3): 959-967.

Frye, J. J., V. A. Klenchin, C. R. Bagshaw and I. Rayment (2010). "Insights into the importance of hydrogen bonding in the gamma-phosphate binding pocket of myosin: structural and functional studies of serine 236." Biochemistry **49**(23): 4897-4907.

Furch, M., S. Fujita-Becker, M. A. Geeves, K. C. Holmes and D. J. Manstein (1999). "Role of the salt-bridge between switch-1 and switch-2 of Dictyostelium myosin." J Mol Biol **290**(3): 797-809.

George, S. E., K. Simokat, J. Hardin and A. D. Chisholm (1998). "The VAB-1 Eph receptor tyrosine kinase functions in neural and epithelial morphogenesis in C. elegans." Cell **92**(5): 633-643.

Gerthoffer, W. T. (1987). "Dissociation of myosin phosphorylation and active tension during muscarinic stimulation of tracheal smooth muscle." J Pharmacol Exp Ther **240**(1): 8-15.

Gerthoffer, W. T. and J. Pohl (1994). "Caldesmon and calponin phosphorylation in regulation of smooth muscle contraction." Can J Physiol Pharmacol **72**(11): 1410-1414.

Gregersen, H., O. H. Gilja, T. Hausken, A. Heimdal, C. Gao, K. Matre, S. Odegaard and A. Berstad (2002). "Mechanical properties in the human gastric antrum using B-mode ultrasonography and antral distension." Am J Physiol Gastrointest Liver Physiol **283**(2): G368-375.

Grikscheit, T. C., A. Siddique, E. R. Ochoa, A. Srinivasan, E. Alsberg, R. A. Hodin and J. P. Vacanti (2004). "Tissue-engineered small intestine improves recovery after massive small bowel resection." Ann Surg **240**(5): 748-754.

Guo, D. C., H. Pannu, V. Tran-Fadulu, C. L. Papke, R. K. Yu, N. Avidan, S. Bourgeois, A. L. Estrera, H. J. Safi, E. Sparks, D. Amor, L. Ades, V. McConnell, C. E. Willoughby, D. Abuelo, M. Willing, R. A. Lewis, D. H. Kim, S. Scherer, P. P. Tung, C. Ahn, L. M. Buja, C. S. Raman, S. S. Shete and D. M. Milewicz

(2007). "Mutations in smooth muscle alpha-actin (ACTA2) lead to thoracic aortic aneurysms and dissections." Nat Genet **39**(12): 1488-1493.

Guo, H., R. Huang, S. Semba, J. Kordowska, Y. H. Huh, Y. Khalina-Stackpole, K. Mabuchi, T. Kitazawa and C. L. Wang (2013). "Ablation of smooth muscle caldesmon affects the relaxation kinetics of arterial muscle." Pflugers Arch **465**(2): 283-294.

Guo, H. and C. L. Wang (2005). "Specific disruption of smooth muscle caldesmon expression in mice." Biochem Biophys Res Commun **330**(4): 1132-1137.

Guo, W. and F. G. Giancotti (2004). "Integrin signalling during tumour progression." Nat Rev Mol Cell Biol **5**(10): 816-826.

Gusev, N. B. (2001). "Some properties of caldesmon and calponin and the participation of these proteins in regulation of smooth muscle contraction and cytoskeleton formation." Biochemistry **66**(10): 1112-1121.

Gutierrez, J. A. and H. A. Perr (1999). "Mechanical stretch modulates TGF-beta1 and alpha1(I) collagen expression in fetal human intestinal smooth muscle cells." Am J Physiol **277**(5 Pt 1): G1074-1080.

Haeberle, J. R., J. W. Hott and D. R. Hathaway (1985). "Regulation of isometric force and isotonic shortening velocity by phosphorylation of the 20,000 dalton myosin light chain of rat uterine smooth muscle." Pflugers Arch **403**(2): 215-219.

Hatton, J. P., M. Pooran, C. F. Li, C. Luzzio and M. Hughes-Fulford (2003). "A short pulse of mechanical force induces gene expression and growth in MC3T3-E1 osteoblasts via an ERK 1/2 pathway." J Bone Miner Res **18**(1): 58-66.

He, W. Q., Y. J. Peng, W. C. Zhang, N. Lv, J. Tang, C. Chen, C. H. Zhang, S. Gao, H. Q. Chen, G. Zhi, R. Feil, K. E. Kamm, J. T. Stull, X. Gao and M. S. Zhu (2008). "Myosin light chain kinase is central to smooth muscle contraction and required for gastrointestinal motility in mice." Gastroenterology **135**(2): 610-620.

Hecker, L., K. Baar, R. G. Dennis and K. N. Bitar (2005). "Development of a three-dimensional physiological model of the internal anal sphincter bioengineered in vitro from isolated smooth muscle cells." Am J Physiol Gastrointest Liver Physiol **289**(2): G188-196.

Heisenberg, C. P., C. Houart, M. Take-Uchi, G. J. Rauch, N. Young, P. Coutinho, I. Masai, L. Caneparo, M. L. Concha, R. Geisler, T. C. Dale, S. W. Wilson and D. L. Stemple (2001). "A mutation in the Gsk3-binding domain of zebrafish Masterblind/Axin1 leads to a fate transformation of telencephalon and eyes to diencephalon." Genes Dev **15**(11): 1427-1434.

Helfman, D. M., E. T. Levy, C. Berthier, M. Shtutman, D. Riveline, I. Grosheva, A. Lachish-Zalait, M. Elbaum and A. D. Bershadsky (1999). "Caldesmon inhibits nonmuscle cell contractility and interferes with the formation of focal adhesions." Mol Biol Cell **10**(10): 3097-3112.

Holmberg, A., C. Olsson and G. W. Hennig (2007). "TTX-sensitive and TTX-insensitive control of spontaneous gut motility in the developing zebrafish (Danio rerio) larvae." J Exp Biol **210**(Pt 6): 1084-1091.

Hori, Y., T. Nakamura, D. Kimura, K. Kaino, Y. Kurokawa, S. Satomi and Y. Shimizu (2002). "Functional analysis of the tissue-engineered stomach wall." Artif Organs **26**(10): 868-872.

Horiuchi, K. Y. and S. Chacko (1989). "Caldesmon inhibits the cooperative turning-on of the smooth muscle heavy meromyosin by tropomyosin-actin." Biochemistry **28**(23): 9111-9116.

Horiuchi, K. Y., H. Miyata and S. Chacko (1986). "Modulation of smooth muscle actomyosin ATPase by thin filament associated proteins." Biochem Biophys Res Commun **136**(3): 962-968.

Huizinga, J. D. and E. J. White (2008). "Progenitor cells of interstitial cells of Cajal: on the road to tissue repair." Gastroenterology **134**(4): 1252-1254.

Hurd, T. R., M. G. Leblanc, L. N. Jones, M. DeGennaro and R. Lehmann (2013). "Genetic modifier screens to identify components of a redox-regulated cell adhesion and migration pathway." Methods Enzymol **528**: 197-215.

Huxley, H. E. (2007). "Evidence about the structural behaviour of myosin crossbridges during muscle contraction." Adv Exp Med Biol **592**: 315-326.

Ikebe, M. and S. Reardon (1990). "Phosphorylation of smooth muscle caldesmon by calmodulin-dependent protein kinase II. Identification of the phosphorylation sites." J Biol Chem **265**(29): 17607-17612.

Ingber, D. E. (2002). "Cancer as a disease of epithelial-mesenchymal interactions and extracellular matrix regulation." Differentiation **70**(9-10): 547-560.

Ingber, D. E. (2003). "Mechanobiology and diseases of mechanotransduction." Ann Med **35**(8): 564-577.

Ingber, D. E., J. A. Madri and J. D. Jamieson (1981). "Role of basal lamina in neoplastic disorganization of tissue architecture." Proc Natl Acad Sci U S A **78**(6): 3901-3905.

Italiano, G., A. Calabro, S. Spini, E. Ragazzi and F. Pagano (1998). "Functional response of cavernosal tissue to distension." Urol Res **26**(1): 39-44.

Jang, S. M., J. W. Kim, D. Kim, C. H. Kim, J. H. An, K. H. Choi and S. Rhee (2013). "Sox4-mediated caldesmon expression facilitates skeletal myoblast differentiation." J Cell Sci.

Jorgensen, E. M. and S. E. Mango (2002). "The art and design of genetic screens: caenorhabditis elegans." Nat Rev Genet **3**(5): 356-369.

Kad, N. M., A. S. Rovner, P. M. Fagnant, P. B. Joel, G. G. Kennedy, J. B. Patlak, D. M. Warshaw and K. M. Trybus (2003). "A mutant heterodimeric myosin with one inactive head generates maximal displacement." J Cell Biol **162**(3): 481-488.

Kamm, K. E. and J. T. Stull (1985). "The function of myosin and myosin light chain kinase phosphorylation in smooth muscle." Annu Rev Pharmacol Toxicol **25**: 593-620.

Katsuyama, H., C. L. Wang and K. G. Morgan (1992). "Regulation of vascular smooth muscle tone by caldesmon." J Biol Chem **267**(21): 14555-14558.

Keller, R., L. A. Davidson and D. R. Shook (2003). "How we are shaped: the biomechanics of gastrulation." Differentiation **71**(3): 171-205.

Kelsh, R. N. and J. S. Eisen (2000). "The zebrafish colourless gene regulates development of non-ectomesenchymal neural crest derivatives." Development **127**(3): 515-525.

Khaled, W., S. Reichling, O. T. Bruhns, H. Boese, M. Baumann, G. Monkman, S. Egersdoerfer, D. Klein, A. Tunayar, H. Freimuth, A. Lorenz, A. Pessavento and H. Ermert (2004). "Palpation imaging using a haptic system for virtual reality applications in medicine." Stud Health Technol Inform **98**: 147-153.

Khau Van Kien, P., F. Mathieu, L. Zhu, A. Lalande, C. Betard, M. Lathrop, F. Brunotte, J. E. Wolf and X. Jeunemaitre (2005). "Mapping of familial thoracic aortic aneurysm/dissection with patent ductus arteriosus to 16p12.2-p13.13." Circulation **112**(2): 200-206.

King, G. G., P. D. Pare and C. Y. Seow (1999). "The mechanics of exaggerated airway narrowing in asthma: the role of smooth muscle." Respir Physiol **118**(1): 1-13.

Kintses, B., M. Gyimesi, D. S. Pearson, M. A. Geeves, W. Zeng, C. R. Bagshaw and A. Malnasi-Csizmadia (2007). "Reversible movement of switch 1 loop of myosin determines actin interaction." EMBO J **26**(1): 265-274.

Kito, Y. and H. Suzuki (2003). "Modulation of slow waves by hyperpolarization with potassium channel openers in antral smooth muscle of the guinea-pig stomach." J Physiol **548**(Pt 1): 175-189.

Klein, R. D. and B. J. Meyer (1993). "Independent domains of the Sdc-3 protein control sex determination and dosage compensation in C. elegans." Cell **72**(3): 349-364.

Kordowska, J., R. Huang and C. L. Wang (2006). "Phosphorylation of caldesmon during smooth muscle contraction and cell migration or proliferation." J Biomed Sci **13**(2): 159-172.

Kuang, S. Q., C. S. Kwartler, K. L. Byanova, J. Pham, L. Gong, S. K. Prakash, J. Huang, K. E. Kamm, J. T. Stull, H. L. Sweeney and D. M. Milewicz (2012). "Rare, nonsynonymous variant in the smooth muscle-specific isoform of myosin heavy chain, MYH11, R247C, alters force generation in the aorta and phenotype of smooth muscle cells." Circ Res **110**(11): 1411-1422.

Kwan, K. M., E. Fujimoto, C. Grabher, B. D. Mangum, M. E. Hardy, D. S. Campbell, J. M. Parant, H. J. Yost, J. P. Kanki and C. B. Chien (2007). "The Tol2kit: a multisite gateway-based construction kit for Tol2 transposon transgenesis constructs." Dev Dyn **236**(11): 3088-3099.

Langevin, H. M., D. L. Churchill and M. J. Cipolla (2001). "Mechanical signaling through connective tissue: a mechanism for the therapeutic effect of acupuncture." FASEB J **15**(12): 2275-2282.

Langevin, H. M., D. L. Churchill, J. R. Fox, G. J. Badger, B. S. Garra and M. H. Krag (2001). "Biomechanical response to acupuncture needling in humans." J Appl Physiol (1985) **91**(6): 2471-2478.

Lawson, J. D., E. Pate, I. Rayment and R. G. Yount (2004). "Molecular dynamics analysis of structural factors influencing back door pi release in myosin." Biophys J **86**(6): 3794-3803.

Lee, J. W. and R. Juliano (2004). "Mitogenic signal transduction by integrin- and growth factor receptor-mediated pathways." Mol Cells **17**(2): 188-202.

Lee, K. M., K. Y. Tsai, N. Wang and D. E. Ingber (1998). "Extracellular matrix and pulmonary hypertension: control of vascular smooth muscle cell contractility." Am J Physiol **274**(1 Pt 2): H76-82.

Lee, Y. H., C. Gallant, H. Guo, Y. Li, C. A. Wang and K. G. Morgan (2000). "Regulation of vascular smooth muscle tone by N-terminal region of caldesmon. Possible role of tethering actin to myosin." J Biol Chem **275**(5): 3213-3220.

Levental, I., K. R. Levental, E. A. Klein, R. Assoian, R. T. Miller, R. G. Wells and P. A. Janmey (2010). "A simple indentation device for measuring micrometer-scale tissue stiffness." J Phys Condens Matter **22**(19): 194120.

Levental, K. R., H. Yu, L. Kass, J. N. Lakins, M. Egeblad, J. T. Erler, S. F. Fong, K. Csiszar, A. Giaccia, W. Weninger, M. Yamauchi, D. L. Gasser and V. M. Weaver (2009). "Matrix crosslinking forces tumor progression by enhancing integrin signaling." Cell **139**(5): 891-906.

Levin, R. J. (2002). "The physiology of sexual arousal in the human female: a recreational and procreational synthesis." Arch Sex Behav **31**(5): 405-411.

Li, X. D., T. E. Rhodes, R. Ikebe, T. Kambara, H. D. White and M. Ikebe (1998). "Effects of mutations in the gamma-phosphate binding site of myosin on its motor function." J Biol Chem **273**(42): 27404-27411.

Li, Y., H. D. Je, S. Malek and K. G. Morgan (2004). "Role of ERK1/2 in uterine contractility and preterm labor in rats." Am J Physiol Regul Integr Comp Physiol **287**(2): R328-335.

Li, Y., M. Reznichenko, R. M. Tribe, P. E. Hess, M. Taggart, H. Kim, J. P. DeGnore, S. Gangopadhyay and K. G. Morgan (2009). "Stretch activates human myometrium via ERK, caldesmon and focal adhesion signaling." PLoS One **4**(10): e7489.

Liao, D., C. Sevcencu, K. Yoshida and H. Gregersen (2006). "Viscoelastic properties of isolated rat colon smooth muscle cells." Cell Biol Int **30**(10): 854-858.

Lin, T., M. J. Greenberg, J. R. Moore and E. M. Ostap (2011). "A hearing loss-associated myo1c mutation (R156W) decreases the myosin duty ratio and force sensitivity." Biochemistry **50**(11): 1831-1838.

Lo, C. M., H. B. Wang, M. Dembo and Y. L. Wang (2000). "Cell movement is guided by the rigidity of the substrate." Biophys J **79**(1): 144-152.

Loufrani, L., B. I. Levy and D. Henrion (2002). "Defect in microvascular adaptation to chronic changes in blood flow in mice lacking the gene encoding for dystrophin." Circ Res **91**(12): 1183-1189.

Lu, C., Y. Liu, X. Tang, H. Ye and D. Zhu (2006). "Role of 15-hydroxyeicosatetraenoic acid in phosphorylation of ERK1/2 and caldesmon in pulmonary arterial smooth muscle cells." Can J Physiol Pharmacol **84**(10): 1061-1069.

Mabuchi, K. and C. L. Wang (1991). "Electron microscopic studies of chicken gizzard caldesmon and its complex with calmodulin." J Muscle Res Cell Motil **12**(2): 145-151.

Malnasi-Csizmadia, A., J. L. Dickens, W. Zeng and C. R. Bagshaw (2005). "Switch movements and the myosin crossbridge stroke." J Muscle Res Cell Motil **26**(1): 31-37.

Margossian, S. S. and S. Lowey (1973). "Substructure of the myosin molecule. 3. Preparation of single-headed derivatives of myosin." J Mol Biol **74**(3): 301-311.

Masi, A. T. and E. G. Walsh (2003). "Ankylosing spondylitis: integrated clinical and physiological perspectives." Clin Exp Rheumatol **21**(1): 1-8.

McCluggage, W. G. (2004). "A critical appraisal of the value of immunohistochemistry in diagnosis of uterine neoplasms." Adv Anat Pathol **11**(3): 162-171.

Metzger, M., C. Caldwell, A. J. Barlow, A. J. Burns and N. Thapar (2009). "Enteric nervous system stem cells derived from human gut mucosa for the treatment of aganglionic gut disorders." Gastroenterology **136**(7): 2214-2225 e2211-2213.

Miettinen, M. M., M. Sarlomo-Rikala, A. J. Kovatich and J. Lasota (1999). "Calponin and h-caldesmon in soft tissue tumors: consistent h-caldesmon immunoreactivity in gastrointestinal stromal tumors indicates traits of smooth muscle differentiation." Mod Pathol **12**(8): 756-762.

Miller, C. E., K. J. Donlon, L. Toia, C. L. Wong and P. R. Chess (2000). "Cyclic strain induces proliferation of cultured embryonic heart cells." In Vitro Cell Dev Biol Anim **36**(10): 633-639.

Moiseeva, E. P. (2001). "Adhesion receptors of vascular smooth muscle cells and their functions." Cardiovasc Res **52**(3): 372-386.

Moore, J. R., L. Leinwand and D. M. Warshaw (2012). "Understanding cardiomyopathy phenotypes based on the functional impact of mutations in the myosin motor." Circ Res **111**(3): 375-385.

Morano, I., G. X. Chai, L. G. Baltas, V. Lamounier-Zepter, G. Lutsch, M. Kott, H. Haase and M. Bader (2000). "Smooth-muscle contraction without smooth-muscle myosin." Nat Cell Biol **2**(6): 371-375.

Moreland, S. and R. S. Moreland (1987). "Effects of dihydropyridines on stress, myosin phosphorylation, and V0 in smooth muscle." Am J Physiol **252**(6 Pt 2): H1049-1058.

Murphy, R. A. (1989). "Contraction in smooth muscle cells." Annu Rev Physiol **51**: 275-283.

Nelson, S. R., M. Y. Ali, K. M. Trybus and D. M. Warshaw (2009). "Random walk of processive, quantum dot-labeled myosin Va molecules within the actin cortex of COS-7 cells." Biophys J **97**(2): 509-518.

Oldenhof, A. D., O. P. Shynlova, M. Liu, B. L. Langille and S. J. Lye (2002). "Mitogen-activated protein kinases mediate stretch-induced c-fos mRNA expression in myometrial smooth muscle cells." Am J Physiol Cell Physiol **283**(5): C1530-1539.

Opas, M. (1989). "Expression of the differentiated phenotype by epithelial cells in vitro is regulated by both biochemistry and mechanics of the substratum." Dev Biol **131**(2): 281-293.

Orr, A. W., B. P. Helmke, B. R. Blackman and M. A. Schwartz (2006). "Mechanisms of mechanotransduction." Dev Cell **10**(1): 11-20.

Pan, W. K., B. J. Zheng, Y. Gao, H. Qin and Y. Liu (2011). "Transplantation of neonatal gut neural crest progenitors reconstructs ganglionic function in benzalkonium chloride-treated homogenic rat colon." J Surg Res **167**(2): e221-230.

Pannu, H., V. Tran-Fadulu, C. L. Papke, S. Scherer, Y. Liu, C. Presley, D. Guo, A. L. Estrera, H. J. Safi, A. R. Brasier, G. W. Vick, A. J. Marian, C. S. Raman, L. M. Buja and D. M. Milewicz (2007). "MYH11 mutations result in a distinct vascular pathology driven by insulin-like growth factor 1 and angiotensin II." Hum Mol Genet **16**(20): 2453-2462.

Park, J. M., T. Yang, L. J. Arend, J. B. Schnermann, C. A. Peters, M. R. Freeman and J. P. Briggs (1999). "Obstruction stimulates COX-2 expression in bladder smooth muscle cells via increased mechanical stretch." Am J Physiol **276**(1 Pt 2): F129-136.

Parker, K. K., A. L. Brock, C. Brangwynne, R. J. Mannix, N. Wang, E. Ostuni, N. A. Geisse, J. C. Adams, G. M. Whitesides and D. E. Ingber (2002). "Directional control of lamellipodia extension by constraining cell shape and orienting cell tractional forces." FASEB J **16**(10): 1195-1204.

Paszek, M. J. and V. M. Weaver (2004). "The tension mounts: mechanics meets morphogenesis and malignancy." J Mammary Gland Biol Neoplasia **9**(4): 325-342.

Paszek, M. J., N. Zahir, K. R. Johnson, J. N. Lakins, G. I. Rozenberg, A. Gefen, C. A. Reinhart-King, S. S. Margulies, M. Dembo, D. Boettiger, D. A. Hammer and V. M. Weaver (2005). "Tensional homeostasis and the malignant phenotype." Cancer Cell **8**(3): 241-254.

Piazzesi, G., M. Reconditi, M. Linari, L. Lucii, P. Bianco, E. Brunello, V. Decostre, A. Stewart, D. B. Gore, T. C. Irving, M. Irving and V. Lombardi (2007). "Skeletal muscle performance determined by modulation of number of myosin motors rather than motor force or stroke size." Cell **131**(4): 784-795.

Pierobon, P., S. Achouri, S. Courty, A. R. Dunn, J. A. Spudich, M. Dahan and G. Cappello (2009). "Velocity, processivity, and individual steps of single myosin V molecules in live cells." Biophys J **96**(10): 4268-4275.

Prajapati, R. T., M. Eastwood and R. A. Brown (2000). "Duration and orientation of mechanical loads determine fibroblast cyto-mechanical activation: monitored by protease release." Wound Repair Regen **8**(3): 238-246.

Provost, E., J. Rhee and S. D. Leach (2007). "Viral 2A peptides allow expression of multiple proteins from a single ORF in transgenic zebrafish embryos." Genesis **45**(10): 625-629.

Raghavan, A., G. Zhou, Q. Zhou, J. C. Ibe, R. Ramchandran, Q. Yang, H. Racherla, P. Raychaudhuri and J. U. Raj (2012). "Hypoxia-induced pulmonary arterial smooth muscle cell proliferation is controlled by forkhead box M1." Am J Respir Cell Mol Biol **46**(4): 431-436.

Raghavan, S., M. T. Lam, L. L. Foster, R. R. Gilmont, S. Somara, S. Takayama and K. N. Bitar (2010). "Bioengineered three-dimensional physiological model of colonic longitudinal smooth muscle in vitro." Tissue Eng Part C Methods **16**(5): 999-1009.

Rayment, I., H. M. Holden, M. Whittaker, C. B. Yohn, M. Lorenz, K. C. Holmes and R. A. Milligan (1993). "Structure of the actin-myosin complex and its implications for muscle contraction." Science **261**(5117): 58-65.

Rayment, I., W. R. Rypniewski, K. Schmidt-Base, R. Smith, D. R. Tomchick, M. M. Benning, D. A. Winkelmann, G. Wesenberg and H. M. Holden (1993). "Three-dimensional structure of myosin subfragment-1: a molecular motor." Science **261**(5117): 50-58.

Rich, A., S. A. Leddon, S. L. Hess, S. J. Gibbons, S. Miller, X. Xu and G. Farrugia (2007). "Kit-like immunoreactivity in the zebrafish gastrointestinal tract reveals putative ICC." Dev Dyn **236**(3): 903-911.

Riedl, J., A. H. Crevenna, K. Kessenbrock, J. H. Yu, D. Neukirchen, M. Bista, F. Bradke, D. Jenne, T. A. Holak, Z. Werb, M. Sixt and R. Wedlich-Soldner (2008). "Lifeact: a versatile marker to visualize F-actin." Nat Methods **5**(7): 605-607.

Risse, P. A., L. Kachmar, O. S. Matusovsky, M. Novali, F. R. Gil, S. Javeshghani, R. Keary, C. K. Haston, M. C. Michoud, J. G. Martin and A. M. Lauzon (2012). "Ileal smooth muscle dysfunction and remodeling in cystic fibrosis." Am J Physiol Gastrointest Liver Physiol **303**(1): G1-8.

Roberts, R. R., M. Ellis, R. M. Gwynne, A. J. Bergner, M. D. Lewis, E. A. Beckett, J. C. Bornstein and H. M. Young (2010). "The first intestinal motility patterns in fetal mice are not mediated by neurons or interstitial cells of Cajal." J Physiol **588**(Pt 7): 1153-1169.

Roberts, R. R., J. F. Murphy, H. M. Young and J. C. Bornstein (2007). "Development of colonic motility in the neonatal mouse-studies using spatiotemporal maps." Am J Physiol Gastrointest Liver Physiol **292**(3): G930-938.

Robertson, C. I., D. P. Gaffney, 2nd, L. R. Chrin and C. L. Berger (2005). "Structural rearrangements in the active site of smooth-muscle myosin." Biophys J **89**(3): 1882-1892.

Roopnarine, O. and L. A. Leinwand (1998). "Functional analysis of myosin mutations that cause familial hypertrophic cardiomyopathy." Biophys J **75**(6): 3023-3030.

Roovers, K. and R. K. Assoian (2003). "Effects of rho kinase and actin stress fibers on sustained extracellular signal-regulated kinase activity and activation of G(1) phase cyclin-dependent kinases." Mol Cell Biol **23**(12): 4283-4294.

Rosenfeld, S. S. and H. L. Sweeney (2004). "A model of myosin V processivity." J Biol Chem **279**(38): 40100-40111.

Rovner, A. S., P. M. Fagnant and K. M. Trybus (2003). "The two heads of smooth muscle myosin are enzymatically independent but mechanically interactive." J Biol Chem **278**(29): 26938-26945.

Sanders, K. M., S. D. Koh, S. Ro and S. M. Ward (2012). "Regulation of gastrointestinal motility--insights from smooth muscle biology." Nat Rev Gastroenterol Hepatol **9**(11): 633-645.

Sata, M. and M. Ikebe (1996). "Functional analysis of the mutations in the human cardiac beta-myosin that are responsible for familial hypertrophic cardiomyopathy. Implication for the clinical outcome." J Clin Invest **98**(12): 2866-2873.

Seiler, C., J. Abrams and M. Pack (2010). "Characterization of zebrafish intestinal smooth muscle development using a novel sm22alpha-b promoter." Dev Dyn **239**(11): 2806-2812.

Seiler, C., G. Davuluri, J. Abrams, F. J. Byfield, P. A. Janmey and M. Pack (2012). "Smooth muscle tension induces invasive remodeling of the zebrafish intestine." PLoS Biol **10**(9): e1001386.

Seow, C. Y. and J. J. Fredberg (2001). "Historical perspective on airway smooth muscle: the saga of a frustrated cell." J Appl Physiol (1985) **91**(2): 938-952.

Sharir, A., T. Stern, C. Rot, R. Shahar and E. Zelzer (2011). "Muscle force regulates bone shaping for optimal load-bearing capacity during embryogenesis." Development **138**(15): 3247-3259.

Shaw, A. and Q. Xu (2003). "Biomechanical stress-induced signaling in smooth muscle cells: an update." Curr Vasc Pharmacol **1**(1): 41-58.

Shepherd, I. and J. Eisen (2011). "Development of the zebrafish enteric nervous system." Methods Cell Biol **101**: 143-160.

Shimada, T., N. Sasaki, R. Ohkura and K. Sutoh (1997). "Alanine scanning mutagenesis of the switch I region in the ATPase site of Dictyostelium discoideum myosin II." Biochemistry **36**(46): 14037-14043.

Shwartz, Y., Z. Farkas, T. Stern, A. Aszodi and E. Zelzer (2012). "Muscle contraction controls skeletal morphogenesis through regulation of chondrocyte convergent extension." Dev Biol **370**(1): 154-163.

Siegman, M. J., T. M. Butler, S. U. Mooers and A. Michalek (1984). "Ca2+ can affect Vmax without changes in myosin light chain phosphorylation in smooth muscle." Pflugers Arch **401**(4): 385-390.

Sivarao, D. V., H. L. Mashimo, H. S. Thatte and R. K. Goyal (2001). "Lower esophageal sphincter is achalasic in nNOS(-/-) and hypotensive in W/W(v) mutant mice." Gastroenterology **121**(1): 34-42.

Small, J. V. and M. Gimona (1998). "The cytoskeleton of the vertebrate smooth muscle cell." Acta Physiol Scand **164**(4): 341-348.

Smith, B. A., B. Tolloczko, J. G. Martin and P. Grutter (2005). "Probing the viscoelastic behavior of cultured airway smooth muscle cells with atomic force microscopy: stiffening induced by contractile agonist." Biophys J **88**(4): 2994-3007.

Smith, C. W. and S. B. Marston (1985). "Disassembly and reconstitution of the Ca2+-sensitive thin filaments of vascular smooth muscle." FEBS Lett **184**(1): 115-119.

Smolock, E. M., D. M. Trappanese, S. Chang, T. Wang, P. Titchenell and R. S. Moreland (2009). "siRNA-mediated knockdown of h-caldesmon in vascular smooth muscle." Am J Physiol Heart Circ Physiol **297**(5): H1930-1939.

Snow, C. J. and C. A. Henry (2009). "Dynamic formation of microenvironments at the myotendinous junction correlates with muscle fiber morphogenesis in zebrafish." Gene Expr Patterns **9**(1): 37-42.

Sobue, K., Y. Muramoto, M. Fujita and S. Kakiuchi (1981). "Purification of a calmodulin-binding protein from chicken gizzard that interacts with F-actin." Proc Natl Acad Sci **78**(9): 5652-5655.

Somara, S. and K. N. Bitar (2006). "Phosphorylated HSP27 modulates the association of phosphorylated caldesmon with tropomyosin in colonic smooth muscle." Am J Physiol Gastrointest Liver Physiol **291**(4): G630-639.

Somara, S., R. R. Gilmont, J. R. Martens and K. N. Bitar (2007). "Ectopic expression of caveolin-1 restores physiological contractile response of aged colonic smooth muscle." Am J Physiol Gastrointest Liver Physiol **293**(1): G240-249.

Somogyi, K. and P. Rorth (2004). "Evidence for tension-based regulation of Drosophila MAL and SRF during invasive cell migration." Dev Cell **7**(1): 85-93.

St Johnston, D. (2002). "The art and design of genetic screens: Drosophila melanogaster." Nat Rev Genet **3**(3): 176-188.

Sternlicht, M. D., M. J. Bissell and Z. Werb (2000). "The matrix metalloproteinase stromelysin-1 acts as a natural mammary tumor promoter." Oncogene **19**(8): 1102-1113.

Sternlicht, M. D., A. Lochter, C. J. Sympson, B. Huey, J. P. Rougier, J. W. Gray, D. Pinkel, M. J. Bissell and Z. Werb (1999). "The stromal proteinase MMP3/stromelysin-1 promotes mammary carcinogenesis." Cell **98**(2): 137-146.

Suveges, D., Z. Gaspari, G. Toth and L. Nyitray (2009). "Charged single alpha-helix: a versatile protein structural motif." Proteins **74**(4): 905-916.

Sweeney, H. L. and A. Houdusse (2010). "Structural and functional insights into the Myosin motor mechanism." Annu Rev Biophys **39**: 539-557.

Sweeney, H. L., S. S. Rosenfeld, F. Brown, L. Faust, J. Smith, J. Xing, L. A. Stein and J. R. Sellers (1998). "Kinetic tuning of myosin via a flexible loop adjacent to the nucleotide binding pocket." J Biol Chem **273**(11): 6262-6270.

Szpacenko, A., J. Wagner, R. Dabrowska and J. C. Ruegg (1985). "Caldesmon-induced inhibition of ATPase activity of actomyosin and contraction of skinned fibres of chicken gizzard smooth muscle." FEBS Lett **192**(1): 9-12.

Tanaka, H., M. Hirose, T. Osada, H. Miwa, S. Watanabe and N. Sato (2000). "Implications of mechanical stretch on wound repair of gastric smooth muscle cells in vitro." Dig Dis Sci **45**(12): 2470-2477.

Toyoshima, Y. Y., S. J. Kron, E. M. McNally, K. R. Niebling, C. Toyoshima and J. A. Spudich (1987). "Myosin subfragment-1 is sufficient to move actin filaments in vitro." Nature **328**(6130): 536-539.

Trivedi, D. V., C. David, D. J. Jacobs and C. M. Yengo (2012). "Switch II mutants reveal coupling between the nucleotide- and actin-binding regions in myosin V." Biophys J **102**(11): 2545-2555.

Trybus, K. M., Y. Freyzon, L. Z. Faust and H. L. Sweeney (1997). "Spare the rod, spoil the regulation: necessity for a myosin rod." Proc Natl Acad Sci U S A **94**(1): 48-52.

Trybus, K. M., T. W. Huiatt and S. Lowey (1982). "A bent monomeric conformation of myosin from smooth muscle." Proc Natl Acad Sci U S A **79**(20): 6151-6155.

Tyska, M. J., D. E. Dupuis, W. H. Guilford, J. B. Patlak, G. S. Waller, K. M. Trybus, D. M. Warshaw and S. Lowey (1999). "Two heads of myosin are better than one for generating force and motion." Proc Natl Acad Sci U S A **96**(8): 4402-4407.

Tyska, M. J. and D. M. Warshaw (2002). "The myosin power stroke." Cell Motil Cytoskeleton **51**(1): 1-15.

VanDijk, A. M., P. A. Wieringa, M. van der Meer and J. D. Laird (1984). "Mechanics of resting isolated single vascular smooth muscle cells from bovine coronary artery." Am J Physiol **246**(3 Pt 1): C277-287.

Villefranc, J. A., J. Amigo and N. D. Lawson (2007). "Gateway compatible vectors for analysis of gene function in the zebrafish." Dev Dyn **236**(11): 3077-3087.

Volkmann, N., G. Ouyang, K. M. Trybus, D. J. DeRosier, S. Lowey and D. Hanein (2003). "Myosin isoforms show unique conformations in the actin-bound state." Proc Natl Acad Sci U S A **100**(6): 3227-3232.

Wallace, K. N., S. Akhter, E. M. Smith, K. Lorent and M. Pack (2005). "Intestinal growth and differentiation in zebrafish." Mech Dev **122**(2): 157-173.

Wallace, K. N., A. C. Dolan, C. Seiler, E. M. Smith, S. Yusuff, L. Chaille-Arnold, B. Judson, R. Sierk, C. Yengo, H. L. Sweeney and M. Pack (2005). "Mutation of smooth muscle myosin causes epithelial invasion and cystic expansion of the zebrafish intestine." Dev Cell **8**(5): 717-726.

Waller, G. S., G. Ouyang, J. Swafford, P. Vibert and S. Lowey (1995). "A minimal motor domain from chicken skeletal muscle myosin." J Biol Chem **270**(25): 15348-15352.

Walsh, R., C. Rutland, R. Thomas and S. Loughna (2010). "Cardiomyopathy: a systematic review of disease-causing mutations in myosin heavy chain 7 and their phenotypic manifestations." Cardiology **115**(1): 49-60.

Wang, C. L. (2001). "Caldesmon and smooth-muscle regulation." Cell Biochem Biophys **35**(3): 275-288.

Wang, C. L., J. M. Chalovich, P. Graceffa, R. C. Lu, K. Mabuchi and W. F. Stafford (1991). "A long helix from the central region of smooth muscle caldesmon." J Biol Chem **266**(21): 13958-13963.

Wang, P. and K. N. Bitar (1998). "Rho A regulates sustained smooth muscle contraction through cytoskeletal reorganization of HSP27." Am J Physiol **275**(6 Pt 1): G1454-1462.

Wang, Z., H. Jiang, Z. Q. Yang and S. Chacko (1997). "Both N-terminal myosin-binding and C-terminal actin-binding sites on smooth muscle caldesmon are required for caldesmon-mediated inhibition of actin filament velocity." Proc Natl Acad Sci U S A **94**(22): 11899-11904.

Ward, S. M., A. J. Burns, S. Torihashi and K. M. Sanders (1994). "Mutation of the proto-oncogene c-kit blocks development of interstitial cells and electrical rhythmicity in murine intestine." J Physiol **480 (Pt 1)**: 91-97.

Webb, L. X. (2002). "New techniques in wound management: vacuum-assisted wound closure." J Am Acad Orthop Surg **10**(5): 303-311.

Westaby, S. (1999). "Aortic dissection in Marfan's syndrome." Ann Thorac Surg **67**(6): 1861-1863; discussion 1868-1870.

White, H. D., B. Belknap and M. R. Webb (1997). "Kinetics of nucleoside triphosphate cleavage and phosphate release steps by associated rabbit skeletal actomyosin, measured using a novel fluorescent probe for phosphate." Biochemistry **36**(39): 11828-11836.

Whittaker, M., E. M. Wilson-Kubalek, J. E. Smith, L. Faust, R. A. Milligan and H. L. Sweeney (1995). "A 35-A movement of smooth muscle myosin on ADP release." Nature **378**(6558): 748-751.

Wirtz, H. R. and L. G. Dobbs (1990). "Calcium mobilization and exocytosis after one mechanical stretch of lung epithelial cells." Science **250**(4985): 1266-1269.

Wolny, M., M. Colegrave, L. Colman, E. White, P. Knight and M. Peckham (2013). "Cardiomyopathy mutations in the tail of beta cardiac myosin modify the coiled-coil structure and affect integration into thick filaments in muscle sarcomeres in adult cardiomyocytes." J Biol Chem.

Woolcock, A. J. and J. K. Peat (1989). "Epidemiology of bronchial hyperresponsiveness." Clin Rev Allergy **7**(3): 245-256.

Word, R. A., J. T. Stull, M. L. Casey and K. E. Kamm (1993). "Contractile elements and myosin light chain phosphorylation in myometrial tissue from nonpregnant and pregnant women." J Clin Invest **92**(1): 29-37.

Wozniak, M. A., R. Desai, P. A. Solski, C. J. Der and P. J. Keely (2003). "ROCK-generated contractility regulates breast epithelial cell differentiation in response to the physical properties of a three-dimensional collagen matrix." J Cell Biol **163**(3): 583-595.

Yengo, C. M., P. M. Fagnant, L. Chrin, A. S. Rovner and C. L. Berger (1998). "Smooth muscle myosin mutants containing a single tryptophan reveal molecular interactions at the actin-binding interface." Proc Natl Acad Sci U S A **95**(22): 12944-12949.

Yeung, T., P. C. Georges, L. A. Flanagan, B. Marg, M. Ortiz, M. Funaki, N. Zahir, W. Ming, V. Weaver and P. A. Janmey (2005). "Effects of substrate stiffness on cell morphology, cytoskeletal structure, and adhesion." Cell Motil Cytoskeleton **60**(1): 24-34.

Yildiz, A., J. N. Forkey, S. A. McKinney, T. Ha, Y. E. Goldman and P. R. Selvin (2003). "Myosin V walks hand-over-hand: single fluorophore imaging with 1.5-nm localization." Science **300**(5628): 2061-2065.

Yildiz, A., H. Park, D. Safer, Z. Yang, L. Q. Chen, P. R. Selvin and H. L. Sweeney (2004). "Myosin VI steps via a hand-over-hand mechanism with its lever arm undergoing fluctuations when attached to actin." J Biol Chem **279**(36): 37223-37226.

Yount, R. G., D. Lawson and I. Rayment (1995). "Is myosin a "back door" enzyme?" Biophys J **68**(4 Suppl): 44S-47S; discussion 47S-49S.

Yu, G., S. Bo, J. Xiyu and X. Enqing (2003). "Effect of bladder outlet obstruction on detrusor smooth muscle cell: an in vitro study." J Surg Res **114**(2): 202-209.

Zeng, W., P. B. Conibear, J. L. Dickens, R. A. Cowie, S. Wakelin, A. Malnasi-Csizmadia and C. R. Bagshaw (2004). "Dynamics of actomyosin interactions in relation to the cross-bridge cycle." Philos Trans R Soc Lond B Biol Sci **359**(1452): 1843-1855.

Zhan, Q. Q., S. S. Wong and C. L. Wang (1991). "A calmodulin-binding peptide of caldesmon." J Biol Chem **266**(32): 21810-21814.

Zhang, H. and L. Zhang (2007). "Regulation of alpha1-adrenoceptor-mediated contractions of the uterine artery by protein kinase C: role of the thick- and thin-filament regulatory pathways." J Pharmacol Exp Ther **322**(3): 1253-1260.

Zheng, P. P., L. A. Severijnen, R. Willemsen and J. M. Kros (2009). "Caldesmon is essential for cardiac morphogenesis and function: in vivo study using a zebrafish model." Biochem Biophys Res Commun **378**(1): 37-40.

Zhong, C., M. S. Kinch and K. Burridge (1997). "Rho-stimulated contractility contributes to the fibroblastic phenotype of Ras-transformed epithelial cells." Mol Biol Cell **8**(11): 2329-2344.

Zhu, L., D. Bonnet, M. Boussion, B. Vedie, D. Sidi and X. Jeunemaitre (2007). "Investigation of the MYH11 gene in sporadic patients with an isolated persistently patent arterial duct." Cardiol Young **17**(6): 666-672.